Immobilisation of SRB on Different Support Materials

by

Onita Basu

B.A.Sc., The University of British Columbia, 1995

A thesis submitted in partial fulfilment of the requirements for the degree of
Master of Applied Science in the Faculty of Graduate Studies
(Department of Civil Engineering, Environmental Engineering Programme)

We accept this thesis as conforming to the required standard

THE UNIVERSITY OF BRITISH COLUMBIA

November, 1999

In presenting this thesis in partial fulfilment of the requirements
for an advanced degree at the University of British Columbia, I
agree that the Library shall make it freely available for reference
and study. I further agree that permission for extensive copying of
this thesis for scholarly purposes may be granted by the head of my
department or by his or her representatives. It is understood that
copying or publication of this thesis for financial gain shall not
be allowed without my written permission.

Department of _____ Civil Engineering _____

The University of British Columbia
Vancouver, Canada

Date _____ November 17th, 1999 _____

ABSTRACT

The attachment and growth of sulphate reducing bacteria to solid supports, under autotrophic conditions, made from different materials was studied in this project.

The study of the immobilisation of SRB to different support surfaces was conducted in two parts. In the first study, glass beads, ceramic beads, molecular sieve, Teflon/plastic pieces, and zeolite supports were used. The purpose of this study was to determine if the selected analytical techniques were appropriate methods to monitor the biomass and sulphate concentrations present in the batch flasks. Both the turbidimetric and methylthymol blue methods of sulphate analysis are considered valid techniques to monitor sulphate concentrations. TKN is considered an appropriate method for enumerating SRB biomass, whereas measurements using the total solids and protein led to erroneous results. In the second study, foam, basalt, Ringlace and alginate beads were used as immobilisation surfaces. The amount of biomass immobilised on the different materials was monitored and compared to the total biomass in the system in an effort to quantify which support would be suitable for an immobilised bioreactor system. In order of decreasing immobilisation, compared to freely suspended biomass, is alginate beads (84%) > foam (79%) > Ringlace (37%), while the biomass on the basalt was below the detection limit of the TKN analysis.

A study of SRB growth in the complex and defined media showed that SRB were able to grow in both nutrient mediums. However, the specific activity of the SRB in the complex media was greater than that in the defined media, 0.097 and 0.015/h, respectively. The CO_2 uptake was first initiated in the defined media solution at a rate of 1.81×10^{-05} mol CO_2/(L.h), while the uptake of CO_2 in the complex media was initiated after approximately 150 hours at a rate of 0.38×10^{-05} mol CO_2/(L.h).

TABLE OF CONTENTS

LIST OF TABLES

LIST OF FIGURES

NOMENCLATURE

A_{CO2} = area of the CO_2 peak

Acomp = A_{N2} = area of N_2 peak

d = diameter (m)

D = F/V = dilution rate (h^{-1})

F = volumetric flowrate (m^3/h))

k_o = zero order rate constant (kg/m^3/s)

K_s = substrate conversion rate (mg/L)

Ksp = solubility product

η_T = total effectiveness factor (dimensionless)

P = protein concentration (mg/mL)

P_F = final protein concentration (mg/mL)

P_I = initial protein concentration (mg/mL)

R = A_{co2}/Acomp = ratio of CO_2 peak area to the peak area of N_2+CO_2

r = the volumetric rate of reaction (kg/m^3/s),

rs = -dS/dt = the rate of substrate consumed (kg/m^3/s)

rx = dx/dt = the rate of biomass produced (kg/m^3/s),

s.a. = surface area (m^2)

SD = standard deviation

S = substrate concentration (mg/L)

S_I = initial substrate concentration (mg/L)

S_F = final substrate concentration (mg/L)

[SO_4] = sulphate concentration (mol/L).

T = organic nitrogen mass (μg)

T_I = initial organic nitrogen mass (μg)

T_F = final organic nitrogen mass (μg)

t = time

td = (ln 2)/μ = doubling time (hours)

Nomenclature (con't)

μ = specific growth rate (time^{-1}).

μ_{max} = maximum specific growth rate (time^{-1})

V = volume of solution in the batch flasks (L)

V = volume in the reactor (m^3)

Vs = sample digestion volume (mL).

x = biomass concentration (kg/m^3)

X = the mass of biomass (mg)

X_m = immobilised cell concentration (mg/L)

Y_{SO_4} = molar growth yield = (g biomass/ mol sulphate)

Y_{xs} = biomass yield coefficient (mg biomass/mg substrate)

ACKNOWLEDGMENTS

CHAPTER 1: INTRODUCTION

Wastewaters containing high levels of toxic metals, sulphate and a low pH can negatively impact the environment. The treatment of these aqueous streams is important to protect the natural environment and human health. Treatment processes include chemical precipitation, reverse osmosis and ion exchange, however these treatment methods may be too expensive to be economically attractive. Therefore it is important to find a more economically attractive alternative, and bioremediation may provide this option.

Removal of metals from wastewaters through cell adsorption, with dead biomass, has been studied as a possible treatment technique for removing metals from wastewater (Eccles, 1995, Mattuschka and Straube, 1993). However, both living and dead biomass can accumulate metals. Living cells can assist in the removal of heavy metals through cell wall adsorption, intracellular accumulation, and extracellular polymeric substance (EPS) as well as through precipitation. Whereas dead biomass accumulates metals strictly through the process of cell wall adsorption.
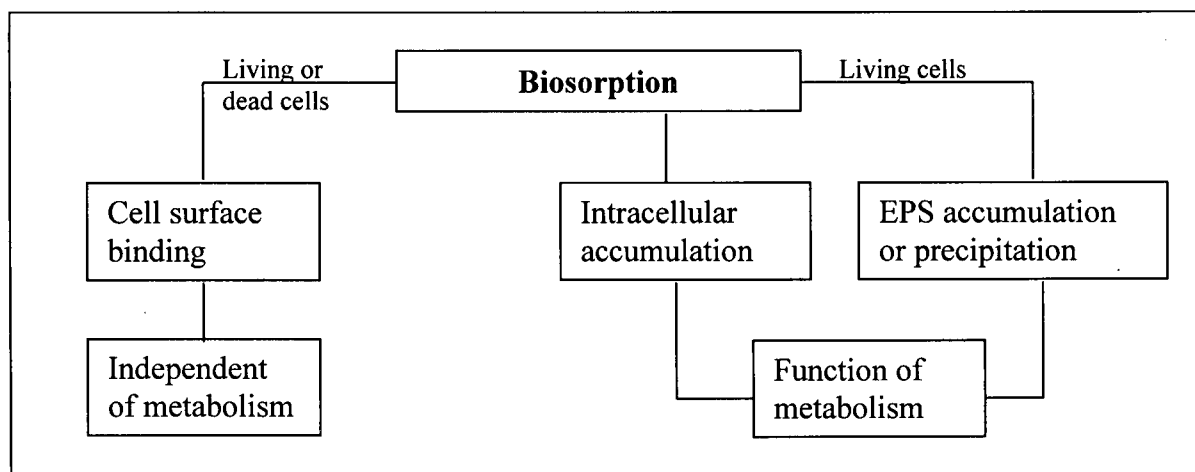
Figure 1.1: Relationship between biosorption and microbe metabolism.
(Source: Chang et. al., IAWQ Conference, 1998)

Binding of metals to the cell wall is independent of the metabolic traits of the organism while intracellular accumulation, EPS accumulation and precipitation are functions of metabolism (refer to Figure 1.1). Therefore, a treatment technique, which utilises living biomass, has the additional advantages of intracellular metal accumulation, as well as EPS metal accumulation/precipitation. A process that can take advantage of living biomass will have a greater ability to remove metals than a biological process relying strictly on cell adsorption.

In particular, sulphate reducing bacteria (SRB) reduce sulphate to hydrogen sulphide, which reacts with heavy metals in solution to form insoluble metal sulphide precipitates. This process also has the potential to recover metal sulphides from the effluent, which allows for recycling of the metal sulphides to the front end of metal refining processes, recovery of the sulphides as a saleable products, or simply as the isolation of hazardous sludge (Barnes et. al., 1991). As well, this biological process may be more economical than more traditional chemical treatment methods of heavy metal, high sulphate containing effluent streams; since metal sulphide precipitates tend to be denser and produce less sludge volume than metal hydroxide sludge making them less expensive to transport (Rowley et. al., 1994).

1.1 Motivation

An immobilised growth system prevents bacterial washout at high flowrates, and provides a larger surface area for bacterial colonisation, resulting in the potential for increased rates of removal. Previous work on attachment of SRB to surfaces has mainly dealt with heterotrophic growth conditions (Maree and Strydom, 1985, Bass et. al., 1996, Kolmert et. al., 1997). Energy sources for heterotrophic growth of SRB are present in two main forms: organic waste, and bulk chemicals. Both of these types of energy sources may lead to competition between SRB and other bacteria, such as methanogens; whereas SRB can outcompete methanogens under autotrophic conditions. As well, the use of organic waste may lead to secondary pollution concerns while the growth of SRB under autotrophic conditions (CO_2/H_2) does not cause secondary pollutants. Although one study did compare SRB immobilisation under autotrophic conditions, it only compared two materials, pumice and basalt (Van Houten et. al., 1994). This study looks at the growth of SRB to different

types of surfaces, under autotrophic conditions. The intention was to select suitable materials that were rapidly colonised by SRB, and would support high cell densities. In addition, the materials selected should not inhibit the sulphate reduction.

In this project, various support media were examined for their potential to promote rapid bacterial colonisation by determining which physical properties seemed to encourage bacterial adhesion. The following media were selected for comparison: glass beads, molecular sieve, ceramic beads, Teflon-plastic, zeolite, foam, basalt, Ringlace and calcium-alginate immobilised beads. The selection process for these materials is discussed in Chapter Two.

1.2 Layout of the Thesis

Chapter Two covers the literature review section of the thesis. In this section the general environmental conditions that cause acid rock drainage (ARD) will be discussed. Examples of the chemical properties of ARD will be given, followed by a discussion of chemical treatment for ARD; as well as the advantages of metal sulphide precipitates compared to metal hydroxide precipitates. A discussion of biological treatment methods for ARD will next be presented, followed by an overview on SRB. This section covers the general distribution of SRB and aims at explaining the growth conditions selected in this study. The last part of the literature review will include a section on bacterial immobilisation and biofilm formation, specific to anaerobic systems. This will be followed by a summary of the literature review, with the purpose of pointing out some of the gaps in that available data that this project hopes to fill. This will be followed by the objectives of the thesis.

In Chapter Three the methods and materials of the experiments will be discussed. This will include how the SRB were cultured and handled, as well as describing in detail how each experiment was performed, including the experimental protocols for each. The theory on the analysis of the various tests will also be covered in this section of the thesis.

In Chapter Four the results will be presented and discussed. This includes the results of biomass concentration versus time on the support materials and in solution as well as the total biomass. The results of the protein assay are compared with the results from the TKN assay. The measured specific growth rates will be presented and compared with values reported in literature. Results of sulphate reduction will be presented and compared with reported values. The CO_2 uptake rates in the defined and complex media will be stated. The SEM images of the bacteria attached to the surfaces are presented. As well, the experimental procedures will be reviewed for their suitability in this project.

In Chapter Five the conclusions made from this project and recommendations for future work will be presented. The appendices include the raw and calculated data from the experiments.

CHAPTER 2: LITERATURE REVIEW

Heavy metals can be found in acid rock drainage, bottom ashes and flue ashes from incineration processes, and electro-plating or circuit board processing industrial effluent. As well, metal refining sites that process metal sulphides often have groundwater contaminated with both heavy metals and sulphate (Barnes et. al., 1991). Elevated levels of sulphates are present in acid rock drainage due to bacterial oxidation of pyrite. In industrial effluents, sulphates are present from spent sulphuric acid (Van Houten et. al., 1994, Maree and Strydom, 1985, 1987). Sulphate levels in chemical industry effluent can range from 200-50,000 mg/L (Van Houten, 1996).

One of the most conventional treatment methods for the removal of heavy metals is chemical reduction using reducing agents such as sodium sulphide or lime treatment (Sengupta, 1993). Lime treatment produces large volumes of metal hydroxides mixed with gypsum. The large volumes of sludge produced are not recyclable and have increasing disposal costs as waste management laws become stricter (Fujie et. al., 1994, Rowley et. al., 1994). As a result, there is an increasing demand for economically viable and environmentally sound alternatives for managing acid rock drainage and other sulphate containing waste streams.

Although many types of effluents contain high levels of sulphates and metals, ARD from mine sites is one of the largest sources. In the United States over 17,000 km of streambeds are affected by ARD (Elliot et. al., 1998). In Canada, there are approximately 10,000 abandoned mines and 6,000 abandoned tailing sites; and an estimated 875 million tonnes of mining wastes capable of causing ARD (CIELAP, 1996). Because mining has such a large impact, ARD will be considered in more detail in the literature review. The treatment of similar effluents from other sources, while not considered here would be similar.

2.1 Acid Rock Drainage

ARD from mining operations originates from drainage from underground tunnels, surface runoff from open pit mines, and drainage from waste rock and tailings deposits. ARD is caused by the exposure of sulphide ores, mainly pyrite, to air and water which results in the production of acid and high levels of sulphates and dissolved metals in water. Sulphide minerals normally lie beneath the earth where air and water penetration is minimised; under these conditions, the acid generation process has little effect on the ground water. However, when the sulphide containing rocks are exposed to air and water through processes like mining, the acid generation process increases (Sengupta, 1993).

Both chemical and bacterial reactions are involved in the production of ARD. The exclusion of air or moisture to the exposed rocks will stop the acid generation process. Inhibiting bacterial activity can also slow down the rate of acid generation. The quantity of ARD produced is restricted by the amount of acid neutralising minerals present. Calcite, $CaCO_3$, is the most common acid consuming mineral; and it consumes 1-2 moles H^+/mole $CaCO_3$, through the production HCO_3^- and H_2CO_3 (Sengupta, 1993).

In the first step of the reaction process (that produces ARD), iron sulphide is oxidised to dissolved iron (ferrous), sulphate and hydrogen ions. The formation of the hydrogen ions decreases the pH of the water. If enough oxygen is present in the water, the ferrous ion then oxidises to ferric iron. When the pH of the environment is greater than about 3.5, the ferric iron will precipitate out as iron hydroxide while further decreasing the pH. Any ferric iron that does not precipitate out can facilitate the oxidation of more iron sulphide, thereby generating more ferrous iron, sulphate and hydrogen ions.

Certain iron and sulphur oxidizing bacteria species can accelerate the rate of the reaction by increasing the rate of the ferrous-iron oxidation step. The most commonly associated bacteria with ARD generation are *Thiobacillus ferrooxidans*. They can increase the rate of acid formation by up to a factor of five (Sengupta, 1993). The reactions which cause ARD are shown below (Sengupta, 1993):

$$FeS_2 + 7/2O_2 + H_2O \rightarrow Fe^{2+} + 2SO_4^{2-} + 2H^+ \qquad (2.1)$$

$$Fe^{2+} + 1/2O_2 + H^+ \leftrightarrow Fe^{3+} + 1/2H_2O \qquad (2.2)$$

$$Fe^{3+} + 3H_2O \leftrightarrow Fe(OH)_3\downarrow + 3H^+ \qquad (2.3)$$

$$FeS_2 + 14Fe^{3+} + 8H_2O \rightarrow 15Fe^{2+} + 2SO_4^{2-} + 16H^+ \qquad (2.4)$$

Overall Reaction:
$$FeS_2 + 15/4O_2 + 7/2O_2 \rightarrow Fe(OH)_3\downarrow + 2SO_4^{2-} + 4H^+ \qquad (2.5)$$
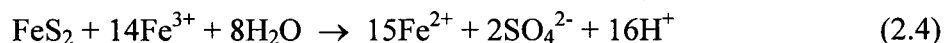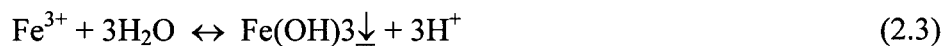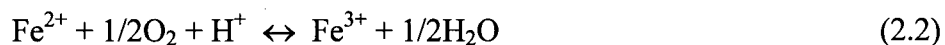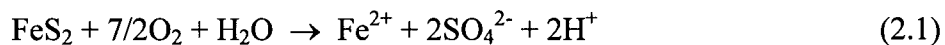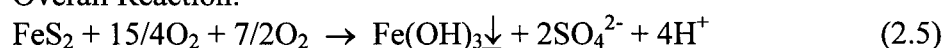
Acid rock drainage from the tailings and waste rock produced by mining operations are often low in pH and high in metal concentrations due to microbial, chemical and hydrological processes that act on the waste. The acid environment tends to mobilise metals which are usually toxic to biota, in addition the acidic conditions are less favourable than near-neutral pH growth conditions for many organisms (Ledin and Pederson, 1996). Examples of the chemical properties of ARD are given in Table 2.1.

Table 2.1: Examples of ARD Water Quality

Measurement (mg/L) except pH	Seepage from an Abandoned Uranium Mine Tailings Pond (Ontario)	Seepage from a Silver Mine Waste Rock Pile (British Columbia)	Mine Water from an Underground Copper Mine (British Columbia)
pH	2.0	2.8	3.5
Sulphate	7440	7650	1500
Acidity	14600	43000	---
Iron	3200	1190	10.6
Manganese	5.6	78.3	6.4
Copper	3.6	89.8	16.5
Aluminium	588	359	---
Lead	0.67	2	0.1
Cadmium	0.05	0.5	0.143
Zinc	11.4	53.2	28.5
Arsenic	0.74	25	0.05
Nickel	3.2	8.0	0.06

(Source: Sengupta, 1993)

Once a mine site is decommissioned, the problems associated with ARD do not stop. This is because acidic drainage is still produced by rainwater and groundwater infiltrating the mine site. Two brief site descriptions of decommissioned mines with ARD drainage are given below. The purpose of describing the sites is to show the levels of contaminants contained within their respective drainage waters and to illustrate that these waters require treatment. It is the existence of such mining sites that helps provide the motivation for looking at economical ways to treat ARD.

The Berkley Pit

The Berkley Pit is perhaps one of the best examples of ARD in North America. It is an abandoned open pit mine in Butte, Montana. Before 1983, it produced over 20 billion lbs. of copper, 4.9 billion lbs. of zinc, 3.7 billion lbs. of manganese, and 2.9 million oz of gold. Since 1982, the pit has been filling with water. The Berkley Pit is the highest acid producing mine in the United States. The pit water has a pH $\cong$ 2.7 near the surface of the water, a sulphate concentration of 4850 mg/L and concentrations of metals ranging from 433 mg/L copper, 202 mg/L total iron, 212 mg/L zinc, and 153 mg/L magnesium (Sengupta, 1993). These levels will increase with depth in the pit, partially due to the formation of hydroxide species which form solid particles and sink toward the bottom of the pit; as they fall any ions adsorbed to the hydroxide floc will sink as well.

About 40% of the water flow into the Berkley Pit is from underground mines while the remaining 60% stems from surface sources. By the early 1990's, the water depth in the pit was 213 meters. At its present rate of water infiltration, the pit is expected to start overflowing in 2011. Clearly, the Berkley Pit is an example of a mine site that requires a major practical process for the treatment of acidic pit water before it starts overflowing and damaging the surrounding environment.

The Britannia Mine

The Britannia mine is considered to be the worst source of metal contamination in North America by Environment Canada (Vancouver Sun, 1996). The Britannia mine is located

50 km north of Vancouver, BC. Approximately 48,000,000 tonnes of ore was mined for copper, silver, zinc, and gold between 1905-1973. Unlike the Berkley Pit, the Britannia mine is mainly underground with over 160 km of mine shafts and tunnels. There are three main access portals to the mine: 2200, 2700, and 4100 adits. The 2200 and 2700 were sealed off at the time of the mine closure to route mine drainage to a single outlet that would discharge at depth into Howe Sound.

Currently all three portals have some drainage that discharges to the surrounding environment. The drainage from the 2700 portal is not considered an environmental problem. The 2200 portal has flow rates ranging from 0-10,000,000 L/d, with copper levels up to 120 mg/L, zinc 50 mg/L, cadmium 0.4 mg/L, iron 60 mg/L, aluminium 74 mg/L and sulphate concentrations ranging from 200 to 2000 mg/L with a pH of 2 to 4. The 2200 drains into a freshwater creek and raises the copper level to toxic concentrations for fish. The 4100 portal drainage ranges from 4,000,000 to 40,000,000 l/d, with copper and zinc levels from 12-28 mg/L, cadmium 0.1 mg/L, and iron and aluminium 30 mg/L. The sulphate concentration ranges from 1200-1800 mg/L with a pH of 3 to 4.

Despite it's reputation as one the worst metal contaminated sites in North America, along with the adverse impact the drainage water has on aquatic life in local stream beds, as well as pilot plant tests run by a local Vancouver Company (1996) looking at both lime treatment and a combined chemical/biological treatment, there was still no active treatment occurring at the Britannia Mine as of September 1999 (Rowley et. al., 1997).

2.2 Treatment Options

Preventing the formation of ARD is the preferred option to actually treating ARD. In newer mines this is facilitated by the use of covers, the addition of chemicals to the waste rock pile, and subaqueous disposal (Ledin and Pederson, 1996, Sengupta, 1993). However, in cases where these methods have not been implemented it is necessary to treat the ARD directly. This is most commonly accomplished through the addition of chemicals to raise the pH of the mine water and precipitate out the metals as hydroxides. Other, more recent methods include the use of natural and artificial wetlands which take advantage of bacterial sulphate reduction, and microbial metal accumulation; and the use of sulphate reducing bacteria bioreactors (Ledin and Pederson, 1996, Barnes et. al., 1991, Webb et. al., 1998).

The use of chemical treatment as an option and some of the limits associated with this method are compared below to the potential of biological treatment with SRB. A brief comment on the use of wetlands will be mentioned followed by a review of a SRB bioreactor treatment system that is being used to treat the groundwater of a metal refining site.

2.2.1 Chemical Treatment

Chemical treatment of mine waters involves the additions of chemicals such as lime, limestone, sodium carbonate and/or sodium hydroxide. This raises pH of the water and results in the metals precipitating out as metal-hydroxides. The disadvantage to this method is that large volumes of sludge are produced composed mainly of calcium sulphate and metal hydroxide.

In general, lime neutralisation is popular because (Murdock et. al., 1994):

- it can treat a wide range of acidities and flowrates,
- it is easy to handle and inexpensive,
- it is a proven technology with moderate operating costs.

10

The general precipitation reactions for metal hydroxides are:

$$M^{2+} + SO_4^{2-} + Ca^{2+} + 2OH^- + H_2O \rightarrow M(OH)_2\downarrow + CaSO_4\bullet2H_2O\downarrow \qquad (2.6)$$

$$2M^{3+} + 3SO_4^{2-} + 3Ca^{2+} + 6OH^- + H_2O \rightarrow 2M(OH)_3\downarrow + 3CaSO_4\bullet2H_2O\downarrow \quad (2.7)$$
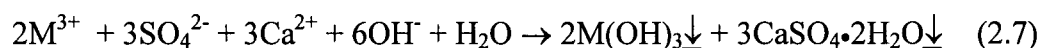
In the above reactions, it can be observed that both metal hydroxides and calcium sulphate dihydrate (gypsum) precipitate out of solution. The additional precipitation of gypsum increases the volume, and cost, of sludge that requires disposal.

The precipitation of metal hydroxides is a function of the solubility of the metal species, which is affected by pH. Metals such as Fe^{3+}, Sn^{2+}, and Hg^{2+} will readily precipitate at low pH (3-4), while others such as Al^{3+}, Cu^{2+}, and Pb^{2+} precipitate at a slightly higher pH (5-6). An even higher pH is required to precipitate metals such Fe^{2+}, Zn^{2+}, Cd^{2+} and Ni^{2+}. The solubility of various metal sulphides as a function of pH is shown in Figure 2.1, and the solubility of various metal hydroxides as a function of pH is shown in Figure 2.2. These figures indicate that it might be possible to remove some metals more readily as sulphides (including Cd, Cu, Fe, Pb, Ni, Ag, and Zn) at lower pH values.

Table 2.2: K_{SP} Values of Various Metals in Water (pH = 7.0)

Metal	Ksp, as a hydroxide	Ksp, as a sulphide
Cadmium	2×10^{-14}	3.6×10^{-29}
Copper	2×10^{-19}	8.5×10^{-36}
Iron	1.1×10^{-36} (Fe^{3+})/2×10^{-15} (Fe^{2+})	3.7×10^{-19}
Lead	2.5×10^{-16}	7×10^{-27}
Nickel	2×10^{-16}	2×10^{-21}
Silver	---	2×10^{-49}
Zinc	4.5×10^{-23}	1.2×10^{-23}

Source(Brady and Humiston, 1986, Sawyer, McCarty et al., 1978)

Compared in Table 2.2 are the Ksp values of various metal hydroxides and metal sulphides at neutral pH. The Ksp value of sulphide precipitates is generally lower than that of the respective metal hydroxides, this indicates that the sulphide precipitates are less soluble than

their metal hydroxide precipitates. For instance, the solubility of $Cd(OH)_2$ and CdS in pure water can be calculated as follows:

$$Cd(OH)_2 \leftrightarrow Cd^{2+} + 2OH^- \qquad Ksp = 2x10^{-14} \qquad (2.8)$$
$$2x10^{-14} = X \qquad (2X)^2$$
$$[Cd^{2+}] = X = ((2x10^{-14})/4)^{1/3} = 1.7x10^{-5} \, M = 1.9 \, mg/L$$

$$CdS \leftrightarrow Cd^{2+} + S^{2-} \qquad Ksp = 3.6x10^{-29} \qquad (2.9)$$
$$3.6x10^{-29} = X \qquad (2X)^2$$
$$[Cd^{2+}] = X = ((3.6x10^{-29})/4)^{1/3} = 2.1X10^{-10} \, M = 2.3 \, x10^{-5} \, mg/L$$
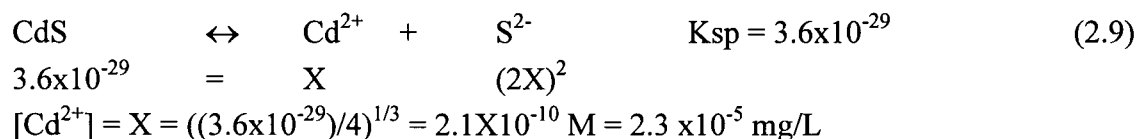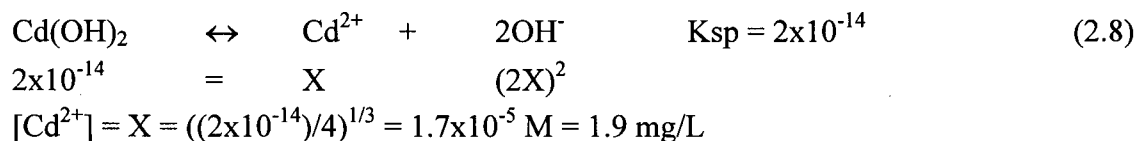
It is clear, from the above calculations that the level of cadmium in solution after precipitation with sulphide is significantly less than its hydroxide counterpart.
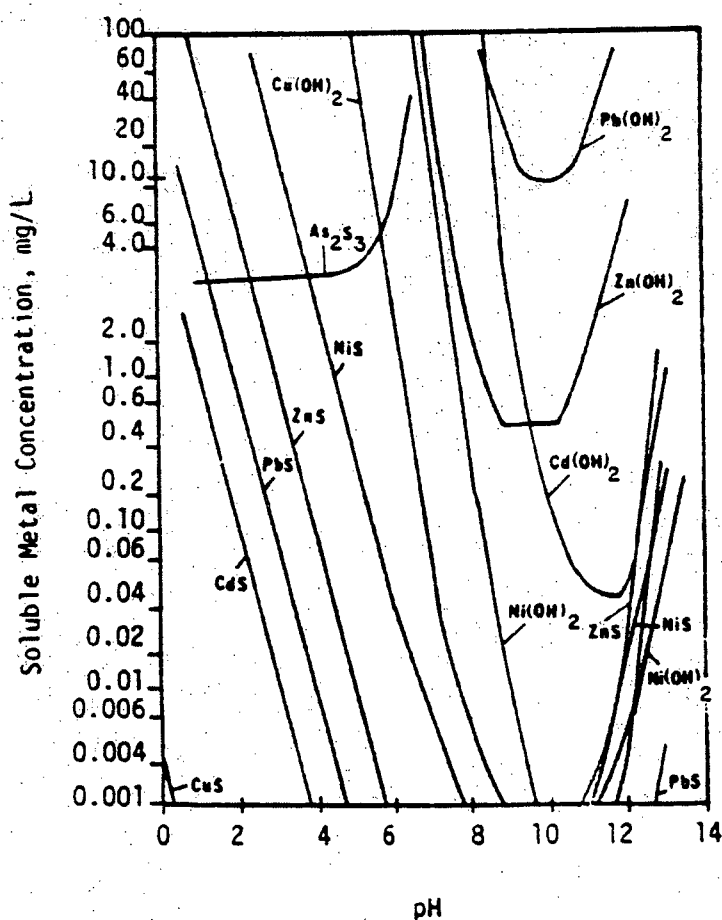
Figure 2.1: Sulphide Precipitation Diagram.
(Source: Peters and Ku, 1985)

12
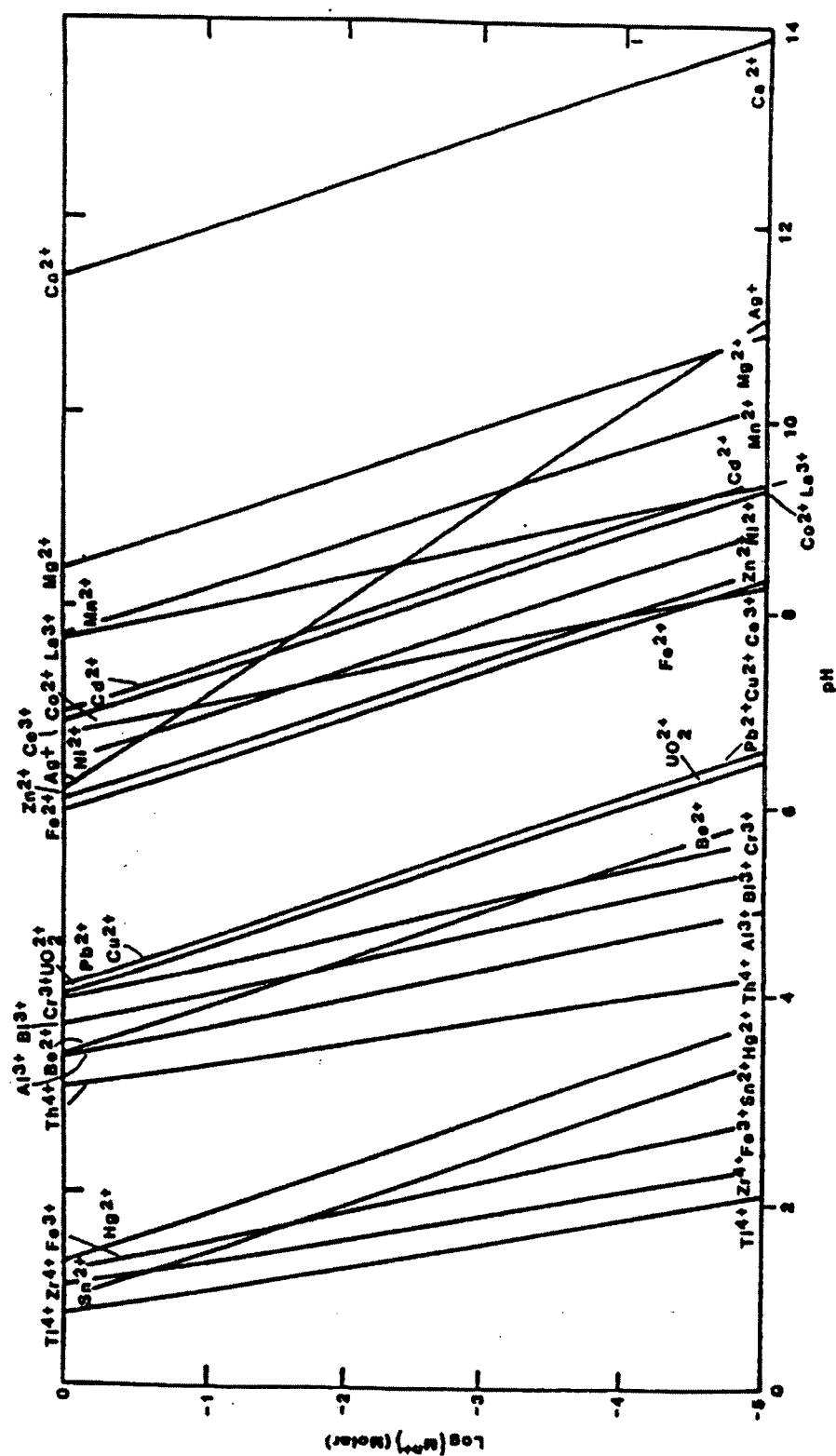
Figure 2.2: Metal Hydroxide Precipitation Diagram.
(Source: Monhemius, A.J., 1977)

As mentioned earlier, many traditional treatment techniques for removal of heavy metals from effluent streams rely on the formation of metal hydroxide precipitates. However, in systems where sulphate is available, the formation of metal sulphides over metal hydroxides has many advantages (De Vegt et. al., 1995, Rowley et. al., 1994, Hammack et. al., 1994):

- Metal sulphides form more rapidly than metal hydroxides, and form a denser sludge.
- Metal sulphides are less soluble (lower Ksp) than metal hydroxides.
- Metal sulphide precipitates are more stable over a wider pH range than metal hydroxides.

2.2.2 Passive Treatment

The use of natural and constructed wetlands, which take advantage of natural microbial processes, is a passive biological option for the treatment of ARD. Wetlands are stagnant, anoxic ponds that contain a variety of plant species such as cattails and mosses (Ledin and Pederson, 1996). Metals can be immobilised by sulphate reducing bacteria and/or by plant root uptake. In addition, the ARD tends to be neutralised and is diluted within the wetland. A schematic of a wetland type treatment is shown in Figure 2.3.
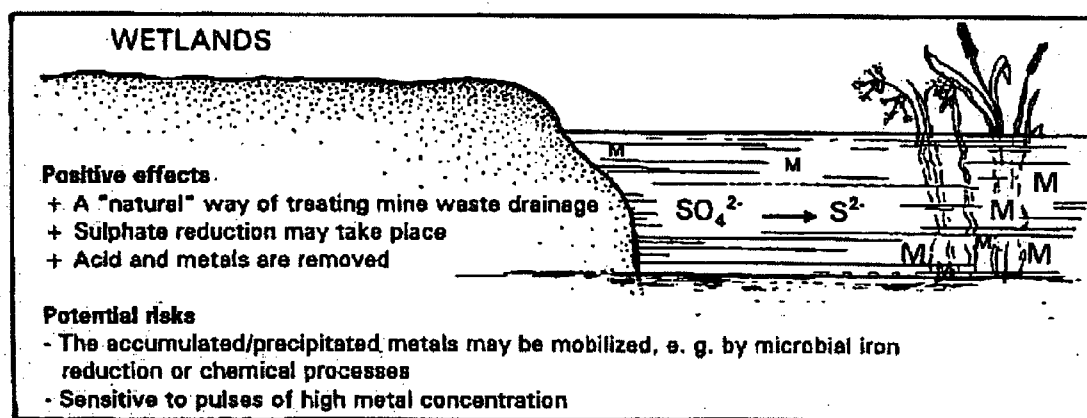
Figure 2.3: Wetlands for ARD Treatment.
(Source: Ledin and Pederson, 1996)

Wetlands can increase the alkalinity of ARD and remove metals through plant uptake, sorption onto organic material, metal hydrolysis, and biological sulphate reduction. Wetlands

14

are considered a low cost, passive treatment method but the utilisation of wetlands may be limited in colder areas where bacterial processes are inhibited at low temperatures. Wetlands are most effective for treating low flow ARD that is not highly acidic but still contains high levels of metals (Hackl, 1997).

2.2.3 Ex-situ Biological Processes

The advantages of metal sulphide precipitates over metal hydroxide precipitates were discussed in Section 2.2.1 from a chemical perspective. However, a biological process, which converts sulphate to sulphides would prevent the need to add sulphate as a chemical to remove metals (Uhrie et. al., 1996). In fact, the possibility of a biological reactor containing SRB to treat ARD has been studied previously (Tuttle et al., 1969, Maree and Strydom, 1985, 1987, Barnes et. al., 1991). These systems all used complex organics as a carbon source for the bacteria present. More recently, the potential of SRB bioreactors using autotrophic growth conditions has been studied (Du Preez et. al., 1992, Van Houten et. al., 1994, 1996). However, these studies were all completed at bench scale level. The Paques UASB Process, described in this section, is the first full scale system to utilise a SRB bioreactor for the treatment of heavy metal, high sulphate containing effluent (Barnes et al., 1991, De Vegt and Buisman, 1995).

The Paques UASB Process

Sulphate reducing bacteria have been used to treat groundwater contaminated with heavy metals and high sulphate levels from a zinc refinery in Budelco, the Netherlands. The composition of the groundwater at the Budelco refinery site is shown in Table 2.3. As mentioned previously, the SRB will convert the sulphate to sulphide, which will then react with the metals in solution and precipitate out as a metal sulphide. The overall reaction can be represented as:

Metal Sulphate + Carbon Substrate $\rightarrow$ Metal Sulphide$\downarrow$ + CO_2 + H_2O + Biomass (2.10)
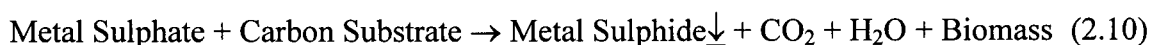
This process uses an upflow anaerobic sludge blanket (UASB) reactor to treat the groundwater. It has been shown to withstand large changes in the influent composition and can rapidly recover from process upsets. The metal sulphide sludge produced from this system can be recycled to the front end of the metal refinery to recover both the metals and convert the sulphide to saleable sulphur.

The bioreactor is capable of operation under non-sterile conditions since the sulphide produced by the SRB is an inhibitor for other microorganisms. The main competitor with SRB is methanogens. However, at the high sulphate levels present in the Budelco groundwater, the SRB can outcompete the methanogens helping to control their numbers.

Table 2.3: Ground Water Analysis of Budelco Zinc Refinery

Component	Concentration (mg/L)
Sulphate	1300
Zinc	135
Cadmium	1.5
Copper	0.8
Cobalt	0.1
Iron	4
Calcium	320
Ammonium	1

(Source: Barnes et. al., 1991)

Shown in Figure 2.4 is a schematic of the biological treatment process. The process includes an influent buffer tank, feed tanks for nutrients, ethanol, alkali and a flocculent. An inline mixer is included to promote mixing of the various feeds with the influent before entering the reactor. An inline heater exchanger is used to test the process at different temperatures. A stripper is included to remove hydrogen sulphide from the gas product stream and soluble sulphide from the aqueous stream.

The flocculent is required to prevent bacterial washout at residence times less than 30 hours. It promotes the formation of bacterial flocs, which will have a heavier mass than free suspended cells, allowing for an increased flowrate through the system (shorter residence time) before washout occurs.

The process uses ethanol as a feed source for the SRB. SRB do not completely oxidise ethanol, and acetate is a by-product of this reaction. Although SRB can then oxidise acetate to CO_2, the degradation is at a slower rate than that of ethanol leading to an accumulation of acetate in the system. At high concentrations of acetate, SRB growth becomes inhibited. To overcome this problem the Budelco site encouraged the growth of methanogens, which can completely degrade the acetate. The methanogen growth was accomplished by adding methanol to the system, as methanogens will outcompete SRB for this food source.
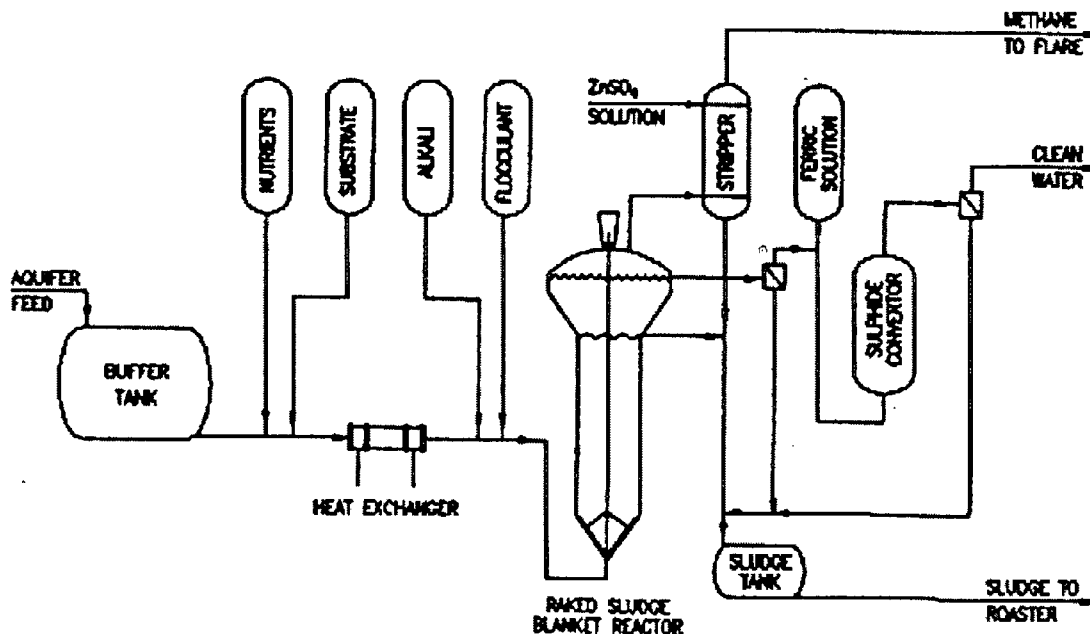
Figure 2.4: Paques UASB Process Pilot Plant.
(Source: Barnes et. al., 1991)

The groundwater pH is around 4.5, so an alkali tank is used to help maintain the pH near neutral in the reactor since SRB have an optimal growth at around pH 7.5, although they are capable of growth from around pH 5-9. The carbonate and sulphide byproducts produced by SRB also help to provide buffering to the system.

17

Shown in Table 2.4 are the results from the full scale demonstration plant. The Paques UASB process demonstrates that SRB can be used to effectively treat contaminated groundwater from the refinery. The final plant design includes a tilted plate settler and a sand filter to provide final polishing to the effluent and lower the final zinc concentration to 0.05-0.15 mg/L.

Table 2.4: Budelco Full Scale Plant Results (initial trials)

Component	Influent (mg/L)	Effluent (mg/L)	Percentage Removal %
Sulphate	1200	160	86.7
Zinc	230	0.3	98.7
Cadmium	1.2	<0.01	99.2
Iron	54	2	96.3
Lead	9	.02	99.8
Copper	2.1	0.03	98.6
Cobalt	0.2	0.02	90

(Source: De Vegt and Buisman, 1995)

The two main problems encountered in this system were the formation of acetate as a byproduct of SRB ethanol oxidation and bacterial washout. Methanogens were introduced into the system to counteract the first problem. The other problem encountered using the sludge blanket system was overcome by adding a flocculent to the system in order to decrease bacteria washout at residence times below 30 hours.

2.3 SRB Overview

2.3.1 The Sulphur Cycle

The three oxidation states of sulphur found in nature are -2 (sulphides), 0 (elemental sulphur), and +6 (sulphate). The change in oxidation states of sulphur is mainly mediated through microbial processes. Shown in Figure 2.5 is the microbial mediated sulphur cycle as well as the aerobic and anaerobic environments required for each stage to occur.
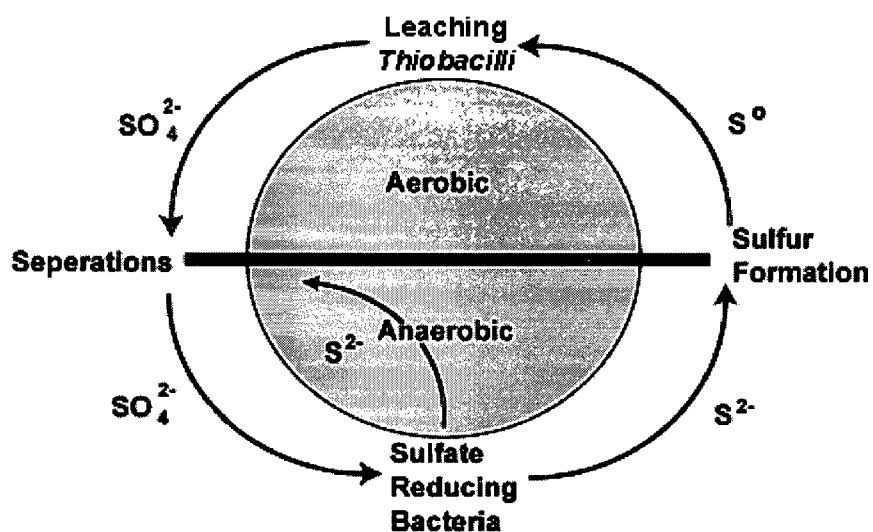
Figure 2.5: Microbial Mediated Sulphur Cycle.
(Source: Van Houten, 1996)

The majority of sulphur is found in the form of sulphate and sulphide in minerals such as gypsum, $CaSO_4.2H_2O$, and pyrite, FeS_2, or iron sulphide. These minerals are mainly present in sediments and rocks, below the surface of the earth. Sulphide is present in the following equilibrium states:

$$H_2S \leftrightarrow HS^- \leftrightarrow S^{2-} \qquad (2.11)$$

low pH   neutral pH   high pH

Below a pH of 6, H_2S predominates, while above a pH of 6, HS^- and S^{2-} are the main species. The latter are highly soluble in water, whereas H_2S is not and easily volatilises into the gas phase and is typically recognised for its unpleasant rotten egg like odour.

Under aerobic conditions at neutral pH, sulphide rapidly oxidises to sulphur, although the reaction is catalysed by the presence of sulphur oxidizing bacteria. Since this reaction takes place spontaneously, bacterial mediated steps usually occur when H_2S is rising from sediment and crosses the anoxic/oxic boundary. Elemental sulphur is chemically stable but can be oxidised by sulphur oxidizing bacteria to sulphate. The sulphate ion is chemically very stable, under normal environmental conditions, and does not reduce easily. However, under anaerobic conditions, sulphate reducing bacteria can reduce sulphate ions to sulphide (Madigan et. al., 1996).

2.3.2 Distribution of SRB

SRB can be found in a vast variety of places including soils, fresh water, marine water, hot springs and geothermal areas, oil and gas reservoirs, estuarine muds, sewage, corroding iron, and sheep rumen. They can tolerate temperatures ranging from -5 to $75°C$ and pH values ranging from 5 to 9 (Perry, 1995). In fact, SRB activity has been noted in ARD with pH values of 3-4, although it is possible that the SRB were actually in microniches with higher pH values (Widdel, 1988, Elliot et. al., 1998). Most SRB can also utilise sulphite and thiosulphite as electron acceptors in addition to sulphate (Cypionka and Pfennig, 1986). Some SRB have been observed using nitrate and fumarate as electron acceptors under sulphate limiting conditions (Widdel, 1988).

2.3.3 Cultivation and Media

All SRB are anaerobic bacteria and most are gram negative (Middleton and Lawrence, 1977). Growth of SRB occurs in the absence of oxygen, although they may survive a temporary exposure to oxygen and then become active again if anaerobic conditions are reestablished

(Widdel, 1988). Gram-negative mesophilic SRB can be grown in a defined media without complex nutrients such as yeast extract or peptone, although they can be used to stimulate the growth of a number of SRB species (Widdel and Bak, 1992). It is recommended that SRB be kept in the dark to prevent the growth of photosynthetic sulphur bacteria; as these bacteria can alter the redox potential of the system to the disadvantage of the SRB. Also, some SRB are light sensitive and display inhibited growth during exposure (Widdel and Bak, 1992).

2.3.4 Electron Donors

SRB fall into two general categories: incomplete and complete oxidisers. Complete oxidisers reduce organic compounds to CO_2 and incomplete oxidisers reduce organic compounds to acetate and CO_2 (Odom, 1993). SRB and methanogens often compete with one another for the use of electron donors as they can both utilise many of the same electron donors (Song et. al., 1988). However, SRB can often outcompete methanogens under limiting electron donor availability conditions (Vroblesky et. al., 1996).

SRB can utilise a variety of compounds as electron donors, and, in general use sulphate as a terminal electron acceptor. Electron donor sources are usually restricted to low molecular weight organic compounds such as acetate, lactate, ethanol and butyrate. Often these compounds are the fermentative products from other anaerobic bacterial processes but some species can also grow with hydrogen. The main groups of electron donors utilised by SRB are (Widdel, 1988):

- Lactate
- Hydrogen
- Formate
- Acetate
- Propionate
- Butyrate and Higher Straight-Chain Fatty Acids
- Branched Chain Fatty Acids
- Monovalent Acids
- Dicarboxylic Acids
- Hydrocarbons (lactate, ethanol).

The reactions, of the most common selected electron sources can be summarised as follows (Van Houten, 1996):

Butyrate + $\frac{1}{2}SO_4^{2-} \rightarrow$ 2Acetate + $\frac{1}{2}HS + \frac{1}{2}H^+$	$\Delta G^o = -27.8$	(2.12)
$4H_2 + SO_4^{2-} + 2H^+ \rightarrow 4H_2O + H_2S$	$\Delta G^o = -38.1$	(2.13)
Acetate + $SO_4^{2-} \rightarrow 2HCO_3^- + HS^-$	$\Delta G^o = -47.6$	(2.14)
Lactate + $\frac{1}{2}SO_4^{2-} \rightarrow$ Acetate + $HCO_3^- + \frac{1}{2}HS + \frac{1}{2}H^+$	$\Delta G^o = -80.0$	(2.15)
Ethanol + $\frac{1}{2}SO_4^{2-} \rightarrow$ Acetate + $\frac{1}{2}HS + \frac{1}{2}H^+ + H_2O$	$\Delta G^o = -80.0$	(2.16)
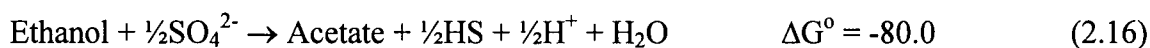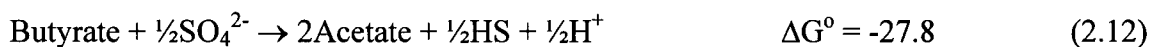
(G^o values from Thauer, 1977)

As shown above, ethanol is more energetically favourable for the SRB than hydrogen, and as such SRB may grow faster with ethanol as a feed substrate. However, other concerns that need to be considered when selecting an electron donor are the cost of the electron donor/sulphate removed and the formation of any secondary pollutants that may need to be treated (Du Preez et. al., 1992).

Carbon and Energy Sources

Listed in Table 2.5 are carbon and energy sources that have been studied for industrial applications using SRB. These sources can be divided up into two main groups: organic waste material and bulk chemicals.

Organic waste materials are not considered a suitable carbon and electron source as these materials can introduce additional pollution to the heavy metal contaminated wastewater. ARD does not contain organic compounds, and so the addition of organic waste will require a secondary treatment process to remove any remaining pollutants in order to produce a clean effluent (Van Houten, 1996). A study using sewage sludge, molasses, pulp mill wastewater, had difficulty in removing all of the COD from the wastewater (Maree and Strydom, 1985). Organic waste is also comprised of a variety of compounds, such as alcohols, and lower fatty acids. These compounds are used by SRB, methanogens, and acetogens, which may result in competition between these three bacteria types in the reactor (Van Houten, 1996).

Table 2.5: Summary of Carbon/Energy Sources used in Previous Studies

Carbon/Energy Source	Comments	Source
Organic Waste Material		
Sugar, Molasses, Pulp Mill Wastewater, Sewage Sludge	Molasses may be cheaper to use than lactate or ethanol. Difficulty in removing COD to required levels.	Maree and Strydom, 1985, 1987 Groudeva and Groudev, 1994
Mixed carbon sources: organic pollutants with high COD (~2500 mg/L) + yeast extract + sugar	May need to use a pre-fermentation step, mixed populations of bacteria present.	Visser et. al., 1993 Fujie et. al., 1994
Bulk Chemicals		
Acetate	Bypasses the ethanol degradation step limited by slow degradation of acetate. Slower growth than with ethanol	Allaoui and Forster, 1994
Ethanol and methanol (90% EtOH/10%MeOH)	Acetate forms as a byproduct of ethanol degradation, which is then further converted to CO_2, CH_4 and methane (through the addition of methanogens).	Barnes et. al., 1991 Rowley et. al., 1994
0.8% Lactate	-----	Barnes et. al., 1991 Diels et. al., 1991
0/20/80% CO/CO_2H_2 5/15/80% CO/CO_2H_2 20/0/80% CO/CO_2H_2	SRB outcompete methanogens for hydrogen. No toxic affects if use CO_2/H_2 only.	Du Preez et. al., 1992 Van Houten et. al., 1994, 1996

Bulk chemicals, are more advantageous to use than organic waste, primarily because there is no secondary pollution that requires treatment. Both ethanol and lactate represent substrates that support fast growth of SRB. (Widdel and Hansen, 1991, Postgate, 1994). However, both substrates are rapidly oxidised to acetate. This represents two disadvantages, firstly, acetate is toxic at high concentration to SRB and it is oxidised at a slower rate than either, ethanol and lactate. Therefore, it is possible that the environment will become toxic to the SRB. Secondly, methanogens use acetate, and competition between the two species may arise (Van Houten, 1996).

Another possible bulk chemical source is mixtures of CO, CO_2 and H_2, also known as synthesis gas, which has been demonstrated to be a viable carbon and electron donor source (Du Preez et. al., 1992, Van Houten et al., 1994). SRB have been shown to outcompete methanogens for hydrogen (Vroblesky, 1996). It has also been demonstrated that for larger scale reactors CO_2/H_2 mixtures become more cost effective than using an ethanol based

energy source (refer to Figure 2.6); this was accomplished by comparing the cost of H_2 and ethanol required to treat a theoretical waste stream (Van Houten, 1996). The following assumptions were made in this comparison: a 1:1 and 2:3 ratio of moles ethanol /mole sulphate reduced, that greater than -10 kmol sulphate/hour were to be treated, and that 20 kmol/hour ethanol and 80 kmol/hour hydrogen were required. Synthesis gas can be obtained as an industrial off-gas from (1) the heating plants of steam and methane industries, (2) the partial oxidation of fuel oil, and (3) from coal gasification. (Du Preez et. al., 1992):
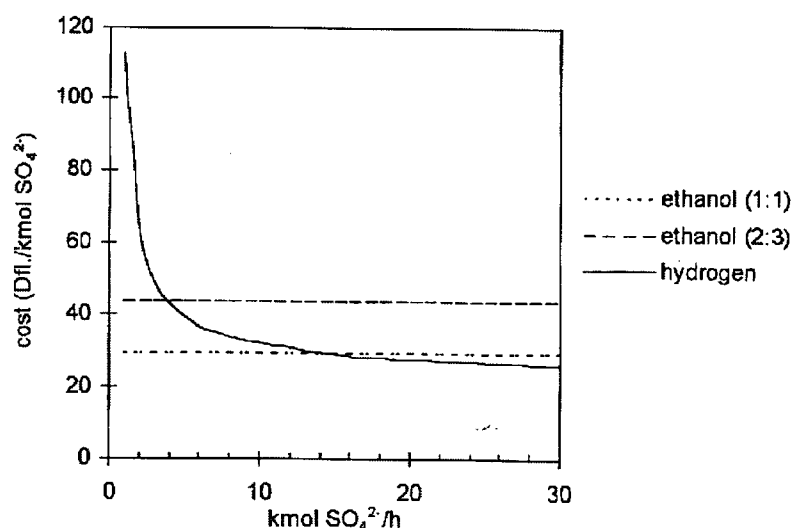
Figure 2.6: Ethanol vs. Hydrogen as Electron Donor Source for SRB.
(Source: Van Houten, 1996)

Synthesis Gas

Van Houten completed a Ph.D. thesis on biological sulphate reduction using synthesis gas in a gas lift reactor (Van Houten, 1996). The reactor configuration is shown in Figure 2.7. This project was divided into three main studies. In the first two parts, H_2/CO_2 were used as the carbon and energy source, while the last part of the study looked at the effects of CO on SRB activity in the gas lift reactor.

The first part studied the growth of SRB on hydrogen and carbon dioxide (80/20% v/v). The purpose of this study was to investigate the feasibility of sulphate reduction in a gas-lift (expanded bed) reactor using immobilised biomass grown on H_2/CO_2 (80/20% v/v). The effect of free H_2S on biomass growth was also investigated. Pumice and basalt were compared for their potential as immobilisation surfaces, during operation of the reactor. No biofilm growth was noted on basalt particles, although the SRB were found to form a stable biofilm on the pumice within 15 days of operation, under turbulent flow conditions. This was attributed to difference in the surfaces of the basalt and pumice. The pumice had large pores, which the SRB were able to colonise and then spread out across the pumice surface. In contrast, the lack of deep pores on the basalt, thus as the bacteria attempt to adhere to the basalt surface, high turbulence and abrasion from other particle knocks the bacteria from the basalt surface. SRB growth was found up to free H_2S concentrations of 450 mg/L; below this concentration a maximum sulphate conversion of 1250 mg/(L.h) was obtained with values ranging from 583 – 1250 mg/(L.h).
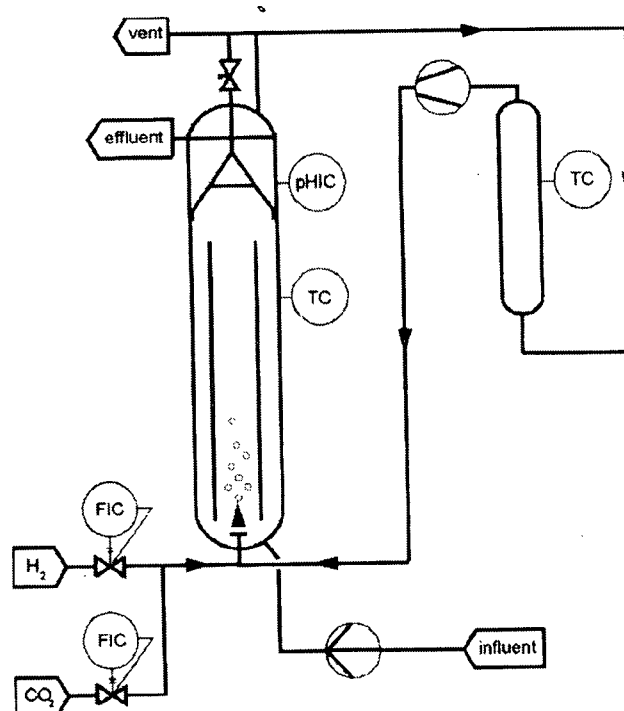
Figure 2.7: Gas Lift Reactor used by Van Houten
(Source: Van Houten, 1996)

The second study investigated the affect of pH on SRB activity, as well as examining the bacterial morphology in the reactor. Bioreactor operation was possible within a pH range of 5.5-8.0 with an optimal pH of 7.5, within this pH range the sulphate conversion rates varied between 4.2–2.1 g SO_4/g biomass per day within this pH range. The bacterial types in the reactor were found to consist of *Desulfovibrio* species. and *Acetobacterium* species.

Since synthesis gas, consists of H_2, CO_2, and CO, the third study investigated the affects of carbon monoxide on sulphate reduction. The H_2 level was kept constant in the reactor while the CO_2 and CO levels were changed. Inhibition of SRB activity was noted at 5%CO, which resulted in a decrease in sulphate reduction from 12-14 g SO_4/(L.d) to 6-8 g SO_4/(L.d). Increasing the CO levels up to 20% was not found to further decrease the sulphate reduction rate, it was also found that adding a recycle loop to the reactor increased the conversion up to 10 g SO_4/(L.d).

2.3.5 Hydrogen Utilising SRB Species

SRB can grow both autotrophically and heterotrophically on hydrogen. For instance *Desulfovibrio* species require acetate as a carbon source while *Desulfobacterium* species can use CO_2 as the carbon source (Van Houten, 1996). *Desulfovibrio* are usually curved and often motile, they can use H_2 but require acetate in addition to CO_2 as a carbon source for growth. *Desulfobulbus* species are generally oval shaped although some types form slender rods. They can grow with H_2 as an electron donor and CO_2 as their carbon source. *Desulfobacterium* species are a nutritionally versatile completely oxidizing SRB, capable of autotrophic growth. They range in shape from rods to ovals to nearly spherical shaped cells. A summary of hydrogen utilising SRB is listed in Table 2.6.

Table 2.6: Hydrogen Utilising SRB

Species	Morphology	Width μm	Length μm	Optimum Temp, °C	Hydrogen Utiliser	Spore Formers
[1]*Desulfotomaculumn*						
nigrificans	Rod	0.5-0.7	2-4	55	+	+
orientis	Rod, slightly curved	0.7-1	3-5	37	+	+
ruminis	Rod	0.5-0.7	4-6	37	+	+
[1]*Desulfovibrio*						
desulphuricans	Vibrio	0.5-0.8	1.5-4	30-36	+	-
vulgaris	Vibrio	0.5-0.8	1.5-4	30-36	+	-
gigas	Large Vibrio	0.8-1	6-11	30-36	+	-
africanus	Vibrio	0.5-0.6	2-3	30-36	+	-
salexigens	Vibrio	0.5-0.8	2-3	30-36	+	-
[1]*Desulfobacter*						
hydrogenophilus	Rod	1-1.3	2-3	28-32	+	-
curvatus	Vibrio	0.5-1	1.7-3.5	28-32	+, poorly	-
[2]*Desulfobacterium*						
autotrophicum	Oval	0.9-1-3	1.5-3	20-26	+	-
macestii	Rod	0.7	1.9-2	35	+	-
[1]*niacini*	Spheroid	1.5	3	29	+	-
[2]*Desulfosarcina*						
variabilis	Oval or Rod	1-1.5	1.5-2.5	33	+	-

(Source: [1] Widdel, 1988, [2] Widdel and Bak, 1992)

Few microbial species can use hydrogen for growth, they include sulphur reducers, denitrifying bacteria, methane bacteria and homoacetogenic bacteria (Widdel, 1988). Methanogens and SRB both compete for hydrogen in anaerobic systems. However, in systems with sufficient sulphate (non-limiting), SRB will outcompete the methanogens as they have a higher substrate affinity for hydrogen. SRB can also maintain the hydrogen threshold value below that able to be utilised by methanogens (Lens and Visser, 1998). *Desulfovibrio* species can grow relatively fast on hydrogen, *Desulfotomaculumn* species, and *Desulfobus* species can also grow on hydrogen but at slower rates than the *Desulfovibrio* species (Schink, 1988).

Temperature, pH, and Micronutrients

Shown in Table 2.7 is a summary of some of the conditions utilised in previous studies for SRB growth, including temperature and pH. All studies required that nitrogen and phosphorous be present in the nutrient solution to ensure growth of the bacteria. As well, a low redox potential varying between −100 to −350 mV was noted as a requirement for SRB growth.

Table 2.7: Temperature and pH Conditions used in Previous Studies

Temperature, °C	pH	Population and *Redox Potential	Nutrients Added	Source
T = 15-40	5–9	SRB and Mixed E (SRB)= - 100 mV E (Mixed) = - 300 mV	N >5%, P >0.2% of the ethanol consumed	Barnes et. al., 1991
T = 20-38	7-7.7	Mixed Population E (Mixed) = -350 mV	N,P, trace metals	Dudney et. al., 1995
-----	3.5	Mixed Population	N,P	Groudeva and Groudev, 1994
T = 20-38	7.0	SRB	raw sewage sludge	Maree and Strydom, 1985, 1987
no control	N/A	SRB E (SRB) = -150 mV	gypsum	Revis et. al., 1989
T = 30	5-8	SRB	N,P	Rowley et. al., 1994
Room temperature	7.0	SRB E (SRB) = -300 mV (SHE)	Organics, N,P	Uhrie et. al., 1995
T = 30	7.0	SRB	N,P	Van Houten et al., 1994
T = 30 ± 1	6.8	Mixed populations (SRB, SRB+M, M)	N,P	Visser et. al., 1993

*Mixed refers to a mixed SRB and methanogen population, unless indicated all redox potential are compared to a standard calomel electrode; N, P refer to ammonium salts and phosphate salts, respectively.

Experiments with SRB have been run successfully with temperatures ranging from 15-40 °C. The optimal growth temperature for a mixed population of SRB, under neutral pH conditions, has been demonstrated to be approximately 32 °C, refer to Figure 2.7 (Maree and Strydom, 1987).
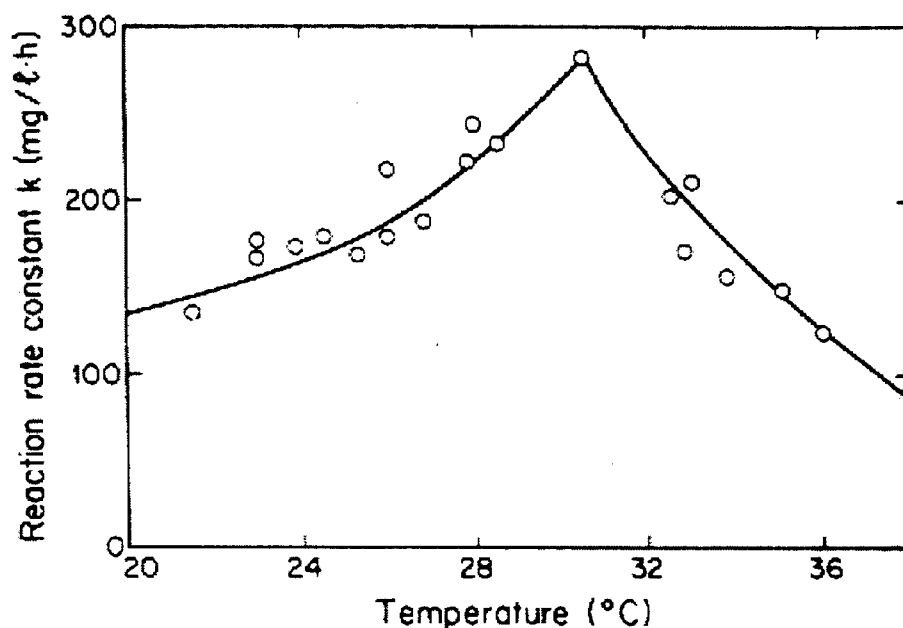
Figure 2.7: Optimal Temperature for Mesophilic SRB
(Source: Maree and Strydom, 1987)

2.3.6 Inhibition of SRB

Hydrogen Sulphide Inhibition

Hydrogen sulphide is a byproduct of the sulphate reduction process performed by SRB. The H_2S is also toxic to the bacteria and can cause growth inhibition as well as cell death. It is assumed that the undissociated H_2S, not HS^- or S^{2-}, causes the inhibition as only neutral molecules can pass through the cell membrane (Lens and Visser, 1998)

Another advantage to using H_2 and CO_2 is it provides gas stripping capability of H_2S which helps to maintain the sulphide level at nontoxic concentrations to the SRB, thus increasing conversion rates of sulphate (Van Houten et. al., 1994). To avoid reaching an inhibitory sulphide level, the carbon source can also be controlled to adjust the conversion rate (Kolmert et. al., 1997).

Metal Inhibition

Although the reduction of sulphate to sulphide by SRB can be used to remove heavy metals from contaminated water by the formation of metal sulphide precipitates, high metal concentrations can still cause inhibition of SRB bacteria. Concentrations of copper, chromium, and cyanide have been reported to inhibit SRB growth (Postgate, 1984, Song et. al., 1988).

SRB inhibition has been found at copper concentrations $\geq 70 - 130$ mg/L, with an IC_{50} estimated at 100 mg/L. Chromium concentrations ≥ 130 mg/L caused a 15% decrease in activity compared to a control with no chromium. SRB were found to be sensitive to cyanide, with concentrations $\geq 5 - 50$ mg/L causing a reduction in activity. The IC_{50} value for cyanide was estimated at 20 mg/L cyanide (Song et. al., 1988).

Toxic limits reported in different studies vary, possibly due to varying levels of sulphide and alkalinity present, which may affect the quantity of heavy metal precipitation. Differences in pH, temperature, and residence times in reactors may also affect the results (Postgate, 1984). It has been reported that the local precipitation of metal sulphides can increase the resistance of organisms to the toxic affects of the metals and it may be possible under long term studies to increase the resistance of SRB to high metal effluent streams (Revis et. al., 1989).

2.4 Immobilisation of Bacteria to Surfaces

The purpose of immobilising SRB on a surface is to increase the biomass concentration in a reactor and to prevent cell washout. Immobilisation of cells refers to the restriction of cell mobility within a defined space and is categorised by two main types: cell entrapment and surface immobilisation. Cell entrapment is when the bacteria are enclosed within a space, while surface immobilisation occurs when the bacteria attach to the surface of a support material.

An immobilised system can, in theory, promote higher substrate conversion rates at higher flowrates than are possible in nonimmobilised systems. Because a continuously stirred bioreactor system (well mixed) will have the same effluent stream composition as the liquid in the reactor, freely-suspended cells are constantly withdrawn from the vessel in the effluent stream. Therefore, an immobilised cell system with a concentration of cells, X_m, not removed from the system may have a higher substrate conversion rate at higher dilution rates, D. The relationship between the dilution rate, steady state substrate concentration and the immobilised cell concentration in a CSTR can be represented by (Doran, 1995):

Equation 2.1

$$\frac{\mu_{max} S}{K_S + S} = \frac{D(S_I - S)Y_{XS}}{(S_I - S)Y_{XS} + \eta_T X_M}$$

Where μ_{max} = maximum specific growth rate (h^{-1}),

K_S = substrate conversion rate (mg/L),

Y_{XS} = biomass yield coefficient (mg biomass/mg substrate),

X_M = immobilised cell concentration (mg/L),

D = F/V = dilution rate (h^{-1}) (where F= volumetric flowrate and V= volume in the reactor),

η_T = total effectiveness factor (dimensionless), and accounts for the extent to which a reaction is affected by internal mass transfer for immobilised cells. Therefore it can be considered as the ratio of the rates of reaction of immobilised cells to free cells.

S = substrate concentration (mg/L).

Shown in Figure 2.8 is the relationship for a CSTR with immobilised cells and without (i.e. $X_M = 0$), at steady state, with $\mu_{max} = 0.1/h$, $K_s = 0.001g/L$, $Y_{XS} = 0.05g/g$ and $S_I = 0.008$ g/L. The plot of substrate conversion rate versus dilution rate shows that for $X_M > 0$, D can be operated at much higher values than $D_{CRITICAL}$ for the suspended cell system. In fact, even when the system is mass transfer limited at $\eta_T = 0.3$, the substrate conversion rates are much higher than the suspended cell system.
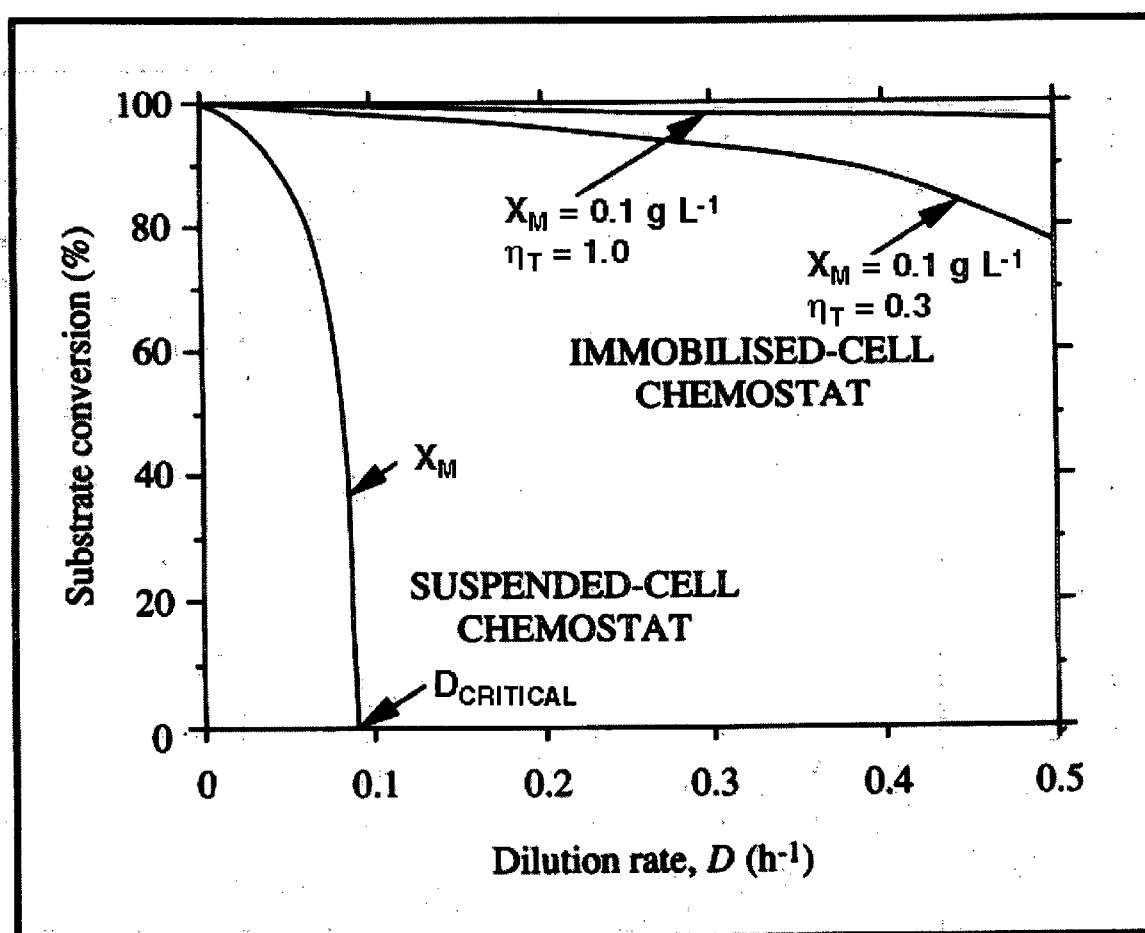
Figure 2.8: Substrate Conversion and Dilution Rate in an Immobilised Cell System.
(Source: Doran, 1995)

Immobilisation may result in high substrate conversions at high dilution rates. However, this is dependent on the ability of the bacteria to colonise the support surface present in the reactor system. Not all supports are colonised to the same degree. Many different surfaces

have been studied to encourage anaerobic microbial colonisation of surfaces in order to allow for improved treatment capability in reactor systems. Listed in Table 2.8 are some of the surfaces used for immobilisation. Also included is any observations made by the authors on how well the support was colonised by the bacteria and any noticeable improvement in substrate conversion rates.

Table 2.8: Surface Immobilised Support Materials used in Anaerobic Studies

Support	Support Properties	Comment	Source
Sand Pumice Sintered Glass (methanogens)	Sand (d=0.7-1.0 mm) Pumice (d=3-4 mm, p=0.431 mL/g) Sintered glass (d=3-3.5 mm, p=0.084 mL/g)	Expanded Bed Reactor: Porous media achieves quicker and better colonisation than nonporous media. Biomass able to colonise an internal structure as well as external, recover quicker from inhibitory substances.	Allaoui and Forster, 1994
Crushed Bunter Sandstone (SRB)	Sand (M= 0, 0.01, 0.1, and 1 gram)	Batch System: More sulphide produced in systems with a support surface than without (1>0.1>0.01>0) (2.5 mM for the system with 1 gram of support and 1.4 mM for the control with no support).	Bass et. al., 1996
Foam Nylon	Foam (porosity 90-96%, pore d=0.064-0.085 cm) Nylon (pore d=0.085 cm)	Packed Bed Reactors: Foam was fund to consistently retain more biomass than nylon. Nylon was found to be less subject to degradation under mechanical abrasion.	Bolte et. al., 1986
Foam Zeolite Glass Beads (Methanogens)	Zeolite (d=5mm) Glass (d=5mm) Foam (pore d=2.21, 0.42, and 0.27 mm)	Packed Bed: Better biofilm development observed with foam than zeolite. No biofilm development observed on glass beads.	Huysman et. al., 1983
Mine Gob Material No support (SRB)	N/A	Batch System: Heavy metals, except for Ni, were removed to below detection limit (0.1 ppm) in the case of the colonised mine gob material as compared to nonsupport system.	Kim and Cha, 1997
Poraver Plastic carriers	Poraver – foam glass particles Plastic carriers – (two types not specified)	Packed Bed and Suspended Carrier: Packed bed system more robust than suspended carriers, which had a decreased capacity during the experiments.	Kolmert et. al., 1997
Hard Stone Quartz sand Plastic No Support (SRB)	Hard Stone (d=1 cm, and finely crushed) Quartz Sand (d=2 mm)	Expanded Bed: Higher rate of sulphate removal in system with hard stone than nonsupport system. No noticeable improvement with quartz sand or plastic support system.	Maree and Strydom, 1985, 1987
Pumice Basalt (SRB)	Pumice (d=0.2-0.5 mm) Basalt (d=0.29 mm)	Gas Lift Reactor: Growth of bacteria started in pores of particles followed by surface coating.	Van Houten, 1996

As mentioned earlier, immobilisation falls under two general categories: surface attachment and cell entrapment. The supports listed in Table 2.8 are examples of surface attachment. Alginate beads can be used as a cell entrapment technique to immobilise SRB. Alginate beads have a pore size within its gel matrix from 5-200 nm in diameter. As well immobilisation with alginate beads has been shown to be a safe, fast and versatile technique (Smidsrod and Skjak-Braek, 1990).

2.4.1 Biofilm Formation

The following section describes some of the properties of biofilm formation that were considered in the selection of support materials for this project.

Biofilms form as the result of adsorption, the production of extracellular polymeric substances, EPS, and growth. Generally, the bacteria uniformly distribute throughout the EPS matrix because the EPS causes biofilms to be gel-like, transport processes tend to control the microbial behaviour in the biofilm (Characklis, 1991).

Many bacteria produce large quantities of EPS and quickly adsorb to a variety of surfaces while others gradually become adsorbed to surfaces over long periods of time. These differences may be due to nutritional conditions, the nature of the substratum surface, and previous macromolecular adhesion to the surface (Characklis, 1991). Nutrient limiting conditions have been suggested as a way to stimulate EPS production and encourage bacterial growth on surfaces (Zobell, 1943). Previous macromolecular adhesion may affect the surface charge of the material and also affect the ability of bacteria to adhere to a surface (Characklis, 1991).

Surface Adsorption

Bacteria have a net negative charge at acidic and neutral pH levels. This creates an inherent preference for materials that have a net positive charge. However, there are many diffusional restraints and chemical interactions that must be overcome before adsorption occurs:

"It is generally conceded that, while the main body of the bacterial cell does not make direct contact with the substratum surface, adsorption is mediated by a process of bridging to the substratum by fine extracellular structures capable of overcoming the repulsion effects by a combination of Brownian displacement, chemical bonding, dipole interactions, and hydrophobic interactions" (Characklis, 1991).

Bacterial adhesion is affected by the hydrophilic and hydrophobic nature of the surface. One study found that bacterial adhesion was more predominant on hydrophilic surfaces (slightly negative charge) than hydrophobic (positively charged) surfaces when the surface tension of the suspending medium is less than the surface tension of the bacteria. In the reverse case, the opposite is observed (Absolom et. al., 1983). Another study which coated pieces of the foam with PVC to decrease its hydrophobic properties found that this decreased the amount of biomass adhering to the surface, suggesting that the more hydrophobic the material the better it is for colonisation (Huysman et. al., 1983).

Some authors have observed increased rates of activity in systems with support material than in systems without support (Bass et. al., 1996, Kim and Cha, 1997, Maree and Strydom, 1985, 1987). It has been postulated that in a batch system a support material provides a greater surface area for growth, which can result in an increase in the amount of active bacteria present and account for observed increases in activity (Bass et. al., 1996).

Surface Roughness

Microbial colonisation on a surface tends to increase with increasing surface roughness (Geesey and Costerton, 1979, Baker, 1984, Characklis, 1984). Some authors have also reported finding attached microbes mostly concentrated in crevices as opposed to smooth surfaces (Geesey and Costerton, 1979, Beeftink and Staugaard, 1986, Meraz, 1995). Whether or not the surface irregularities serve as anchoring points for bacterial adhesion or whether the surface roughness encourages adsorption is still under debate (Schink, 1988).

Pore Size

The pore size of the support surface must be suited for bacterial colonisation. For instance, activated carbon has a large internal surface area, ranging from 500-1600 m^2/g, but most of it cannot be colonised by bacteria since most of the pores are smaller than 50 nm in diameter (Schink, 1988). It has been postulated that the optimal size of surface micropores that promote bacterial colonisation, is 5 times the length of the bacteria (Messing, 1982).

Three types of foam, zeolite, and glass beads were used in a comparative study to monitor the colonisation of surfaces by methanogens (Huysman et. al., 1983). The foams were highly porous and contained pore sizes of 0.27mm, 0.43 mm and 2.21 mm. The zeolite, contained pores in the nm range, while the glass was non porous. The foam systems were colonised rapidly, followed by some surface attachment in the system with zeolite and no colonisation in the glass system. The study found that both the 0.43 mm and 0.27 mm foams had better bacterial colonisation than a foam with a mean pore diameter of 2.21mm, with the former showing a slightly better performance than the smaller pore sized foam (Huysman et al, 1983).

Both pumice and basalt have been studied as possible supports for SRB, with the pumice support material showing a better biofilm formation than the basalt (Van Houten, 1996). The pumice particles were observed to have a very porous, sponge-like structure, while the basalt has a rough surface but lacks deep pores. The preference for the bacteria to colonise the pumice over the basalt, which had negligible biofilm formation, may be due to the more porous structure under turbulent conditions. The SRB can easily enter the pores of the pumice where the liquid turbulence is less and the bacteria have time to adhere to the surface. The SRB have little chance to adhere to the basalt surface due to liquid turbulence and direct collisions with other basalt pieces which can knock the bacteria off the surface.

2.4.2 SRB Biofilm Quantification

Biomass quantification in bacterial studies is often accomplished by using one or more of the following techniques: gravimetric analysis, enumeration techniques, optical density, and protein determination. Gravimetric analysis relies on measuring the weight of a sample. This is either accomplished by taking a wet weight or dry weight sample. A wet weight sample involves monitoring the increase in weight of a known sample volume over the time of the experiment. An increase in weight is expected to be due to an increase in biomass. A dry weight, or total solids, involves drying a known sample at 103 $^{\circ}$C and then weighing it – this is to avoid errors associated with water retention in the sample.

Enumeration of bacterial numbers can be determined using the membrane filter (MF) or the multiple tube fermentation (MTF) techniques. In the MF technique a number of serial dilutions are made. These dilutions are then passed through a 0.45 μm filter paper, which is small enough to retain the bacteria. The bacteria (on the filter paper) are then contacted with a solid agar solution that contains nutrients for growth and incubated. After incubation the number of colonies formed can be counted and the concentration in the original sample determined.

The MTF technique is based on the principle of dilution to extinction. In this test, a number of serial dilutions are made. The next step involves transferring a 1 mL sample from each of the serial dilutions to five test tubes containing a suitable culture medium with an inverted tube inside. The presence of gas is taken as a positive indication of growth. The number of positive to negative samples is compared to an MPN table to estimate the number of bacteria present. These enumeration techniques are very labour intensive and require anaerobic conditions for the SRB to grow.

The optical density method is a fast technique that measures the optical density of a sample. An increase in optical density is attributed to increasing biomass. However, the optical density readings will be skewed in a study with SRB due to interference from metal sulphide precipitates.

Another way to determine the biomass of a sample is to measure the concentrations of the cell constituents, such as protein, organic carbon, or organic nitrogen. These methods rely on either comparing the sample to a known standard or by measuring the total amount of the constituent in a sample. In the former case, such as with proteins, absorbance measurements of the sample are taken and compared to a standard curve of a known protein. In the latter case, if the molecular weight of the bacteria is known, the biomass can be determined by comparing the measured amount of the cell constituent, such as total organic carbon, to the known molecular weight.

Microscopy can also be used to quantify biomass. Microscopy is a useful tool as it can be used to monitor the development of a biofilm to a surface. It is possible to use phase contrast imaging in conjunction with a light microscope to enumerate bacteria that grow in monolayers. Microscope imaging also allows for observation of the types of bacterial species present in the biofilm. As SRB do not form monolayers, light microscopy was discarded as a method of enumeration. However, scanning electron microscope imaging is a useful tool for observing where the SRB adhere to surfaces as well as to observe the morphological characteristics of the bacteria.

The organic nitrogen, total solids and protein determinations were considered as possible methods to measure the biomass in the system, while scanning electron microscopy was used to observe where the bacteria adhered to the support surfaces. These techniques are discussed in more detail in the Methods and Materials Chapter of the thesis.

2.4.3 Cell Growth Kinetics in a Batch System

In a batch culture, the rate of cell growth changes based on which phase of cell growth is occurring in the batch system: the lag phase, growth phase, stationary phase and death phase.

The lag phase begins immediately after inoculation, during this stage the rate of growth is close to zero as the cells adapt to their new environment.

The exponential growth phase: after the lag phase, the rate of growth increases and continues until the stationary phase. If the growth rate is exponential this will appear as a straight line on a plot of ln (biomass) versus time. In this stage the rate of cell division is determined by their ability to process nutrients.

The stationary phase: as the nutrients in the batch system become limiting or as inhibitory products accumulate, the growth rate slows until the population remains stationary. In this phase either the cells have exhausted the substrates required for growth and/or the rate of cell death is equal to that of cell growth.

The death phase: The nutrients in the system have been exhausted, or the environmental conditions in the batch system no longer support growth. In this phase the rate of cell death is greater than cell growth.

In a closed system where growth is the only factor affecting the biomass concentration, the rate of cell growth during the growth phase can be described as:

Equation 2.2

$$r_x = \frac{dx}{dt} = ux$$

Where: rx = dx/dt = the rate of biomass produced ($kg/m^3/s$),

x = biomass (kg/m^3)

μ = the specific growth rate (s^{-1}).

If the specific growth rate is constant, it can be integrated as follows:

Equation 2.3

$$\int_{x_o}^{x} \frac{1}{x}dx = u \int_{t=0}^{t} dt$$

$$\ln x = \ln x_o + \mu t$$

From the above equation, a plot of ln x versus time gives a straight line with slope μ, the specific growth rate.

2.4.4 Reactor Selection

Once a preliminary batch study has been completed, and a suitable immobilisation surface for SRB determined, the next step is to continue the studies under continuous flow conditions in a reactor. Various reactor designs have been studied for the removal of sulphate and/or heavy metals from wastewater. A summary of some of the reactor designs, considered to date, along with potential advantages, is listed in Table 2.9.

Of the reactors listed in Table 2.9, the membrane bioreactor and the gas-lift (expanded bed) type reactor appear to have interesting potential. It has been reported that most bioreactor systems require some degree of nutrient addition to ensure the viability of the cells (Barnes et. al., 1991, Diels et. al., 1991, Van Houten et. al., 1994, Dudney et. al., 1995). Due to the set up of a membrane reactor, a lower addition of nutrient to the cells may be possible since there is direct feed of the nutrients to the biofilm and the microbial community. However, it is unclear if the membrane surface provides the optimum conditions necessary to maximise removal of heavy metals and sulphides from wastewater streams.

Biomineralization is a good tool for lowering metal levels in effluents to less than 1 ppm. The membrane allows the bacteria to remove the metals from one stream while the cells are kept viable by another nutrient stream. This separation of streams allows treatment of water with minimal consumption of nutrients like carbon and phosphate (Diels et. al., 1991). The dynamic development of the system is controlled by the diffusion reaction for both the substrate and the inhibiting product. At low membrane thickness the substrate can easily diffuse through the membrane and the metabolic products produced in the later stages control the system. At a higher thickness, the diffusion of the substrate decreases and substrate gradients appear, which results in controlling the system during the initial phase (Lefebvre et. al., 1997).

Positive results have been reported in both packed and expanded bed type reactors (Maree and Strydom, 1987, Groudeva and Groudev, 1994, Allaoui and Forster, 1994, Van Houten et. al., 1994). Similarly, the gas uplift reactor with pumice particles has been proven to work successfully in the removal of heavy metals and sulphates from effluent streams (Van Houten et. al., 1994). The advantage of the fluidised bed over a packed bed reactor is that channelling is minimised, the drawback is they can be more complicated to design.

Table 2.9: Comparison of Different Reactors with Immobilisation Surfaces

Technique	Advantages	Source
1. Expanded Bed Reactors	• porous media (pumice and sintered glass) had better colonisation than non porous media (sand).	Allaoui and Forster, 1994
2. Tubular Membrane Reactor and Flat Sheet Reactor (Asymmetric) Zifron Membrane (Symmetric)	• metals recuperated on glass beads, • separation of nutrient and effluent stream, • Cd recovery 99.9% • combination of membrane immobilisation and nutrient diffusion keeps bacteria in stationary phase promoting biomineralization of heavy metals, • better results were achieved with the symmetric membrane.	Diels et. al., 1991
3. PVA Membranes	• metal removal by biosorption.	Grappelli et. al., 1995
4. Packed Bed Reactor	• optimum pH 7 but buffering capacity of effluent allowed workable conditions at 3.5, • removal of heavy metals down to ppb level, • glass beads used as packing material, • it took 5 months to obtain maximum SRB activity.	Groudeva and Groudev, 1994
5. Packed Bed Reactor	• 90% removal of sulphate with hard stone vs. 40% with sludge blanket, • hard stone media yielded best results.	Maree and Strydom, 1985, 1987
6. Gas-Uplift Reactor (SRB population only)	• biofilm stable under turbulent flow conditions, • open structure of pumice assists in microbe attachment.	Van Houten et. al., 1994

2.5 Summary

The literature review section of this thesis covered the environmental conditions associated with ARD. The chemical treatment of ARD, which relies on raising the pH of the ARD to form metal hydroxide precipitates, was compared to the advantages of precipitating metals as sulphides. This was extrapolated further to the potential use of a biological process using SRB to treat ARD. An example of a current process using a SRB bioreactor to treat heavy metal contaminated effluent was illustrated. The two main problems encountered in this system were the formation of acetate as a byproduct of ethanol oxidation from the SRB and bacterial washout. Methanogens were introduced into the system to counteract the first problem and a flocculent was added to the system to overcome the second.

A review of the general conditions required to cultivate SRB was also included in the literature review. The selection of growth conditions were (1) deciding upon a suitable carbon source and energy source, (2) determining a nutrient media that promoted bacterial growth based on that carbon and energy sources, (3) the pH of the nutrient media, and (4) the incubation temperature of the bacteria. In general low molecular weight organic sources are suitable carbon and energy sources for SRB. However, these organic sources may not always be readily available at an industrial site and they may not be cost effective. In addition, if organic sources are introduced into a system as a feed source for SRB, any unconsumed organics will require treatment prior to discharge. Based on this data, CO_2/H_2 were selected as the carbon and energy sources for the SRB, experiments were designed to determine the appropriate nutrient media and the temperature selected for the experiments was 32 ± 1 °C, under neutral pH conditions.

An immobilised growth system allows bacteria to remain fixed on the media and prevent bacterial wash out at high dilution rates; this allows for a large mean cell-residence times with short hydraulic retention rates. The Paques UASB Process used a reactor with freely suspended cells and also encountered problems with bacterial washout at residence times below 30 hours. In order to overcome this problem a flocculent was added to the system in order to promote bacterial granulation and prevent washout. Another way to combat this

issue would be to use a support surface, or attached growth system, that would allow for bacterial colonisation, and prevents bacterial washout at higher flow rates.

While many studies have looked at immobilisation of bacteria to surfaces, only a limited number of studies have looked at SRB immobilisation. In particular there is a shortage of data on the attachment of SRB to surfaces under autotrophic conditions.

2.5.1 Selection of Support Materials

Previous work on SRB indicates that porous structured media is better colonised than nonporous media (Diels et. al., 1990, Allaoui and Forster, 1994, Van Houten et. al., 1994,). Other properties that have been noted to encourage bacterial adhesion or bacterial growth are the surface charge and hydrophobicity, surface roughness, and surface area (Huysman et. al., 1983, Schink, 1988, Characklis, 1991, Bass et. al., 1996,).

Based on these factors, and the desire to study a large number of different types of materials available at low cost. The following support materials were used in this study: foam, basalt, zeolite, glass beads, alginate beads, Teflon, Ringlace, molecular sieve, and ceramic beads. Foam was selected as a highly porous material because porous material is better colonised than nonporous material (Allaoui and Forster, 1994, Huysman et. al., 1983). It was also selected as a low cost support material. Glass beads were selected as they have a net positive surface charge which was thought to encourage bacterial adhesion. Both the basalt and the zeolite were selected as low cost, natural rock formations with rough surfaces. The ceramic beads and molecular sieve were chosen due to availability and to see if additional surface area encouraged bacterial growth. Ringlace is a commercial product sold as a biomass support used in aerobic wastewater treatment. We wanted to see if SRB would attach to it. The Teflon-plastic pieces were chosen because Teflon is hydrophobic in nature and may encourage biofilm attachment. Finally, the alginate beads were selected to see if entrapped cells would have a higher sulphate reduction rate than surface immobilised cells.

2.6 Thesis Objectives

Immobilised growth systems prevent bacterial washout at high flowrates and provide a larger surface area for bacterial colonisation (resulting in the potential for increased rates of removal). Previous work with attachment of SRB to growth surfaces has mainly looked at heterotrophic growth conditions (Maree and Strydom, 1985, Bass et. al., 1996, Kolmert et. al., 1997). One study looked at immobilisation of pumice and basalt under autotrophic conditions, but not other materials (Van Houten et. al., 1994). The use of waste organics as the carbon and energy source for bacteria can lead to secondary pollution and bulk chemicals such as ethanol may not be as cost effective as the growth of SRB under autotrophic conditions (CO_2/H_2) (Van Houten, 1996, Du Preez et. al., 1992). The focus of this study is to look at the ability of SRB to attach to different types of growth surfaces, under autotrophic conditions, in order to determine what types of growth surfaces promote rapid bacterial colonisation for SRB.

The central objective of this thesis is to compare attachment and growth of sulphate reducing bacteria to solid supports made from different materials. In order to obtain this objective the following sub-objectives were addressed (1) the selection of a suitable medium for autotrophic growth of SRB, (2) the development of a technique for quantifying biomass concentrations on the support materials and in suspension, (3) the measurement of SRB growth on different support materials. Static batch cultures were used instead of a continuous flow bioreactor due to time constraints.

In order to accomplish these objectives the following parameters were measured: biomass growth on the support materials and in solution, CO_2 uptake, and sulphate reduction. SEM images were used to determine how and where the SRB preferentially (if any) colonised the different surfaces. By measuring the increase in biomass, it is possible to determine the specific growth rates of the bacteria in the different systems. Measuring the biomass also allows for the determination of immobilised compared to freely suspended bacteria. The nutrient uptake rate (CO_2) in the system was monitored to observe if the rate of bacterial growth was affected by changes in the media composition. The sulphate reduction rate was

measured to determine the reaction order in an autotrophic system. As well, the sulphate reduction data and the biomass growth were used to determine the growth yield, Y_{SO_4}, in the different systems.

CHAPTER 3.0: METHODS AND MATERIALS

3.1 Overview of Experiments

During this project three experiments were conducted: (1) the comparison of SRB growth in different nutrient media, (2) growth of SRB on nine different support materials and (3) monitoring the rate of CO_2 uptake by SRB. This chapter will describe the experimental procedures and the analytical methods that were used during this project.

The comparison of SRB growth in different media was done so as to select a nutrient solution that supported growth under autotrophic conditions. The ratio of yeast extract and bactopeptone in the nutrient solution was investigated to see if the SRB would grow in a defined media under autotrophic conditions. The biomass growth, sulphate reduction and the rate of CO_2 uptake were monitored in these experiments.

The second set of experiments was broken up into two sections: set 1 and set 2. One of the main objectives of the set 1 experiments was to establish the analytical techniques to be used to quantify the biomass in the system as well as to measure the sulphate reduction rate of the SRB. In the set 2 experiments, the biomass growing on the support and in solution, respectively, was quantified. The sulphate reduction rate was also measured in these experiments. The yield, Y_{SO_4}, was calculated based on the mass of biomass produced per mole of sulphate reduced. The second set of growth experiments was conducted over two weeks during which we did not want the nutrients to become limited. The purpose of the CO_2 experiments was to measure the CO_2 uptake rate to estimate the time at which CO_2 needed to be recharged to the growth bottles. A secondary objective was to monitor the CO_2 in both complex and defined media to observe if there was any difference in the uptake rates. The accompanying sections outline the individual procedures and, where required, the basic principles involved in performing the experiments.

3.2 Comparison of SRB Growth in Different Media

The initial experiments consisted of establishing a suitable nutrient solution for SRB growth under autotrophic conditions. Six types of nutrient media were prepared and 1 mL of inoculum was added to the batch flasks. Complete blackening in the flask was taken as an indicator of active bacterial growth, and was considered to have occurred when the solution in the flasks was completely black and opaque after the vial was shaken. Once a suitable nutrient solution was established (based on the time for complete blackening to occur), successive experiments were performed to grow the bacteria in a defined media instead of a complex media. Again SRB growth was monitored by observing the length of time required for complete blackening to occur in the batch flasks. No quantitative measurements were gathered for this section of the experiments.

3.2.1 SRB Growth

A SRB mixed culture grown under mixed conditions suitable for both heterotrophic and autotrophic growth was obtained from the Biomet Mining Corporation, Vancouver, Canada. An inoculum was prepared from this culture by growing under batch conditions for 3-5 days prior to inoculation of the batch flasks used in the experimental procedures. The cultures were grown under autotrophic conditions. Initially the SRB culture was taken directly from the stock and grown in a complex media, either the Biomet, ethanol, or Modified Van Houten (MVH) media respectively. The set 2 experiments were carried out in a defined media based on the MVH nutrient solution. The complex media all contained yeast extract and/or bactopeptone, which tend to promote faster growth but can cause interference with protein tests since these chemicals contain protein as well. A defined media that doesn't contain yeast extract or bactopeptone, will cause less interference when quantifying the biomass samples.

3.2.2 Nutrient Solutions

Six nutrient solutions, described in Table 3.1, were prepared and tested for growth of SRB. The solutions were prepared with distilled water and autoclaved for 15 minutes at 121 °C. All chemicals except bactopeptone, yeast extract, and thioglycolic acid were added to the solution before autoclaving. Once the solution had cooled to room temperature, 1 M HCl was used to adjust the pH level to 7. The pH meter calibration was checked each time with pH 4 buffer solution. A Mettler Toledo Model 465 pH probe was used to adjust the pH of the nutrient solution. The nutrient media selection process for the 2 sets of experiments is shown in Figure 3.1.
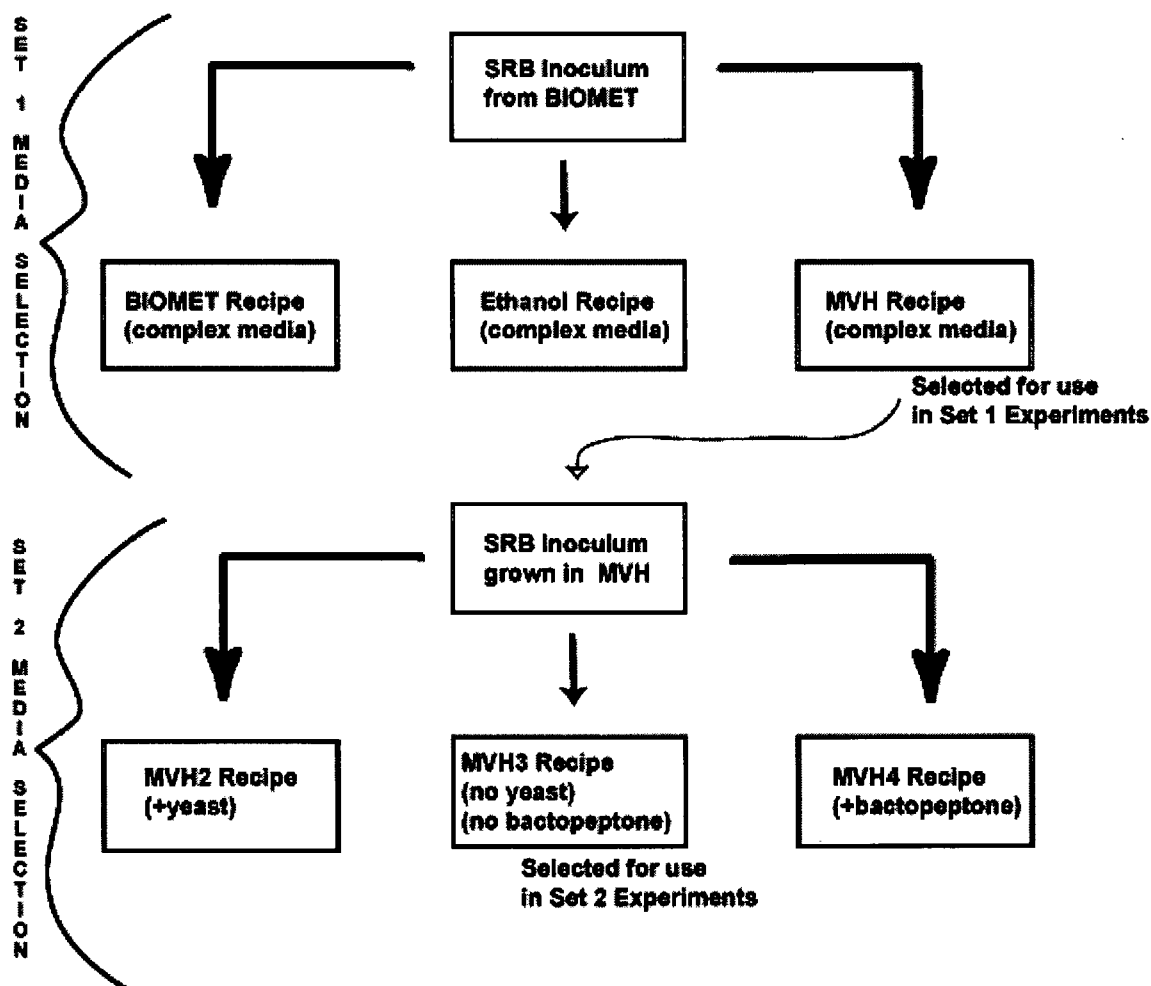
Figure 3.1: Nutrient Solution Selection Process

Once the nutrient media was prepared, 40 mL was transferred to a 160 mL batch flask and 1 mL of inoculum was added (refer to the Inoculation Protocol on page 53 for further details). The samples were placed in an incubator at 31 °C and the bottles were monitored daily, for up to 10 days, for blackening in the flasks, which was taken as an indication of SRB activity.

The Modified Van Houten (MVH) nutrient media is a simplified version of another nutrient media used to growth SRB under autotrophic conditions (Van Houten et. al., 1994). The MVH media is the same except for the stock salt solution and the exclusion of a vitamin solution and a trace element solution. The vitamin and trace elements solutions require an additional 21 chemicals but only compromises 2.2 mL of the 1 litre volume (Stams, 1992). Communication with both Michael Rowley of the Biomet Mining Corporation and Susan Baldwin, respectively, indicated that a simpler media could be prepared which would still allow for growth of the SRB; as such the MVH solution was prepared and tested for SRB growth.

Table 3.1: Nutrient Solutions

Ingredient	Biomet [+]	Ethanol	MVH [++]	MVH2	MVH3	MVH4
	Amount added (g) (made up to 1000 mL in dH2O)					
Bactopeptone	0.012	----	0.216/0.10	----	----	0.1
Yeast Extract	0.013	1.03	0.204/0.10	----	0.1	----
Thioglycolic Acid [1]	----	10 mL	5 mL	5 mL	5 mL	5 mL
Ascorbic Acid [2]	----	10 mL	----	----	----	----
Na_2SO_4	----	----	4.953	4.953	4.953	4.953
KH_2PO_4	0.065	----	0.409	0.409	0.409	0.409
NH_4Cl	----	----	0.297	0.297	0.297	0.297
$MgCl_2.6H_2O$	----	----	0.091	0.091	0.091	0.091
$CaCl_2.2H_2O$	----	----	0.120	0.120	0.120	0.120
Na_2HPO_4	----	----	0.524	0.524	0.524	0.524
KCl	----	----	0.385	0.385	0.385	0.385
$NaHCO_3$	----	----	1.209	1.209	1.209	1.209
Stock Salt Solution [3]	----	----	100/50 mL	50 mL	50 mL	50 mL
Ethanol	----	1.20 mL	----	----	----	----
Methanol	----	0.13 mL	----	----	----	----
$(NH_4)_2SO_4$	0.163	----	----	----	----	----

1. Thioglycolic Acid made up as 3.5 g/350 mL dH_2O
2. Ascorbic Acid made up as 10 g/ L dH_2O
3. Stock Salt Solution: 3.5 g NH_4Cl, 0.60 g KH_2PO_4, 10.00 g $FeSO_4.7H_2O$, 18.35 g $MgCl_2.6H2O$, 6.75 g $CaCl_2.2H_2O$ made up to 1L with dH_2O.
(Sources: + Michael Rowley, personnel communication, 1998, ++ Van Houten et. al., 1994)

3.2.3 Temperature

The temperature of the batch flask experiments were maintained at 31 ± 2 °C by placing the batch flasks in temperature controlled incubators. A Blue M dry type bacteriological incubator and a New Brunswick Scientific Innova 4230 incubator were used for these experiments.

3.2.4 Cultivation

When cultivating SRB with an H_2/CO_2 mixture it is recommended to leave a headspace of 2/3 to 3/4 of the total volume. The amount of inoculum to add should be around 1% (v/v) for faster growing SRB species and up to 5-10% (v/v) for slower growing species. Enrichment cultures should be transferred at least twice into new medium before use to gradually dilute away non SRB and the transfer volume should be kept between 1-10% (v/v) (Widdel and Bak, 1992). Based on this 40 ml of nutrient solution was added to 160 mL Kimble Bottles to allow for 75% headspace, and 1 mL of inoculum was added to the 40 mL nutrient solutions (2.5% v/v).

3.3 Growth on Support Materials

The purpose of these experiments was to evaluate the potential of a wide variety of materials to support growth of sulphate reducing bacteria. The batch growth experiments attempt to quantify the bacterial density in solution and on the growth supports provided in the batch flasks. Two sets of experiments were performed: set 1 and set 2. In set 1, the following support materials were used: molecular sieve, glass beads, ceramic beads, Teflon, and zeolite and the following analyses were performed, total and volatile solids; $\%CO_2$ in headspace, TKN and sulphate concentration. In set 2, the following support materials were used: foam, basalt, calcium alginate beads, and Ringlace. In these experiments the biomass was separated into two samples: the growth in suspension and that attached to the support materials. The following analyses were conducted: TKN, sulphate, and protein. As well, scanning electron microscope (SEM) images were also captured to determine how densely and where the bacteria were colonising the various growth surfaces.

Table 3.2: SRB Growth Surfaces

Growth Surface	Experiment	Comment
Glass Beads (smooth)	Set 1	Sphere, diameter =3 mm, surface area =0.0033m²/g
Davison Molecular Sieve Fisher Scientific	Set 1	Sphere, diameter =3 -5 mm
Ceramic Beads	Set 1	Sphere, diameter =5 mm
Zeolite Canmark Ltd	Set 1	10+ mesh size
Teflon/Plastic Pieces	Set 1	Disc, diameter =20 mm, width= 3mm each disc, cut into quarters.
Basalt Ocean Construction Supplies Ltd	Set 2	Spheroid, diameter =3-5 mm, length =7-11 mm, surface area =3.68 m²/g
Polyurethane Foam	Set 2	Cube, side =15 mm, density =40 kg/m³, surface area =0.184 m²/g
Ringlace Ringlace Products Ltd. 9902 NE Glisan, Portland Oregon	Set 2	Thread-like, length =150 mm section Thread width = 100 μm
Calcium Alginate Beads	Set 2	Sphere, diameter = 3 mm

3.3.1 Preparation of Growth Surfaces

The selection process, for the growth surfaces used in this project, was discussed in Section 2.6.1: Selection of Support Materials. Listed in Table 3.2 are the various growth surfaces used in the first and second set of support material experiments during this project. All growth surfaces were treated in the same manner except for the calcium alginate beads (see preparation below). The method for preparing the calcium alginate beads was adapted from two separate papers (Kueck and Armitage, 1984, Santoyo et. al.,1996).

Preparation of Growth Surfaces

1. Wash growth surface in dilute nitric acid.
2. Rinse growth surface with tap water.
3. Autoclave growth surface (15 min @ 121 °C).
4. Rinse growth surface with tap water.
5. Autoclave growth surface (15 min @ 121 °C).
6. Dry and keep in oven at 40 °C until required (up to 3 days).

Preparation of Calcium Alginate Beads

1. Prepare 0.2 M $CaCl_2$ solution and cool in fridge.
2. Add 1 mL thioglycolic acid to 200 mL distilled H_2O.
3. Add 8 g sodium alginate to the 200 mL distilled H_2O (4% w/v).
4. Mix at 35 °C until well dissolved and no clumps are left in solution.
5. Allow to cool to room temperature.
6. Add 40 mL of SRB inoculum to sodium alginate solution under a N_2 head with constant stirring.
7. Pump alginate/SRB mixture through a 20 gauge needle to add beads dropwise into the 0.2 M $CaCl_2$ solution with continuous slow stirring (this takes about 8 hours).
8. Allow beads to harden in a fridge overnight.

3.3.2 SRB Growth

Media: The media selected is based on a nutrient solution described by Van Houten and is composed of the following per 1000 mL of distilled water: Na_2SO_4 4.95 g, $Na_2HPO_4.2H_2O$ 0.524 g, KH_2PO_4 0.41 g, NH_4Cl 0.30 g, KCl 0.38 g, $MgCl_2.2H_2O$ 0.10 g, $CaCl_2.2H_2O$ 0.11 g, $NaHCO_3$ 1.2 g, thioglycolic acid 5 mL, bactopeptone 0.10 g, yeast extract 0.10 g, and stock

salt solution 50-100 mL. The stock salt solution contains per 2000 mL of distilled water: NH_4Cl 7g, KH_2PO_4 1.2 g, $FeSO_4.7H_2O$ 20 g, $CaCl_2.2H_2O$ 13.5 g, $MgCl_2.6H_2O$ 36.7 g (Van Houten et al., 1994). In some cases the bactopeptone and yeast extract were omitted from the media preparation.

Set 1 Experiments

Bacteria Culture: Bacteria were cultured in 40 mL of nutrient medium in 120 mL serum bottles with rubber stoppers. The bottles were inoculated with 1 mL of inoculum pipetted directly from a 3 day old batch culture grown in 40 mL of the MVH solution. The cultures were grown under autotrophic conditions with a 80%H_2-20%CO_2 atmosphere, and incubated at 31 °C. The CO_2 was injected in to the flasks through the rubber stoppers with a 60 mL Luer-Lok disposable syringe and 20 gauge needle.

Set 2 Experiments

Bacteria Culture: Bacteria were cultured in 40 mL of nutrient medium in 160 mL Kimble bottles with black screw caps and a butyl rubber septum. The method for adding the bacteria to the bottles was adapted from the Hungate Technique for the preparation and use of media under anaerobic conditions (Hungate, 1969). The batch flasks contained 1 mL of inoculum (except in the case of calcium alginate beads, in which case 4 mL of inoculum was immobilised in the beads) pipetted directly from a 5 day old batch culture grown in 40 mL of MVH2 solution. The cultures were grown under autotrophic conditions with a 75%H_2-25%CO_2 atmosphere, and incubated at 31 °C. The CO_2 was injected in to the flasks through the butyl rubber septum with a 50 mL Hamilton Gas Tight syringe and 24 gauge needle.

Inoculation Protocol

1. Autoclave bottles for 15 minutes at 121 °C.
2. If required, add growth surface for SRB (refer to Preparation of Growth Surfaces for more detail).
3. Add 40 mL of the appropriate nutrient solution to each vial, MVH for set 1 experiments and MVH2 for the set 2 experiments.
4. Nitrogen purge the vial (with the nutrient solution) for 5 minutes.

5. Hydrogen purge the vial for 5 minutes.
6. Add 1 mL of SRB inoculum after about 3-4 minutes of hydrogen purging.
7. Cover the vial opening with parafilm to minimise air entering the vial.
8. Quickly stopper the vial once the hydrogen purge is complete.
9. Flush 50 mL gas tight syringe twice with CO_2.
10. Inject CO_2 into the vial. Inject 25 cc CO_2 for set 1 and 30 cc CO_2 for set 2.
11. Check that the incubator temperature is set to 31 $^{\circ}$C.
12. Place the batch flasks in the incubator.
13. Conduct the following tests TSS, VSS, TKN, protein, sulphate, and SEM prep as required. The protocols for these tests are outlined in the analysis sections of this chapter.

Experimental Procedure

One of the purposes of the set 1 experiments was to determine how long the experiments should be run. Three experimental runs were completed during this set of experiments. The length of each run was 9 days, 5 days and 7 days, respectively. In the first run, samples were collected daily between days 3-9, in the second run, samples were collected each day of the experiment, while in the third run samples were collected on each day of the experiment except for day 2. The first set of experiments demonstrated that adequate results could be obtained within 7 days using a complex media. Since the set 2 experiments were conducted in a defined media, the duration of the experiment was increased to 14 days. Samples were collected on days 1, 3, 5, 8, 11, and 14 of the growth experiments. In the case of the Ringlace support, there was a lack of available material and samples were collected on days 8, 11, and 14 only. The data collected for the control on day 1 was assumed to also represent the data for the Ringlace on day 1 as these values for the experiment are measurements of the inoculum biomass concentration and the initial sulphate present in the solution. The batch growth experiments performed involved sacrificial sampling in order to determine the total biomass in the system. On any given day of sampling two or three bottles were selected at random for analysis. The nutrient solution in each vial was filtered through a 0.22 μm Millipore filter paper. The general handling procedure required to gather the samples for analysis is demonstrated in Figure 3.2.

Both the biomass in solution and on the support was collected. This was accomplished by first collecting the biomass in the filtrate on filter paper and then collecting the biomass on the support on a different filter paper. The filtrate was collected, preserved with 2M HCl and placed in a 4 °C fridge for later sulphate analysis. The collected material on the filter paper was rinsed with a weak acid solution, followed by two rinses with distilled water. The filter paper and solids was then placed in a desiccator. The material on the support materials in the batch flasks was then also collected on filter paper. This involved adding distilled water to the flask, vigorously shaking it, and then filtering the water. This process was repeated until the water added to the flask remained clear after shaking.
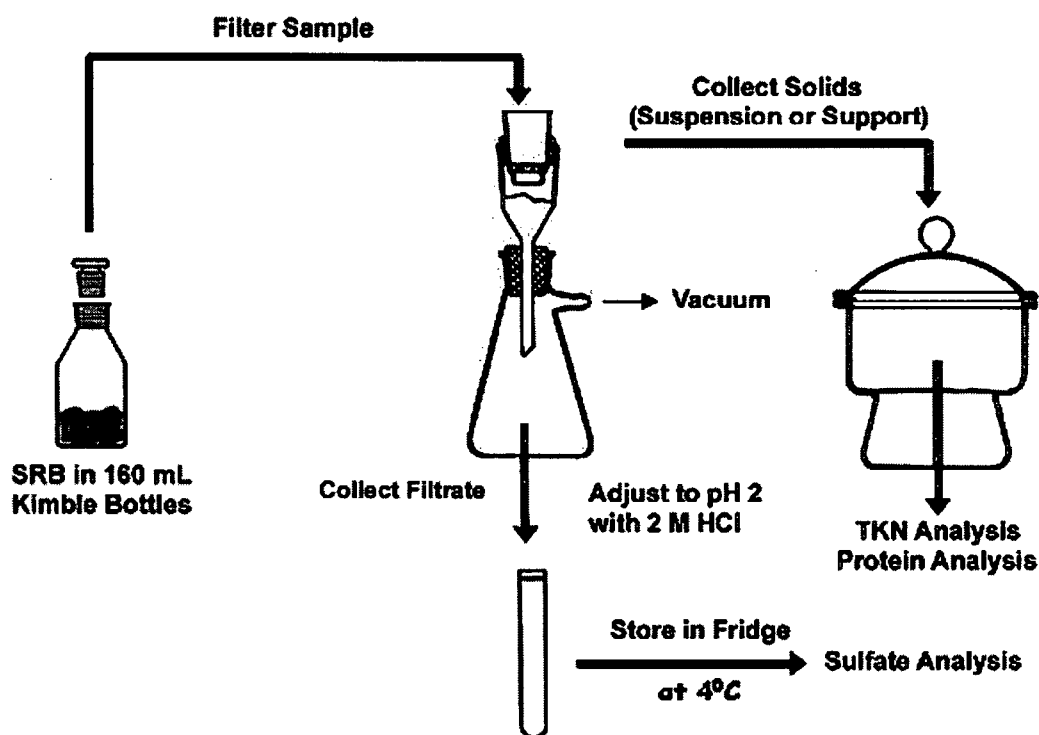
Figure 3.2: Sampling Procedure Flow Diagram

The filter paper with solids was placed in a desiccator. Once all the sampling was complete and the filter paper with the solids had dried they were prepared for protein and/or TKN digestion. The filter papers were placed in digestion tubes and 10 mL 0.5 M NaOH was added, the samples were vortexed and placed in a block digester for 90 minutes at 85 °C. In

55

most cases the filter paper was completely digested after the 90 minutes and the solids resuspended in the NaOH. Two mL of the sample was removed and placed in small labelled glass vials for protein testing. Ten mL of TKN digestion reagent (200 mL H_2SO_4 and 134 g K_2SO_4 dissolved in 1000 mL distilled water) was then added to the digestion tubes and the samples further digested for 6.5 hours. After digestion, the samples were allowed to cool to room temperature, then diluted to 100 mL with distilled water, the samples were placed in the fridge at 4 °C until a TKN analysis was performed.

3.4 CO$_2$ Uptake Experiments

The change in the level of CO_2 in the gas headspace of the batch flasks was monitored over time in complex and defined MVH nutrient solutions. The initial and final biomass concentrations (TKN values) were also measured. Two types of experiments were conducted. One experiment monitored the change in CO_2 in bottles with and without support in the complex media, while the other experiment compared the CO_2 uptake rate in the complex and defined nutrient solutions. The purpose of the first experiment was to determine if recharging of the flasks with CO_2 would be required during the support studies, while the purpose of the second experiment was to observe if the type of nutrient media present in the bottles affected the CO_2 uptake rate.

In the first experiment, bottles were prepared with glass beads, Teflon pieces, molecular sieve, ceramic beads, zeolite and a control in the MVH nutrient solution, bottles were prepared in duplicate for each day of sampling. Each bottle contained 40 mL of nutrient solution and 1 mL of inoculum. The experiment was run for 6 days and samples were collected once daily for the duration of the experiment. The CO_2 in the bottles was measured using the Hamilton-Fisher Gas Partitioner Model 29.

The second experiment consisted of three separate runs, in the first run, three bottles with foam, basalt, and a control, respectively, were prepared in duplicate with MVH2 as the nutrient solution. Each bottle contained 40 mL of nutrient solution and 1 mL of inoculum. This experiment was run for 160 hours before being stopped due to temperature fluctuation problems with the incubator and a blockage that developed in the Shimadzu TOC Analyser Model TOC-500. The second run consisted of two bottles (without support) of MVH2 and MVH3 nutrient solutions, respectively, each prepared in triplicate. Each bottle contained 40 mL of nutrient solution and 1 mL of inoculum. Samples were collected 3 times a day for the first 12 days of the experiments, and 1-2 times a day for the duration of the experiment. A new calibration curve was prepared each time samples were collected. The MVH2 and MVH3 test was run for 800 hours. The third run consisted of bottles of MVH nutrient solution (without support) prepared in duplicate with one control bottle prepared as well.

Each bottle contained 40 mL of nutrient solution and 1 mL of inoculum, except for the control to which no inoculum was added. Samples were collected 3 times daily for the first 150 hours and then 1-2 times daily for duration of the test, this experiment was run for 350 hours. A new calibration curve was prepared each time samples were collected.

3.5 Analytical Methods

3.5.1 Total Solids and Volatile Solids

Total and volatile solids were measured in the set 1 experiments to monitor the increase in biomass over time. Total solids are considered the dry solids mass (contents) of the sample after drying at 103 °C, while volatile solids are considered the fraction of the total solids that volatilises at 500 °C. The difference between the total solids and the volatile solids would be the inorganic solids contents of the sample.

Dry weight measurements were conducted on filtered and washed samples. Initially 5 mL of sample was removed filtered and weighed, later the total medium volume in each flask was filtered and washed. Dilute nitric acid was used in an attempt to acidify and resuspend the metal sulphides; allowing them to pass through the filter paper, the acid wash was then followed by a rinse with distilled water. The samples were placed overnight in an oven at 103 °C, followed by storage in a desiccator until the weight was recorded. If the volatile solids were also being measured the sample was then placed in a Linberg Muffle Furnace at 500 °C for 1 hour, allowed to cool and then weighed. The sampling procedures utilised were adapted from the Section 2540: Solids in Standard Methods (Standard Methods, 1995). The Total and Volatile Solids Sampling Protocol outlines the method for sampling both total and volatile solids while the Total Solids Sampling Protocol was used when only total solids was measured.

Total and Volatile Solids Sampling Protocol

1. Pre-fire a ceramic crucible in a muffle furnace at 500 °C, for at least 1 hour.
2. Allow the crucible to cool to room temperature; either in the muffle furnace or in a crucible holding oven (set at ~ 30 °C).
3. Weigh the empty crucible.
4. Vigorously shake, by hand, the batch flasks.
5. Remove 5 mL of sample from the batch flasks with a wide bore pipette. (Repeat to collect 2 samples from each vial being sampled).
6. Place the crucible in the oven at 103 °C for 1 hour.

7. Remove the crucible and let cool to room temperature.
8. Weigh the crucible.
9. Place the crucible in the muffle furnace at 500 °C for 1 hour.
10. Allow the crucible to cool to room temperature; either in the muffle furnace or in a crucible holding oven (set at 30 °C).
11. Weigh the crucible.

Total Solids Sampling Protocol

1. Prefire ceramic or aluminium crucible in 500 °C oven for at least 1 hour.
2. Filter sample through 0.22 um membrane filter paper.
3. Rinse with one wash of dilute acid.
4. Rinse twice with distilled water.
5. Fire samples in 103 °C oven overnight.
6. Store in a desiccator until ready to record sample weight.
7. Record sample weight.

3.5.2 Total Kjeldahl Nitrogen (TKN) Assay for Biomass Determination

Organic nitrogen was used as an indirect correlation to the biomass in the batch flasks. Organic nitrogen is considered to be organically bound nitrogen in the trinegative state and as such does not actually include all organic nitrogen compounds, but does include most types of organic nitrogen. It does include proteins and peptides, nucleic acids, urea and many synthetic organic materials. From an analytical perspective, organic nitrogen and ammonia can be determined together and are usually referred to as "kjeldhal nitrogen". (Standard Methods, Section 4500: Nitrogen (Organic), 1995).

The total organic nitrogen (TKN) was measured with a Lachat Autoanalyzer QuikChem 800. TKN measures the inorganic and organic nitrogen in a system by converting all organically bound nitrogen, nitrates to ammonia. The level of ammonia in the sample is then measured as indication of the total nitrogen in the system. In this experiment the TKN value is taken to represent only the organically bound nitrogen and can be used as an indirect correlation to the total biomass in the system. All organic nitrogen is assumed bound within the cells of the bacteria being measured. Nitrate and ammonia that is present in the nutrient media will be water soluble.

Since the solution is filtered, followed by a slightly acidic water wash and then two washes with distilled water all of the nitrate, and ammonia that is in solution is assumed to be washed off the cells and through the filter paper. Any remaining nitrogen content is therefore based on organically bound nitrogen. To confirm this theory, nutrient solutions with no bacteria were rinsed through the filter papers and carried through the TKN analysis. No ammonia was expected to remain on the filter paper, since it is water soluble – the TKN values from these tests were used as blanks for the results, with the values being subtracted from the TKN values obtained from the sample results.

The TKN digestion protocol was adapted from Technicon Industrial Systems (1975), while the TKN analysis was adapted from a procedure provided by Lachat (1976).

TKN Sampling and Preparation Protocol

1. Place sample with dry filter paper into TKN digestion tubes.
2. Add 10 mL TKN digestion reagent.
3. Add 1-2 boiling chips to each digestion tubes.
4. Place samples in the digestion block.
5. Set low temperature dial at 120 °C for 3 hours.
6. Set high temperature dial at 350 °C for 3.5 hours.
7. Allow samples to cool to room temperature.
8. Dilute TKN samples to 100 mL.
9. Place samples and standards in sampling tubes for autoanalyser.

3.5.3 Total Protein (DC Bio-Rad Protein Assay)

The Bio-Rad DC protein assay is a colourmetric assay for protein concentration and is based on the Lowry Assay (Lowry et. al., 1951). It provides an indirect measurement of the biomass in the system. This assay was selected, as it is suitable for measuring proteins that have been solubilised in sodium hydroxide solutions up to 0.5 M NaOH. The DC Bio-Rad assay has been modified from the original Lowry Assay to allow for maximum colour development in 15 minutes and with a colour change of not more than 5% in one hour.

This is a two step procedure and is based on the reaction of protein in the samples with an alkaline copper tartrate solution and Folin reagent, which is a phosphomolybodate complex. In the first step, copper reacts with and binds to the protein in the alkaline media. In the second step, the copper treated proteins reduce the Folin reagent (Lowry et. al., 1951). The reduction of the Folin reagent results in the loss of oxygen atoms, which is the cause of the subsequent colour change observed. Maximum absorbance occurs at 750 nm and minimum absorbance at 405 nm. The total protein preparation and sampling procedure has been adapted from instructions provided by Bio-Rad.

Total Protein Preparation and Sampling Protocol

1. Place sample with dry filter paper into digestion tubes.
2. Add 10 mL 0.5 M NaOH to digestion tubes.
3. Place samples in digestion block.
4. Set low temperature dial at 90 °C for 1.5 hours.
5. Allow samples to cool to room temperature.
6. Remove 2 mL of samples for protein test (use remaining for TKN test).

Testing (adapted from the Bio-Rad Procedure):
1. Resuspend bovine gamma globulin protein standard in 0.5 M NaOH.
2. Pipette 100 µL of standard or sample into clean, dry test tube (if necessary, dilute samples by adding 50 µL of sample with 50 µL NaOH).
3. Add 500 µL reagent A (an alkaline copper tartrate solution) and mix well.
4. Add 4.0 mL reagent B (dilute Folin Reagent) and mix well.
5. Incubate at room temperature for 15 – 20 minutes (note that the colour remains relatively constant from 15 – 60 minutes with about a 5% decrease in colour over this time period).
6. Measure OD at 750 nm.
7. Determine concentration of protein standard by plotting standards vs. OD_{750} and then comparing with OD_{750} from samples.

3.5.4 Sulphate Analysis

Two techniques were used to measure sulphate: the barium chloride turbidmetric method and the methylthymol blue colourimetric method.

Turbidimetric Method

Sulphate concentrations were measured from procedure outlined in Section 4500 SO_4 E: Turbidimetric Method (Standard Methods, 1995). The optical density was measured using a Miltron Roy Spectronic 20D spectrophotometer. In this method, sulphate ions are precipitated in an acetic acid medium with barium chloride. The sulphate reacts with the barium forming barium sulphate that appears as a white cloudy suspension in solution. The absorbance value is then recorded at 420 nm and compared to the absorbance values recorded for sulphate standards to determine the sulphate concentration in the samples.

Methylthymol Blue Method

Sulphate concentrations were measured using a Lachat Autoanalyzer QuikChem 8000. The method employed was based on colourimetric changes measured at 460 nm. The analysis method was adapted from written instructions provided by the Lachat Company (1994). As well as procedures outlined in Section 4500 SO_4 F: Automated Methylthymol Blue Method (Standard Methods, 1995)

In this analysis, barium is reacted with methylthymol blue (MTB) in an ethanol solution to form a blue complex. The sample, containing sulphate, is next reacted with the ethanol barium-MTB solution. The sulphate displaces the MTB forming barium sulphate and uncomplexed MTB. Sodium hydroxide is added to the solution to raise the pH, which allows for the measurement of the uncomplexed MTB that is grey in colour. A summary of the reactions is shown below:

$$\text{Barium} + \text{MTB} \rightarrow (\text{Barium-MTB})_{complex} \qquad (3.1)$$

$$(\text{Barium-MTB})_{complex} + \text{sulphate} \rightarrow (\text{Barium-sulphate})_{complex} + \text{MTB} \qquad (3.2)$$

$$\text{MTB} + \text{NaOH} \rightarrow \text{MTB}_{grey} + \text{pH}\uparrow \qquad (3.3)$$

Since one mole of sulphate directly displaces one mole of MTB, the change in colour monitored provides a direct correlation to the sulphate concentration in the sample.

Preparation and Collection of Sulphate Samples

1. Filter sample through 0.22 um Millipore (Durapore) filter paper.
2. Collect filtrate in 15 mL test tube.
3. Adjust filtrate to pH 2 with concentrated HCl.
4. Store in fridge at 4 °C until testing (not to exceed 28 days).
5. Dilute samples before measuring sulphate concentration (approximately200× using the turbidmetric method and 100× using the methylthymol blue method).
6. Prepare standards in the range of 0-100 ppm sulphate.

3.5.5 Gas Analysis/CO_2 Monitoring

The Fisher-Hamilton Gas Partitioner (CA# 11-127) was used to monitor the CO_2 in flasks of the set 1 experiments with molecular sieve, ceramic beads, Teflon, zeolite, and the glass beads. The Shimadzu TOC Analyser Model TOC-500 was used to monitor the CO_2 for the nutrient uptake experiments.

CO_2 Measuring Technique

To use the gas partitioner 0.5 ml of sample is injected using a 1 mL Hamilton Luer-Lok gas tight syringe into the analyser. To use the TOC analyser 25, 50 Or 100 µL of samples is injected using a 25 or 100 µL Hamilton Luer-Lok gas tight syringe into the analyser. The CO_2 values for the gas partitioner are quantified by comparing the total peak area to the CO_2 peak area, providing a percentage value of CO_2 in the sample. The CO_2 values for the TOC analyser are quantified by comparing the CO_2 peak area to a standard curve produced by injecting known amounts of CO_2 into the analyser.

Fisher-Hamilton Gas Partitioner Model 29

The gas partitioner is a gas chromatograph that has been specifically designed to quantitatively measure substances which, are in the gas phase at room temperature. The gas partitioner has a dual-column, dual-detector chromatograph that can separate and monitor carbon dioxide, oxygen, nitrogen, methane, hydrogen sulphide and carbon monoxide.

A continuous flow of helium gas is used as the carrier gas to sweep the samples through the two columns. The columns are packed to selectively hinder the passage of various components in the sample, resulting in the separation of the gases and elution through the system at different times. A detector senses and produces an electrical signal as each component is eluted through the columns. The electrical signal is sent to a recorder where it is recorded as a measurable peak. The height of the peak is proportional to the gas concentration; since a component will always emerge at the same time from the column, the elution time can be used to characterise a particular gas.

Shimadzu TOC Analyser Model TOC-500

The total organic carbon (TOC) analyser combusts samples to CO2 and water at different temperatures and measures the CO_2 produced. It measures total carbon (TC), inorganic carbon (IC), volatile organic carbon (VOC) and total organic carbon (TOC). The samples for TC analysis are passed through an oxidation catalyst and heated to 680 $^{\circ}$C, whereas for the determination of IC, samples are passed through a reaction tube (without a catalyst) at 150 $^{\circ}$C. TOC is the difference in value between the TC and the IC measurement. VOC are composed of low boiling point organic carbons, which evaporate at temperature below about 90 $^{\circ}$C. The IC reaction tube can be used to determine the VOC content if the sample is already well characterised.

The TOC analyser utilises an infrared (IR) detector to measure the CO_2 concentration in the gas. Monatomic molecules such as N_2, O_2 and H_2, which may be present in the gas phase do not absorb IR energy. The amount of IR energy absorbed by the CO_2 present in a sample is

proportional to the gas density and hence concentration of the CO_2 in the sample, according to the Beer-Lambert Law.

A calibration curve was established by injecting known volumes of CO_2 into the TOC analyser and recording the resultant peak area. A syringe was used to withdraw a known volume of gas from the headspace of the sample vials and then injected into the TOC analyser, the resultant area was compared to the calibration curve to establish the volume of CO_2 in the headspace of the batch flasks.

The CO_2 calibration curve was produced by injecting known volumes (and hence concentrations) of CO_2 into the analyser. Medical grade CO_2 was used to establish the CO_2 calibration curve. A section of tubing was attached to the CO_2 cylinder; the tubing was then clamped onto a gas blown bubble. The glass bubble had a rubber septum attached to the top and two stopcocks on either side, tubing was attached to both stopcocks, and one section connected to the gas cylinder and the other placed in a flask with water. Once an adequate flowrate was established – a syringe was pushed through the septum, flushed with CO_2 and then filled to a known volume.

TOC Analyser CO$_2$ Injection Protocol

1. Open the carrier air valve and adjust flow to 150 mL/min.
2. Switch the Main Furnace Oven button to ON.
3. Allow the equipment 1 hour to warm up.
4. Open the CO_2 regulator valve and observe gas bubble percolating through water. Adjust the gas flow until the bubbles are steady but not causing violent bubbling.
5. Flush gas tight syringe with CO_2 and then fill slightly greater than required volume of CO_2.
6. Just before injecting – expel excess CO_2 from syringe.
7. Prepare a standard calibration curve by injecting known volumes (15,10,5, 0 µL) of CO_2 into the TOC analyser of CO_2. Inject each volume in duplicate, or until reproducible areas result.
8. Remove samples form incubator.
9. Inject syringe carefully through the butyl rubber septum of the batch flask and then pump syringe twice. Fill syringe to just past 25 µL.
10. If the area reading is less than the area reading for the 5 µL standard, repeat step 9 using a 50 µL gas sample.

11. Just before injecting – expel excess gas from syringe.
12. Inject sample into the TOC analyser

3.5.6 Scanning Electron Microscope Imaging

The scanning electron microscope images provide the opportunity to visually observe how the sulphate reducing bacteria are adhering to and colonising the different support media being examined. The SEM generates images by shooting a beam of electrons at the surface to be imaged. Electrons are then either backscattered or given off (secondary electrons) by the gold coated specimen. The beam is slowly scanned across the specimen until an area has been imaged by the microscope (Postek et. al., 1980). A Hitachi S-4100 FE SEM (field emission scanning electron microscope) was used to capture the photos.

Before a sample is placed in a SEM it must be prepared properly. This includes fixing the sample, drying the sample, and coating the sample with a conductive material. The fixation protocol for preparing the SEM samples was established with the help of Elaine Humphreys in Biological Sciences (Humphreys, 1999).

Preparation of Samples (Fixation Protocol)

1. Warm up fixing solution, 2.5 M glutaraldehyde solution in a 0.1 M cacodylate buffer at pH 7.0, to 32 °C.
2. Place samples in fixing solution for 30 minutes.
3. Wash samples with 0.1 M cacodylate buffer 3 times for 5 minutes each.
4. Place samples in 0.1 M OsO_4 solution and allow to sit for 30-60 minutes. (The OsO_4 is extremely toxic and should be handled strictly in a fumehood and with gloves).
5. Rinse 1-2 times with distilled H_2O.
6. Dehydrate the sample with successive ethanol solutions of 30%, 50%, 70%, 85%, 95%, and three times with 100% ethanol. Each wash is 5 minutes in duration.
7. Critical Dry Point samples with CO_2.
8. Sputter coat samples with gold.

CHAPTER 4: RESULTS AND DISCUSSION

4.1 SRB Growth in Different Nutrient Media

4.1.1 Nutrient Solution Tests

The nutrient solution tests were divided up into two sections – initially a suitable complex nutrient solution was tested that would allow for active autotrophic growth of SRB in a time period of about 3 days. This nutrient solution was used in the first set of support experiments. The second set of nutrient solution tests, compared defined media for SRB growth. Six nutrient solutions were compared in total. Growth of SRB was considered to have occurred if blackening was observed in the growth vials. The first set (set 1) of support material experiments was carried out in the MVH nutrient solution, while the second set (set 2) of support material experiments was carried out in the MVH2 nutrient solution.

A typical complex nutrient solution for heterotrophic growth of SRB would consist of: 0.5 g/L KH_2PO_4, 1 g/L NH_4Cl, 1 g/L $CaSO_4$, 2 g/L $MgSO_4 \cdot 7H_2O$, 3.5 g/L sodium lactate, 1 g/L yeast extract, 0.1 g/L ascorbic acid, 0.1 g/L thioglycolic acid, 0.5 g/L $FeSO_4 \cdot 7H_2O$ (Postgate, 1984). Initially three complex nutrient solutions were compared: the Biomet, Ethanol and MVH recipes. A complete description of these nutrient solutions can be found in Table 3.1: Nutrient Solutions. Blackening was observed within 3 days with the MVH solution, 5 days with the ethanol solution and only minimal growth was noticed after 21 days with the Biomet solution. The MVH solution was selected as the most suitable nutrient solution for the set 1 experiments since blackening was observed more rapidly in this nutrient solution than the others, as well the ethanol solution was discarded since it provides a readily available carbon source other than CO_2 for the SRB. Although the goal of the project was to study the growth of SRB under autotrophic conditions, the ethanol media was initially included to confirm the

68

viability of the obtained culture in case no growth was observed with the MVH and Biomet recipes.

The second set of nutrient experiments compared the growth of SRB in more defined modifications of the MVH media. Solutions were made up with yeast extract only, bactopeptone only and one solution with neither yeast extract nor bactopeptone (as indicated in Table 4.1: Addition of Yeast and/or Bactopeptone to Nutrient Solutions). The purpose of the defined media is to exclude carbon sources other than CO_2 to the SRB, and to minimise the amounts of yeast extract and bactopeptone, which may interfere with the protein assay used during the set 2 experiments.

Table 4.1: Addition of Yeast and/or Bactopeptone to Nutrient Solutions

	MVH	MVH2	MVH3	MVH4
Yeast	+	-	+	-
Bactopeptone	+	-	-	+

+ indicates addition of substance
– indicates substance omitted

Table 4.2: Blackening as an indication of Activity in Nutrient Solutions

	MVH	MVH2	MVH3	MVH4
Observation*	Rapid blackening by day 3	Some blackening by day 4-5, complete blackening by day 6-7	Rapid blackening by day 3	Rapid blackening by day 3

*all tests performed in triplicate

Based on the results shown in Table 4.2, SRB can grow adequately without the addition of yeast or bactopeptone as nutrients. As expected, the defined media required more time before blackening occurred.

4.1.2 Comparison of MVH, MVH2, MVH3 Nutrient Solutions

The observation of blackening in the nutrient solution tests provided a visual determination of growth in the different media but did not allow a quantitative comparison between the growth differences in the MVH, MVH2 and MVH3 nutrient solutions. In order to do this biomass samples were collected and analysed for TKN to provide an indication of how quickly the SRB grew with and without the presence of yeast extract and bactopeptone. The

69

MVH4 solution was not studied further at this point since it is more common to add yeast extract to nutrient solutions and there was no observed differences in activity between it and the MVH3 solution. The initial and final TKN values for the three nutrient solutions are listed in Table 4.3. Shown in Figure 3.1 are the plots of the natural logarithm of TKN versus time; it can be noticed that the solution with the greater amount of yeast and bactopeptone had a faster initial growth.

Table 4.3: TKN values for the SRB in three MVH solutions

	MVH		MVH2		MVH3	
	(μg N)	SD	(μg N)	SD	(μg N)	SD
Initial TKN	45	---	<20[+]	11	<20[+]	11
Final TKN*	785	---	181	25	256	11

[+]Initial TKN values are based on the values from the blank which had greater values than initial MVH2, and MVH3 TKN values

The MVH2 and MVH3 solutions were allowed to run for 1.5 months and TKN values were also measured at this times, the values were 402 and 369 μg N respectively. These samples were not run in duplicate however, so the confidence interval cannot be stated for these numbers. Based on the approximate error (4-11%) in the final values, shown in Table 4.3, the final error could be expected to be about $\pm$ 44 μg N.

The addition of yeast and bactopeptone has been noted to act as jump start for the SRB growth but is not strictly required (Widdel and Bak, 1992). The final values measured are as expected, based on this, since the MVH nutrient solution with the complex media had the fastest specific growth. It also produced the largest concentration of biomass, which may be due to extra available carbon present in the yeast extract and bactopeptone. The MVH3 solution has yeast extract (but no bactopeptone) and a final TKN value of 256 μg N while the MVH2 solution has a final TKN of 181 μg N on day 14. The higher value for the MVH3 compared to the MVH2 solution may due to the addition of the yeast extract.
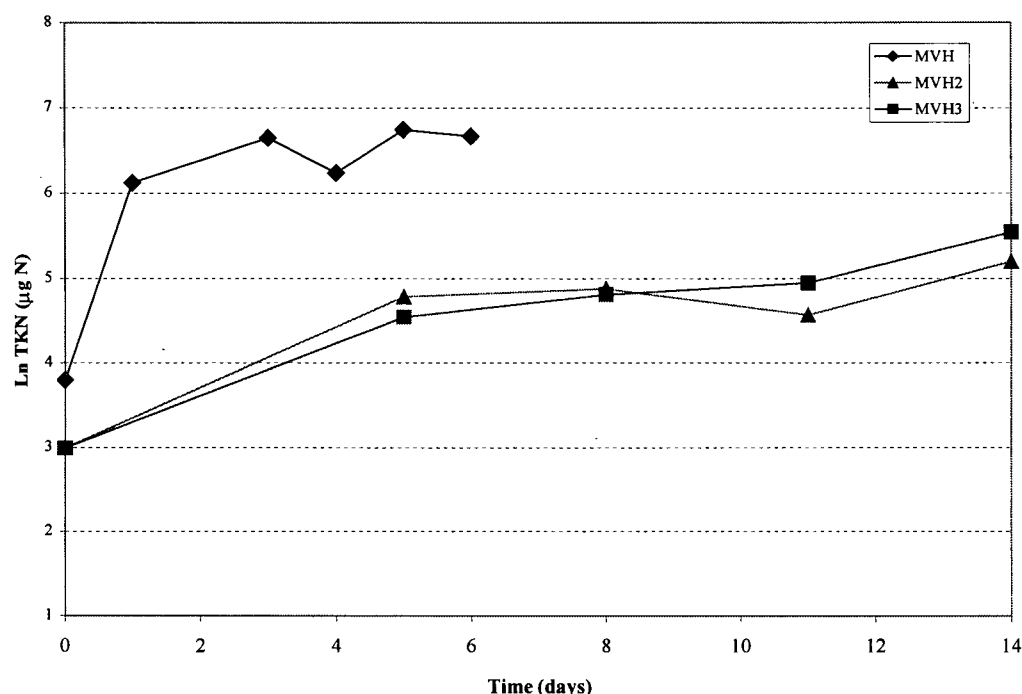
Figure 4.1: First Order Growth Comparison of MVH Nutrient Solutions.

Note: The specific growth of each solution was taken from the slope between points 1 and 2. The values determined were 0.097, 0.015, and 0.013/h for the MVH, MVH2, and MVH3 solutions, respectively.

Table 4.4: Summary of Nutrient Solution TKN and Sulphate Results

	TKN			
	$T_T=T_F-T_I$ $\mu g\ N$	Biomass, X_T mg	$(dSO_4/dt)/X_T$ mg/(L.h.mg)	Yield, Y_{SO_4} g X_T/mol SO_4 reduced
MVH	740	6.50	2.31	8.47
MVH2	161	1.41	2.41	5.59
MVH3	236	2.07	0.85	10.06
	Sulphate			
	dSO_4/dt mg/(L.h)	Initial mg/L	Final mg/L	Reduced mol x 10^{-04}
MVH	15.04 ± 2.79	4117	2318	7.68
MVH2	3.42 ± 0.75	3405	2812	2.53
MVH3	1.75 ± 0.44	3360	2878	2.06

The TKN and sulphate reduction data for the three nutrient solutions are summarised in Table 4.4. The final TKN values follow the expected trend with MVH>MVH3>MVH2. The biomass is calculated based on the assumed mass fraction of nitrogen in one mole of

biomass. The chemical formula is represented by $CH_{1.8}O_{0.5}N_{0.2}$ (Roels, 1983). The conversion from µg N to mg Biomass then is:

Equation 4.1

$$\text{mg } Biomass = TKN(\mu g\, N) \times \left(\frac{24.6}{2.8}\right) \times \left(\frac{1\,\text{mg}}{1000\ \mu g}\right)$$

The specific sulphate reduction rate was determined by dividing the change in sulphate over time by the biomass concentration. This normalises the data between the systems, since a higher initial inoculum concentration would result in a greater amount of sulphate reduced. The values for MVH and MVH2 solutions are similar ranging from 2.31-2.42 mg/(L.h.mg biomass); the value for the MVH3 solution is lower and has a value of 0.85 mg/(L.h.mg biomass). Another method of determining the activity of the bacteria is to establish the growth yield, Y_{SO_4}, this is the mass of biomass produced per mol of sulphate reduced. The growth yield can be shown as:

Equation 4.2

$$Y_{SO_4} = \frac{(X_F - X_I)}{([SO_4]_I - [SO_4]_F) \times V}$$

Where Y_{SO_4} = molar growth yield (g biomass/ mol sulphate),

X = the mass of biomass (g),

V = the volume of solution in the batch flasks (L),

and [SO_4] = the sulphate concentration (mol/L).

The yield coefficients determined range from 5.59-10.06 g/mol SO_4. These values correspond well with previously published research, which had yield coefficients ranging from 4-12.2 g/mol SO_4 in systems using hydrogen as the electron donor (Badziong and Thauer, 1978, Cypionka and Pfennig, 1986). Slightly higher values, ranging from 11-13.5 g/mol SO_4 have been reported in systems using a defined lactate nutrient media, as shown in Table 4.5.

Table 4.5: Yield Coefficients of SRB with Sulphate as electron acceptor

Species	Growth Yield, Y_{SO_4} g /mol SO_4	pH	Nutrient Type	Continuous or Batch	Source
Desulfovibrio vulgaris (Marburg)	4-5	7.2	Hydrogen, Acetate and CO_2	Continuous	Badziong and Thauer, 1978
Desulfovibrio vulgaris (Marburg)	8.3	6.5	Hydrogen, Acetate and CO_2	Continuous	Badziong and Thauer, 1978
Desulfovibrio vulgaris (Marburg)	13.5	7.1	Defined Lactate Sulphate Medium	Batch	Ingvosen and Jorgensen, 1984
Desulfovibrio sapovorans	11.0	7.1	Defined Lactate Sulphate Medium	Batch	Ingvosen and Jorgensen, 1984
Desulfovibrio salexigens	12.0	7.1	Defined Lactate Sulphate Medium	Batch	Ingvosen and Jorgensen, 1984
Desulfotomaculumn orientis	6.6-7.5	6.95	Hydrogen Basal Mineral Medium w/ 1mmol acetate/L	Batch	Klemps et. al., 1985
Desulfotomaculumn orientis	8.5-12.2	6.85	Hydrogen and CO_2, Basal Mineral Medium	Continuous	Cypionka and Pfennig, 1986

4.1.3 CO_2 Monitoring

The CO_2 level in the headspace of the bottles was monitored, with the Shimadzu TOC analyser, over time to observe the rate of decrease in CO_2 over the duration of the experiment. A decrease in CO_2 was taken as an indication that the SRB were utilising it as a carbon source for cell synthesis. A previous study, using radioactively labelled CO_2, showed that in a batch system with H_2 as the electron donor and CO_2 available as the carbon source, 90% of the cell carbon could be attributed to CO_2 (Klemps et. al., 1985).

Complex nutrients such as yeast extract and bactopeptone while not required for growth can stimulate it, by providing extra micronutrients and carbon for cell synthesis (Widdel and Bak, 1992). Thus, it might be expected that the nutrient solution with the yeast extract and bactopeptone will show a faster rate of CO_2 uptake. The CO_2 uptake rates for the MVH, MVH2 and MVH3 nutrient solutions are shown in Figure 4.2, Figure 4.3, and Figure 4.4, and as predicted, the systems with the bactopeptone and/or yeast extract did display faster rates of CO_2 uptake.

73

Interestingly, however is that there appears to be a large lag phase in the complex nutrient solution (MVH) of about 150 hours before the CO_2 level begins to decrease. A similar lag phase from about 100-200 hours is also noticed with the MVH3 experiments, while a shorter lag phase, between 50-75 hours, is apparent with the MVH2 nutrient solution. It is likely that the SRB first utilise the most readily available carbon source, which is provided by the yeast and/or bactopeptone present in the MVH and MVH3 solutions. The MVH2 solution has no other sources of carbon present and in order to grow the SRB must utilise the CO_2 available. As Figure 4.2, Figure 4.3 and Figure 4.4 also show the rate of CO_2 uptake, was initiated in the order of MVH>MVH3>MVH2. The CO_2 experiments confirm that complex nutrients can stimulate growth but also show they are not necessary for growth to occur.

As well, it should be noted that CO_2 measurements were taken from replicate bottles on each day of sampling. Both the MVH and MVH2 replicates had similar uptake rates, respectively. However, in the case of the MVH3 replicates, 2 of the 3 prepared bottles had similar uptake rates, while the third bottle had a slightly longer lag phase and a slower uptake rate. It is possible that a smaller volume of SRB inoculum was added to this bottle, which might account for the slightly lower uptake rate.

Table 4.6: CO_2 Uptake Experiment - Final TKN Values

Solution	Time* (hours)	TKN X (mg)	μg N	SD
MVH	400	4.9	558	25
MVH2	900	3.5	402	35
MVH3	900	3.2	369	42

*Time at which samples were measured

The TKN values were measured at the end of the experiments, this corresponds to 400 hours for the MVH solution and 900 hours for the MVH2 and MVH3 solutions. The results are listed in Table 4.6. The SRB growth in the MVH solution had the highest biomass concentration at 4.9 mg, which is attributed to the additional carbon in the yeast and bactopeptone. The MVH3 and MVH2 values are similar 3.2 and 3.5 mg, respectively.
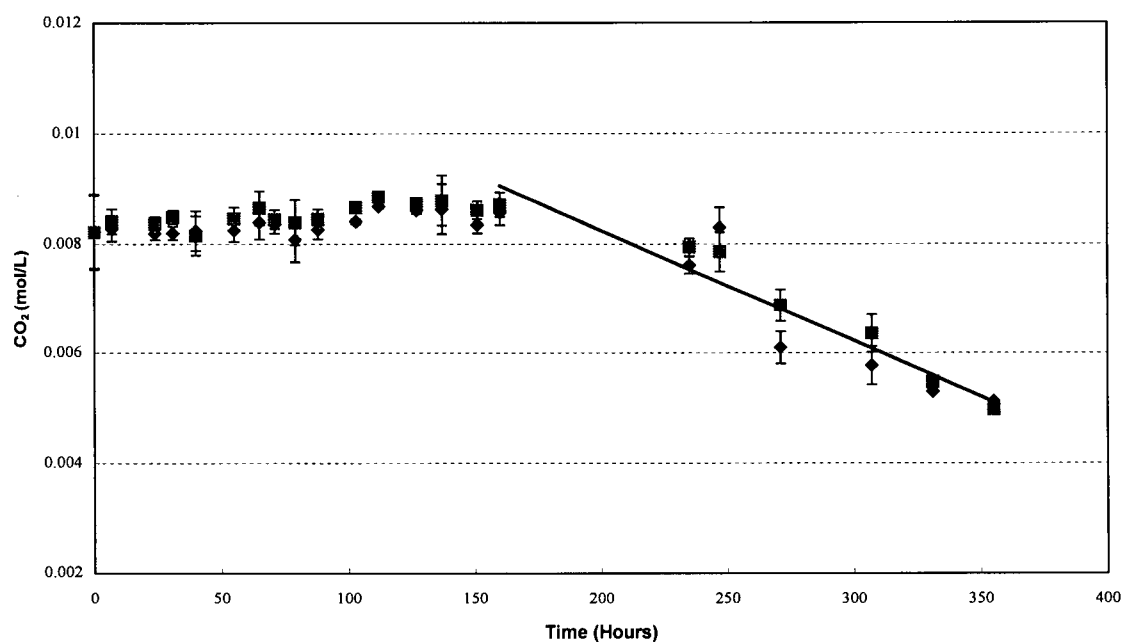
Figure 4.2: CO_2 Uptake in MVH Nutrient Solution.

Note: T = 31 ^{O}C, the CO_2 uptake starts at around 150 hours and decreases at a rate of 1.81 x10^{-05} mol CO_2/(L.h). The error bars represent the standard deviation determined in the calibration curve on each day of sampling.
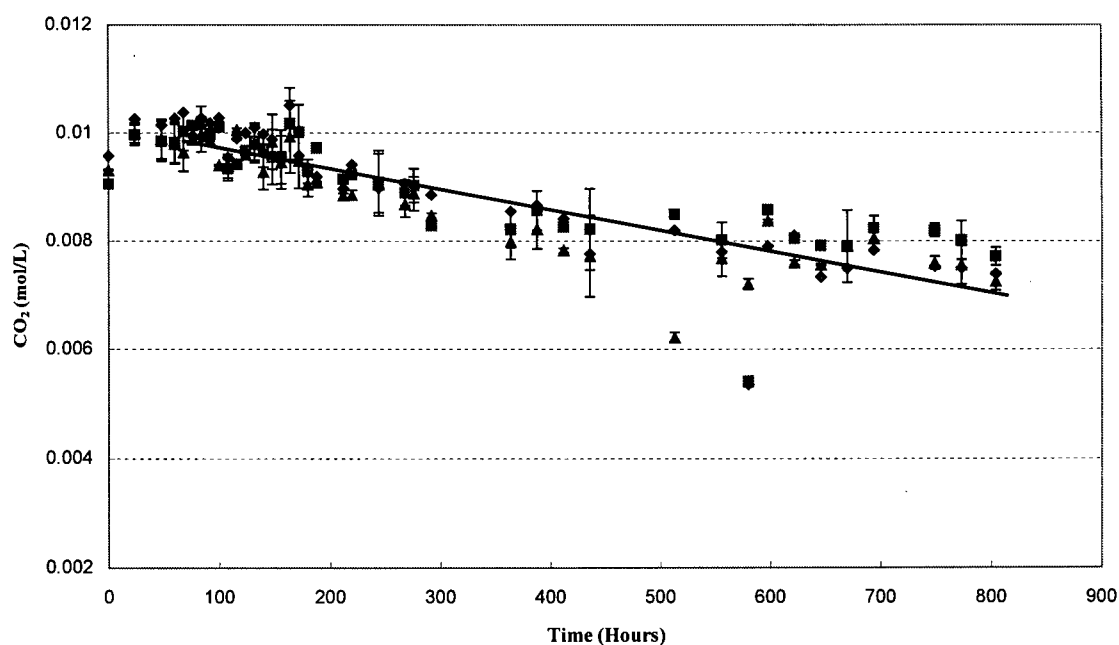
Figure 4.3: CO_2 Uptake in MVH2 Nutrient Solution.

Note: T = 31 ^{O}C, the CO_2 uptake starts between 50-75 hours and decreases at a rate of 0.38 x10^{-05} mol CO_2/(L.h). The error bars represent the standard deviation determined in the calibration curve on each day of sampling.

75
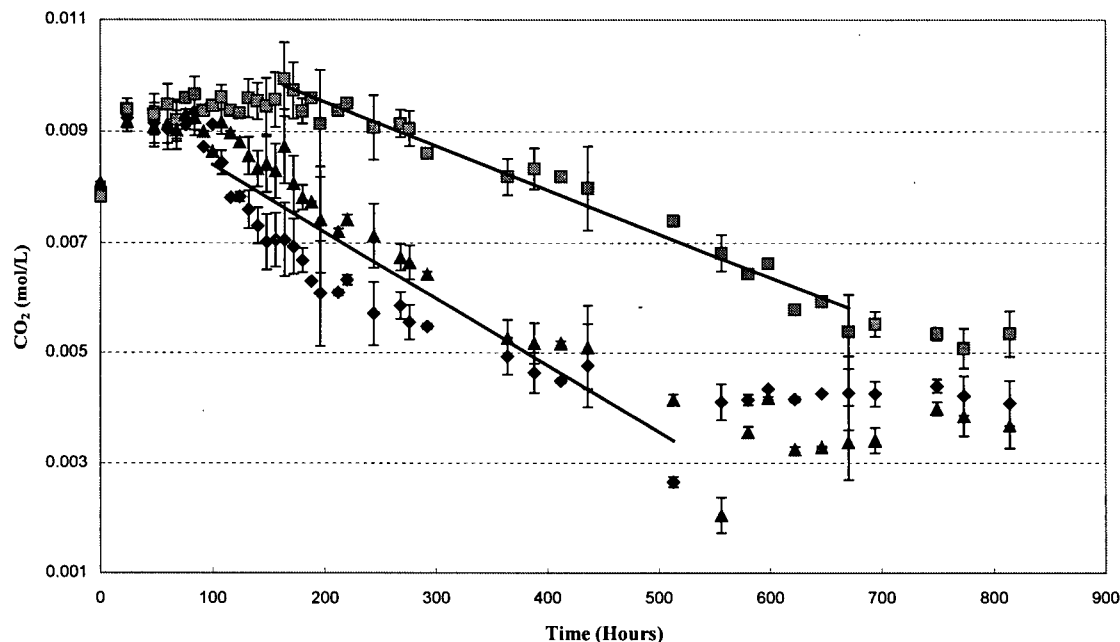
Figure 4.4: CO₂ Uptake in MVH3 Nutrient Solution.

Note: T = 31 °C, the CO₂ uptake starts at about 100 hours for the lower curve at a rate of 1.12 x10⁻⁰⁵ mol CO₂/(L.h), while the CO₂ uptake starts at about 200 hours for the upper curve at a rate of and decreases at a rate of 0.75 x10⁻⁰⁵ mol CO₂/(L.h). The error bars represent the standard deviation determined in the calibration curve on each day of sampling.

It is not possible to report the values in terms of a Yield Coefficient, Y_{CO_2}, since not all of the carbon utilised in the systems with complex media would have come from the CO_2 available. In particular, both the MVH and MVH3 solution had other sources of carbon available due to the addition of the yeast extract and bactopeptone. It is interesting to note that the overall change in the CO_2 was similar for the different nutrient solutions (refer to Table 4.7). However, it must be pointed out that the following assumptions were made: the final time CO_2 activity was observed for both the MVH and MVH2 solutions corresponds to the last time a sample was taken and it was assumed that CO_2 uptake stopped at that time. If the experiments had been run for a longer period of time the change in CO_2 would likely be greater than the values reported. As well, as no other data measuring CO2 uptake rates was found in literature it was not possible to compare the CO_2 uptake rates to other data.

Table 4.7: Change in CO_2 level during Nutrient Solution Experiments

Solution	Rate of CO_2 Uptake mol CO_2/(L.h) $\times 10^{-05}$	Initial Time CO_2 Activity Observed (h)	Final Time CO_2 Activity Observed (h)	Change in CO_2 (mol/L)
MVH	1.81 ± 0.24	150	350	0.004
MVH2	0.38 ± 0.03	50	800	0.003
MVH3	1.12 ± 0.04	100	500	0.004
MVH3	0.75 ± 0.03	200	675	0.004

4.2 Set 1: Growth on Support Materials: Glass, Molecular Sieve, Ceramic Beads, Teflon and Zeolite

The main purpose of the set 1 experiments was to determine if the selected analytical techniques were appropriate methods to monitor the biomass and sulphate concentrations present in the batch flasks. This was accomplished by comparing the results to previously published data.

4.2.1 Solids

Total solids were measured in one experiment with glass beads and a control. In a second experiment total solids was measured for the following supports: glass, molecular sieve, ceramic beads and zeolite. Both experiments were carried out with the complex MVH nutrient solution. The first experiment involved collecting 5 mL samples from the 40 mL nutrient solution, the total biomass was estimated by multiplying the sample weight (expressed in mg/mL) by the total sample volume. The total solids were observed to increase over the first 6 days but then decreased on the 7th day of sampling (refer to Table 4.8). The overall change in the total solids is small and it is unclear if any growth is occurring.

Table 4.8: Total Solids Results

Time (days)	Control (No Support)		Glass Beads	
	Solids (mg)	SD	Solids (mg)	SD
3	46.1	0.4	45.2	0.1
4	48.6	0.2	47.4	0.2
6	52.5	0.4	49.3	0.4
7	44.0	0.1	44.8	0.3

In the second experiment, the entire volume of the sample was filtered, instead of just 5 mL. This was to remove any error in the total solids that may arise due to a lack of homogeneity in the sample volume collected for analysis. As shown in Figure 4.5, the total solids data was scattered and an increase in biomass over time was not observed. Volatile solids measurements, were also monitored during this experiment, however the numbers were

78

below the method detection limit (0.01 mg). The standard deviations for the solids data plotted in Figure 4.5 ranged from 0.4–10 mg, also indicating that the data should be considered with scepticism.
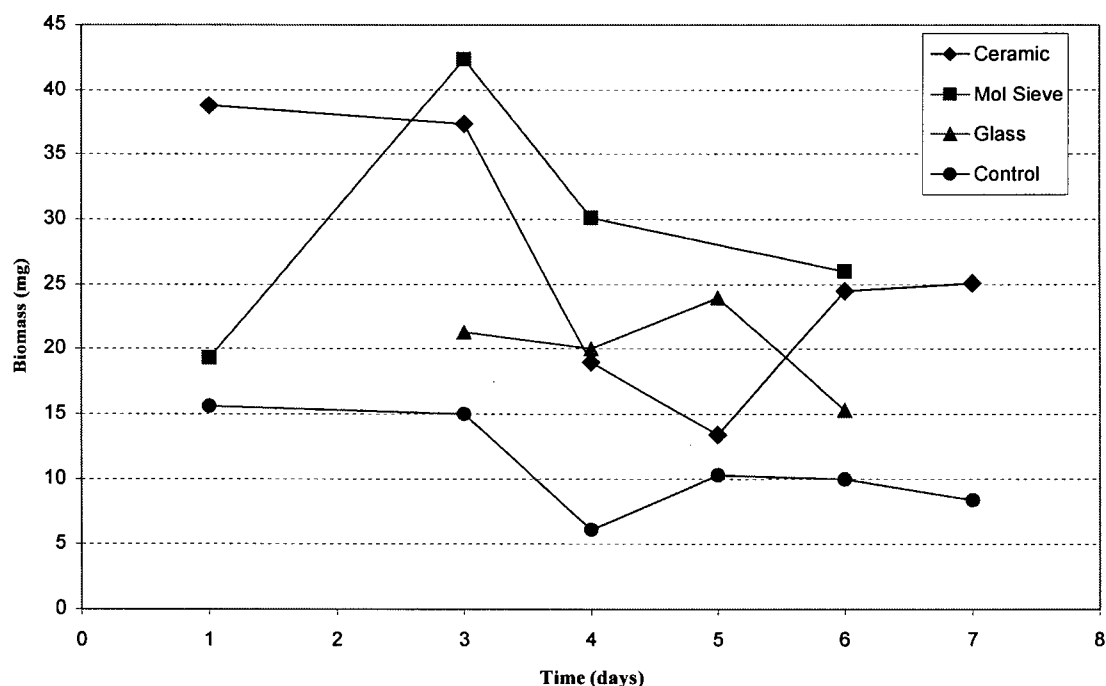
Figure 4.5: Total Solids Results for the Set 1 Experiment Support Surfaces.

The procedure for collecting the solids samples is outlined in Section 3.4.2. The collected solids samples were washed with dilute nitric acid to acidify and resuspend the metal sulphides; allowing them to pass through the filter paper. The main reason for the error in the data may have to do with the amount of mass collected, compared to the weights of the crucibles. Ceramic crucible were used for these experiments and weighed between 18-20 grams each while the final dry weight of the sample was in the order of 0.01-0.04 grams, making it difficult to obtain an accurate weight for the SRB samples. The problems here were also encountered during another project utilising SRB (Pierre Berube, personal communication, 1998). To compensate for this problem, aluminium crucibles, which are lighter in weight, could be used. Although the total volume in the flask was filtered to collect the biomass, a larger initial inoculum could be used to increase the amount of biomass in the sample.

4.2.2 Growth Curves using TKN Measurements

TKN was used as an indirect correlation to the biomass in the batch flasks. The increase in the natural logarithm of TKN over time for the set 1 experiments is shown in Figure 4.6 (control and glass beads), Figure 4.7 (Teflon and zeolite) and Figure 4.8 (molecular sieve and glass beads). The error bars displayed in the figures are based on the standard deviation of the samples. The results from this portion of the experiments show an increase in biomass, or organic nitrogen, over time. The nutrient solution for the set 1 experiments was the MVH solution. By plotting the natural logarithm of the TKN value over time, the specific growth rate, μ, can be determined. A straight line is expected from this type of plot during the exponential growth phase of the SRB (as discussed in the Literature Review Section: Cell Kinetics in a Batch System). The specific growth rates and doubling times of the SRB determined in this experiment are listed in Table 4.9.

The data for the molecular sieve and the ceramic beads support materials appears to follow a first order trend over the duration of the experiment with covariance values of 0.99 and 0.99, respectively, for the first order trend lines fitted to the data. This indicates that the substrates are in excess and that the bacteria are in the growth phase. The covariance values for the first order fits to the zeolite and Teflon data are 0.99 and 0.93, respectively. The MVH control follows a linear trend for the first days and then appears to plateau indicating the bacteria have become substrate limited and are in the stationary phase. The glass support follows a similar trend as the control. The specific growth rates for the control and glass are each based on their respective first two data points as this appears to be the exponential growth phase for these systems – in these cases monitoring more samples would have been desirable to confirm the rapid increase in initial TKN.
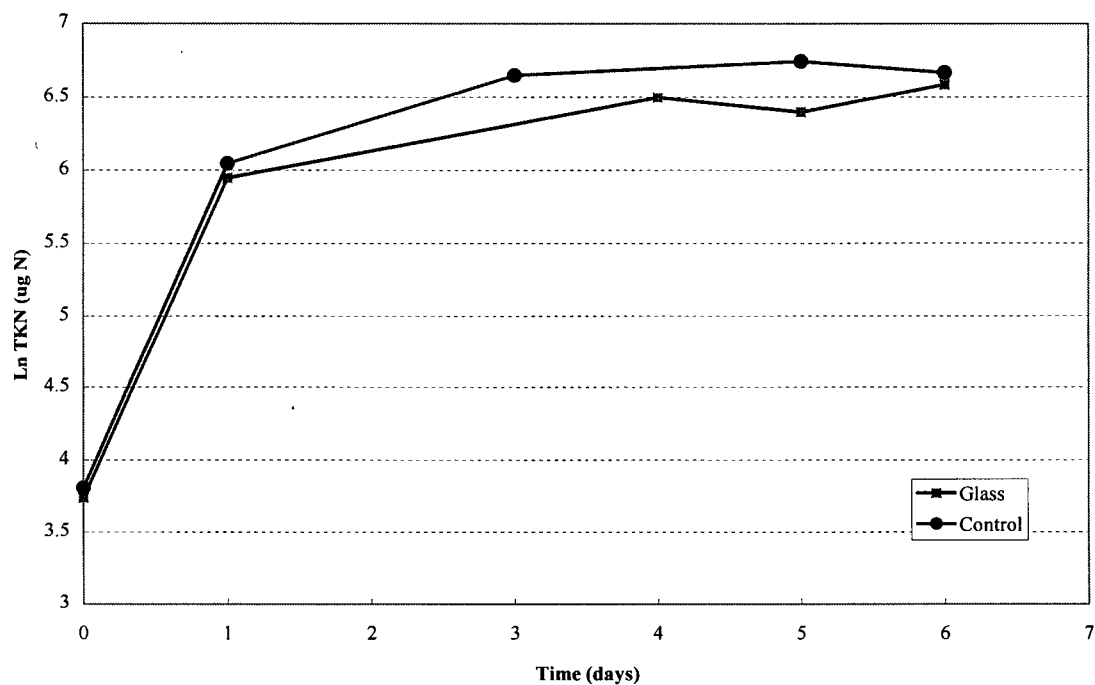
Figure 4.6: Control and Glass Bead Support Growth Curves.

Note: T=31 °C, grown in complex MVH nutrient solution, μ = 0.096 and 0.089 h^{-1} for the control and glass beads, respectively.
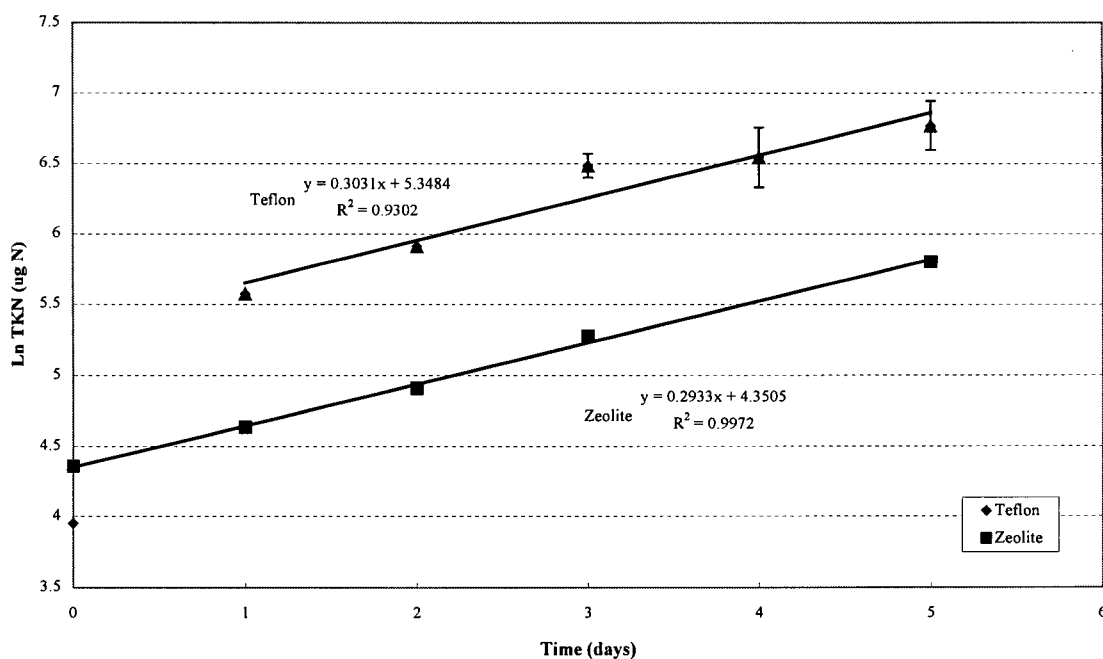
Figure 4.7: Teflon and Zeolite Support Growth Curves.

Note: T=31 °C, grown in complex MVH nutrient solution, μ = 0.0126 and 0.0122 h^{-1} for the Teflon and zeolite, respectively.

81
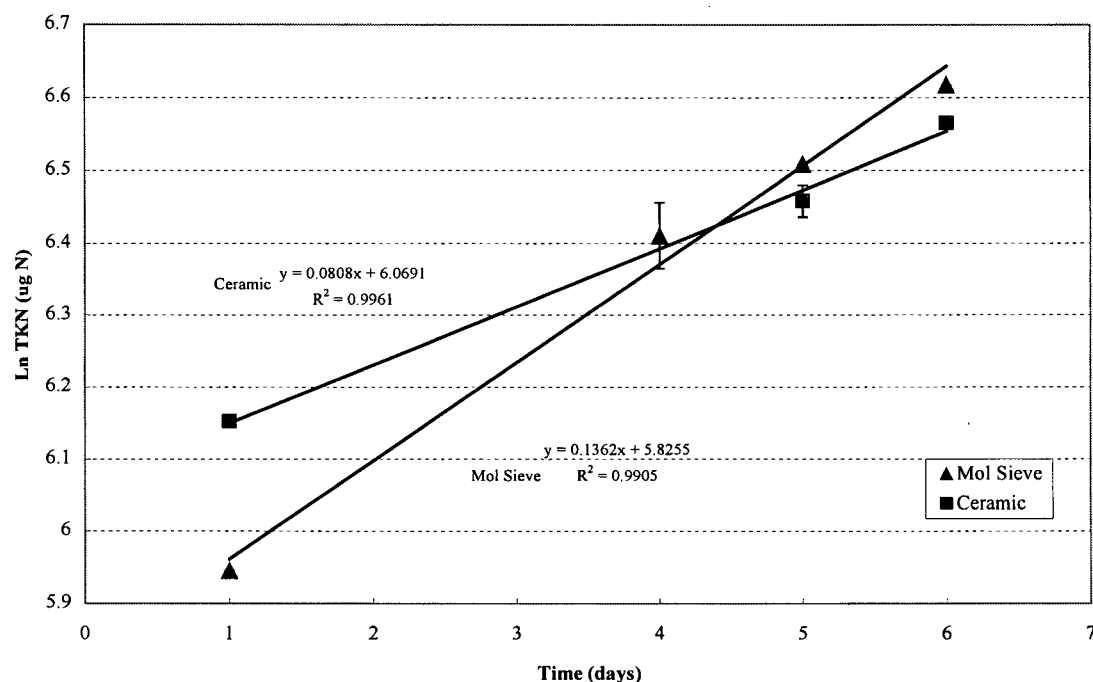
Figure 4.8: Molecular Sieve and Ceramic Bead Support Growth Curves.

Note: T=31 °C, grown in complex MVH nutrient solution, μ = 0.0057 and 0.0034 h^{-1} for the molecular sieve and ceramic beads, respectively.

The specific growth rate, μ, was determined from the following equation:

Equation 4.3

$$\mu = \frac{\ln X - \ln X_0}{t}$$

The doubling time for the control (system with no support) was determined to be 7.2 hours while for the support systems the values range from 7.7 to 206 hours. Batch culture studies with pure SRB species report specific growth values ranging from 0.013 to 0.15/hour, the control in this experiment was established as 0.096 which is within the range of data collected from previous studies (Badziong and Thauer, 1978, Robinson and Tiedge, 1984, Klemps et. al., 1985).

Table 4.9: Set 1 Experiment Specific Growth Rates and Doubling Times

Support	μ (h^{-1})	td (h)
MVH (control)	0.096	7.2
Glass Beads	0.089	7.7
Teflon	0.0126	54.9
Zeolite	0.0122	56.7
Molecular Sieve	0.0057	122
Ceramic Beads	0.0034	206

*based on TKN values

The glass bead system had a doubling time of 7.7 hours, which is similar to that of the control. The Teflon and zeolite appear to have impeded growth with doubling times calculated between 54.9-56.7 hours, while the molecular sieve and ceramic beads support materials appear to have strongly impeded the growth of the SRB with doubling times of 122 and 206 hours respectively.

Total Solids Sampling vs. TKN Data for Biomass Determination

Both TKN data and total solids data was collected for the 7 day experiment with the following supports: molecular sieve, ceramic beads, and glass beads. The solids data is based on the negative difference method in that the final value is subtracted from an initial value while the TKN data is based strictly on a positive result (measurement of TKN). A comparison of the data for the control and molecular sieve is shown in Table 4.10. In all cases with the TKN data a general increase in measurement was recorded over the duration of the experiment, in comparison a consistent increase in solids was not observed with the total solids method.

83

Table 4.10: Molecular Sieve and Control Comparison of Total Solids and TKN data

Time (days)	Total Solids (mg)	Biomass* (mg)	TKN (µg N)
Control			
0	---	0.4	45
1	15.6	4.0	456
3	15.0	6.8	771
5	10.3	7.4	847
6	10.0	6.9	785
Molecular Sieve			
1	19.3	3.4	382
3	42.4	---	---
4	30.1	5.3	608
5	---	5.9	671
6	26.0	6.5	741

*based on TKN values

4.2.3 Sulphate Reduction

Sulphate results for the glass, Teflon/plastic, and zeolite supports and a nonsupport control are presented here. The results for the molecular sieve and ceramic beads have been omitted from this section. Sulphate samples were collected for the molecular sieve and ceramic bead support systems, however equipment problems with the Lachat analyser delayed the testing of these particular samples beyond the recommended storage of 28 days by nearly a month. When these samples were analysed no change in the sulphate concentrations was measured. The sulphate measurements for the control and glass support were determined using the turbidimetric method while the Teflon and zeolite support system sulphate concentrations were determined with the Lachat analyser.

Plots of the sulphate reduction that occurred in the support systems with glass, zeolite and Teflon show an overall decrease in sulphate reduction but do not follow a linear trend pattern. The control appears to demonstrate a linear decrease in sulphate with time, as is demonstrated in Figure 4.9, the covariance, $r^2=0.94$ for the fitted trend line; although the first data point was excluded as an outlier from this trend line. The decrease in sulphate concentration with the glass support system is higher on days 4 and 5 than on day 3, because

84

this was also observed in the control, the data from day 3 was considered to be an outlier and was not included in the results shown in Table 4.11. No sulphate measurements were taken on the first 2 days of sampling as the sulphate concentration was not expected to decrease during this time period. However, samples should have been taken and in subsequent experiments sulphate samples were taken at the start of the runs. Figure 4.10 shows the plots of the Teflon and zeolite support systems. Both the Teflon and zeolite support systems appears to exhibit an initial lag phase where little sulphate reduction is occurring for the first four days and then drops off sharply on the fifth. The error bars in Figures 4.9 and 4.10 are based on standard deviations.

The sulphate reduction data is summarised in Table 4.11; since it was not possible to fit a trend line to the sulphate reduction curves, other than the control, the growth yield, Y_{SO_4}, is based on the difference between the initial and final sulphate concentration values. The calculation may be carried out as shown:

Equation 4.4

$$\frac{X_T}{\Delta SO_4} = \frac{(X_F - X_I)}{[SO_4]_I - [SO_4]_F}$$

In order to used equation 4.3, the initial and final sulphate concentration must be converted from mg/L to moles, this is accomplished by using the following equation:

Equation 4.5

$$\text{mols } SO_4 = \left(\frac{\text{mg } SO_4}{L}\right) \times \left(\frac{\text{mol}}{96.06 \text{g}}\right) \times \left(\frac{1\text{g}}{1000 \text{ mg}}\right) \times V$$

Table 4.11: Summary of Sulphate Reduction Results in Set 1 Experiments

Support	TKN			Sulphate		
	$T_T = T_F\text{-}T_I$ μg N	Biomass mg	Yield, Y_{SO_4} g X_T/mol SO_4 reduced	Initial mg/L	Final mg/L	Reduced mols x 10^{-04}
MVH	740	6.50	8.47	4117	2318	7.68
Glass	681	5.98	16.24	3649	2785	3.69
Teflon	820	7.20	15.98	3552	2477	4.51
Zeolite	253	2.22	4.88	3414	2346	4.56

As mentioned in section 4.1.2 the growth yield, Y_{SO_4}, is one way to analyse the data and expresses the biomass produced in the system with respect to the amount of sulphate reduced. The Y_{SO_4} values range from 4.88-16.16.24 g/mol SO_4, which is similar to values reported in literature which range from 4-13.5 g/mol SO_4 (Badziong and Thauer, 1978, Ingvosen and Jorgensen, 1984, Cypionka and Pfennig, 1986).
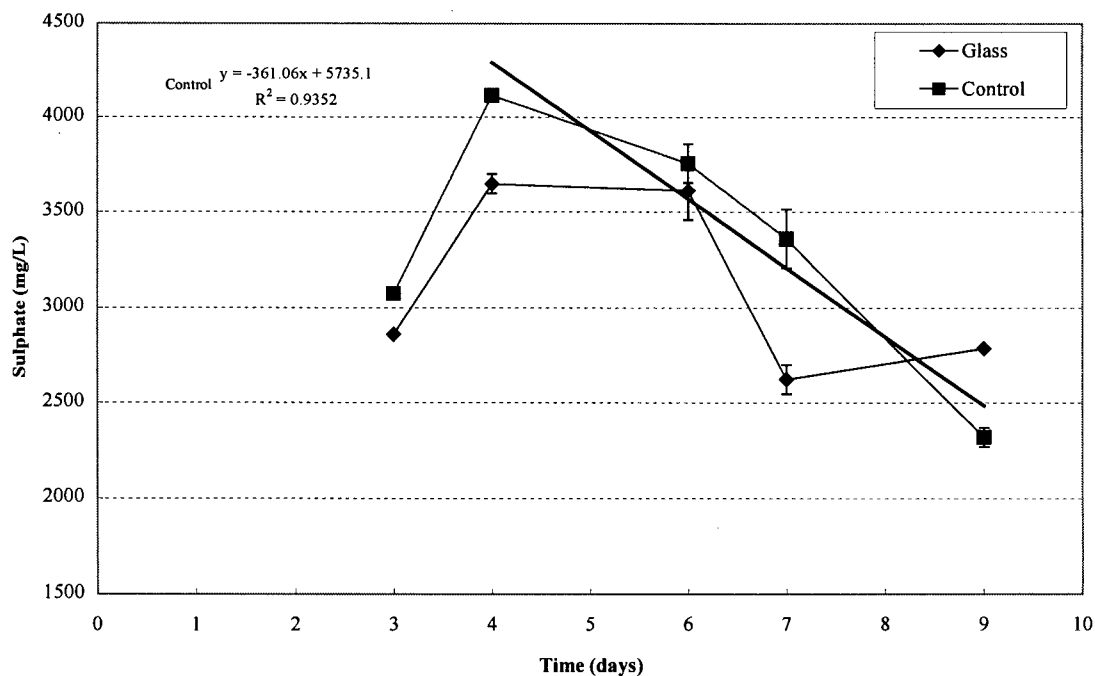
Figure 4.9: Sulphate Reduction with Glass Support.

Note: T = 31 °C, the error bars are based on standard deviations and the experiment was conducted with the complex MVH nutrient solution.
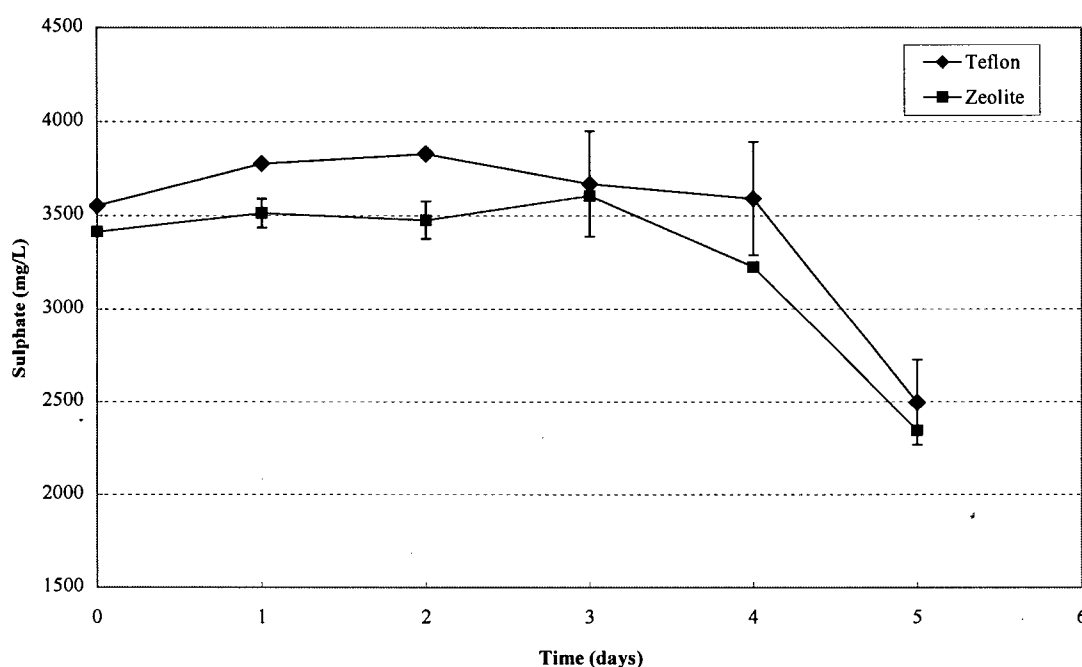
Figure 4.10: Sulphate Reduction with Teflon and Zeolite Supports.
Note: T = 31 °C, the error bars are based on standard deviations and the experiment was conducted with the complex MVH nutrient solution.

4.2.4 CO_2 Monitoring

The gas partitioner was used to monitor the CO_2 in the set 1 batch experiments. The purpose of the gas partitioner was to attempt to observe if the CO_2 level decreased in the headspace of the bottles. This was in an attempt to provide a rough confirmation that the bacteria were utilising the CO_2, as well as to determine the length of time before all the CO_2 was utilised in the flasks. This would provide an indication of when an experiment should be stopped or when CO_2 should be recharged to the flasks in the experiment. Two separate experiments were run using the gas partitioner; one with a control and the following support surfaces: glass beads, molecular sieve, and zeolite. The second experiment was conducted with Teflon and zeolite as support surface.

The gas partitioner measures the following gases: CO_2, O_2, Nitrogen, CO and H_2S; it does not measure the hydrogen gas present in the sample mixture. The y-axis on the graph is the

87

ratio of CO_2 to the gases in the head space, except hydrogen, in the flask and is simply calculated as:

Equation 4.6

$$R = \frac{A_{CO_2}}{(A_{CO_2} + A_{comp})}$$

Where R = ratio of CO_2 peak area to the peak area of N_2+CO_2

A_{CO2} = area of the CO_2 peak

A_{COMP} = combined peak area of N_2, O_2, CO and H_2S present in the headspace, as only N_2 was present, $A_{COMP} = A_{N2}$.

Two peak areas are used in this calculation, as the gases pass through the first column in the gas partitioner, an initial peak (referred to as the composite peak, A_{COMP}) of all the gases, except the carbon dioxide is detected. The second peak that passes through the first column is the carbon dioxide peak. The gases then pass through a second column, which separates out the gases from the composite peak, and are detected by another sensor. The carbon dioxide passes through this column without detection.
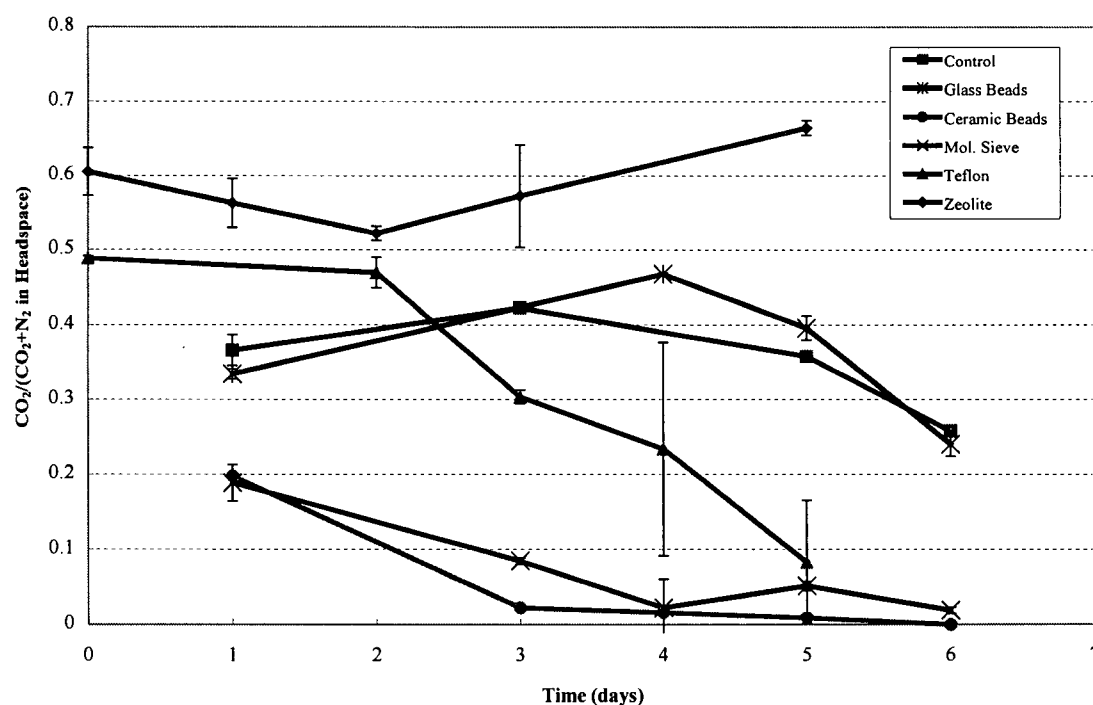
Figure 4.11: CO_2 depletion curves for Set 1 Experiments.

88

The scatter in the data observed in Figure 4.11 is due to the following problems:

- ACOMP is not constant between samples since it was not injected in a consistent fashion during the preparation of the batch experiments. This is considered to be one of the main problems with the data scatter.

- Since ACOMP was assumed to be constant no standard CO_2 injections were run with the gas partitioner, this was a mistake. As CO_2 standards would have compensated for the error in ACOMP because then it would have be possible to directly compare the CO_2 area with that of the standards.

- A leak was detected in the second column of the gas partitioner after the experiments were completed. Although, the data used was from the first column, the leak in the second column resulted in the need to use a higher flowrate than recommended which may have decreased the equipment detection sensitivity.

The only general observation that can be made from Figure 4.11 is that except for the zeolite support, all of the other systems seemed to show some decrease in CO_2, which may be taken as an indication that it was being utilised.

The lack of any noticeable activity in the zeolite flask may indicate that some component of the zeolite had an inhibiting affect on SRB growth or possibly that the system was contaminated with an outside carbon source that the SRB utilised. Both reasons appear to have some validity since growth was observed in the flask but at much more limited quantities compared to the other systems (refer to Table 4.11). The data for the glass beads is scattered. Good trends are observed for the batch flasks with no support, ceramic beads, molecular sieve, and Teflon. It appears as though these support systems have a slightly faster decrease in CO_2 compared to the flasks with no support.

As noted above, the CO_2 data in the set 1 experiments appears to show a general decreasing trend for the most of the systems, except for the batch experiments with zeolite. In general, however the data is quite scattered. The amount of CO_2 injected into the set 1 bottles was 25 cc into 80 mL of headspace this corresponds to approximately 31% CO_2. After 5 days, we

see that the ceramic beads, molecular sieve, and Teflon values are approaching zero. This data does not correspond well with the MVH CO_2 data, which still had measurable levels of CO_2 after 400 hours (16 days).

4.2.5 Discussion of Set 1 Support Surfaces

In the initial phases of this project, the following support surfaces were used: glass beads, molecular sieve, ceramic beads, Teflon/plastic pieces, and zeolite. During this portion of the project the total biomass in the system was measured while the fraction of biomass on the different supports compared to that in solution was not determined. Only visual observations were made at this point to determine if any of the supports seemed to provide a suitable surface for bacterial adhesion.

Glass beads have been used in some previous experiments as surfaces for bacterial colonisation with success (Allaoui and Forster, 1994, Diels et. al., 1990, Groudeva and Groudev, 1990). Another study, however, found that no colonisation occurred while using glass beads as an immobilisation surface (Huysman et. al., 1983). The data obtained from the glass beads shows an increase in biomass over time based on the TKN test. However, less metal sulphide precipitates were observed adhering to the glass beads than with other surfaces, and were easily removed by gently shaking the flasks. The glass bead are not porous, which may also limit the amount of biomass that can attach to the glass surface, whereas the study by Diels (1990) used sintered glass beads which have a porous structure. The growth yield, 16.24, was higher than that determined for control.

Although the data indicates an increase in biomass over time with the zeolite support, no significant concomitment precipitation of metal sulphides was observed. As well, the increase in biomass was significantly less than that measured in the other systems. A relatively low growth yield, 4.88 g/mol SO_4, was observed. Other natural rock types including septolite, pumice, basalt, crushed stones, and zeolite have been examined before (Huysman et. al., 1983, Maree and Strydom, 1985, 1987, Allaoui and Forster, 1994, Van Houten et. al., 1994). In previous studies, although success was found with the growth of

SRB using septolite, pumice and hard stone, a stable biofilm was not observed when basalt or zeolite was used. The results obtained indicate that zeolite surface does not encourage bacterial growth and is not considered to be a suitable support surface for the SRB.

Both the data for the ceramic beads and molecular beads appears fairly good in terms of increase in TKN. As well, both materials appeared to have blackening on their surfaces, possibly due to the porous nature of both materials, allowing for good bacterial adhesion and growth. However, both materials are fairly brittle and were observed to fracture during the batch experiments; resulting in a slight disintegration of the beads over the short time period (5-7 days) in which the experiment was run. It is likely that the beads would degrade further in longer term studies, especially in a continuous flow reactor where more turbulent conditions would exist, thus they are not considered as suitable immobilisation surfaces for SRB growth.

The small Teflon/plastic pieces had an increasing biomass trend observed from the TKN data gathered. As well, good biofilm coating was noticed on the Teflon/plastic pieces, with an apparent initial preference for the Teflon side over the plastic side. A previous study examining the potential of using a plastic support for SRB immobilisation had less successful results (Maree and Strydom, 1985). However, bacteria have shown a preference for adhering to hydrophobic materials (Abolsom et. al., 1983, Huysman et. al., 1987). The hydrophobic properties of the Teflon may encourage bacterial adhesion. The growth yield in this batch system, 15.98 g/ mol SO_4, was greater than that determined for the control.

Review of Set 1 Experiments

One of the primary objectives of the set 1 experiments was to become familiar with and validate the techniques used to monitor the biomass in the system. This was accomplished by comparing calculated data to published data in the literature. A secondary objective was to visually observe if any of the materials appeared to show promising results for bacterial adhesion. The solids test was discarded as a method to measure biomass due to large differences between duplicate samples and difficulty in obtaining an increase in the total solids measurements over the time in which the experiments were conducted. The TKN

analysis was considered valid as a general increase in TKN was observed over the duration of the experiments (as expected), further, and more importantly, the specific growth rates, μ, determined corresponded well with literature values. As well both the turbidimetric and methythymol blue methods of sulphate analysis were considered valid, as the calculated growth yields, Y_{SO_4}, were similar to values reported in the literature. Of the two methods used to measure sulphate, the methylthymol blue method is less labour intensive since it is run on an automated analysis, and as such it was used as the technique to measure sulphate in the set 2 experiments.

4.3 Set 2: Growth on Support Materials: Foam, Basalt, Ringlace, and Alginate Beads

The immobilisation materials used in the set 2 experiments were foam, basalt, Ringlace, and alginate beads. The nutrient solution for the set 2 experiments was the MVH2 solution. It should be noted that although the Teflon support from the set 1 experiments showed promising results as an immobilisation surface, it was not included in the set 2 experiments, which quantified the amount of biomass attached to the surface, due to a lack of available equipment. As in the set 1 experiments, TKN was used as an indirect correlation to the amount of biomass in the batch flasks. In addition, a protein analysis was also run on the samples in a secondary attempt to monitor the increase in biomass during the experiments. The purpose of the protein assay was to provide a check of the TKN estimated biomass concentrations. The biomass determined from the TKN assay were based on the theoretical molecular weight of the bacteria, while the protein biomass concentrations were compared to a Bovine gamma globulin standard. A comparison of the results obtained by measuring TKN and protein are presented below. The amount of biomass immobilised on the different materials was monitored and compared to the total biomass in the system in an effort to quantify which support would be suitable for an immobilised bioreactor system. The sulphate reduction rate in the systems was also monitored and expressed in terms of the growth yield, Y_{SO_4}.

4.3.1 Growth Curves using TKN and Protein Measurements

Total TKN

Plots of the natural logarithm of TKN versus time are shown in Figure 4.12 (Ringlace and alginate beads) and Figure 4.13 (foam and basalt). The error bars displayed in the figures are based on the standard deviations of the samples. The specific growth rates and doubling times of the SRB determined in this experiment are listed in Table 4.12. The trends for the alginate beads and the control have linear portions and then flatten out during the stationary phase of SRB growth after days 8 and 5, respectively. The data for the Ringlace indicates an increasing biomass trend with no apparent decrease in the growth rate.

93

It should be noted that the alginate bead support system has a higher initial TKN concentration (as shown in Figure 4.12) compared to the initial TKN value found in the other support systems in the experiment, including the control. This is due to method of inoculation, in the other growth experiment systems 1 mL of SRB inoculum was added to each batch flask, whereas in the alginate system 4 mL of SRB inoculum was encapsulated within the beads (as described in Chapter 2: Methods and Materials). This resulted in a much higher initial concentration of SRB in the alginate support system.
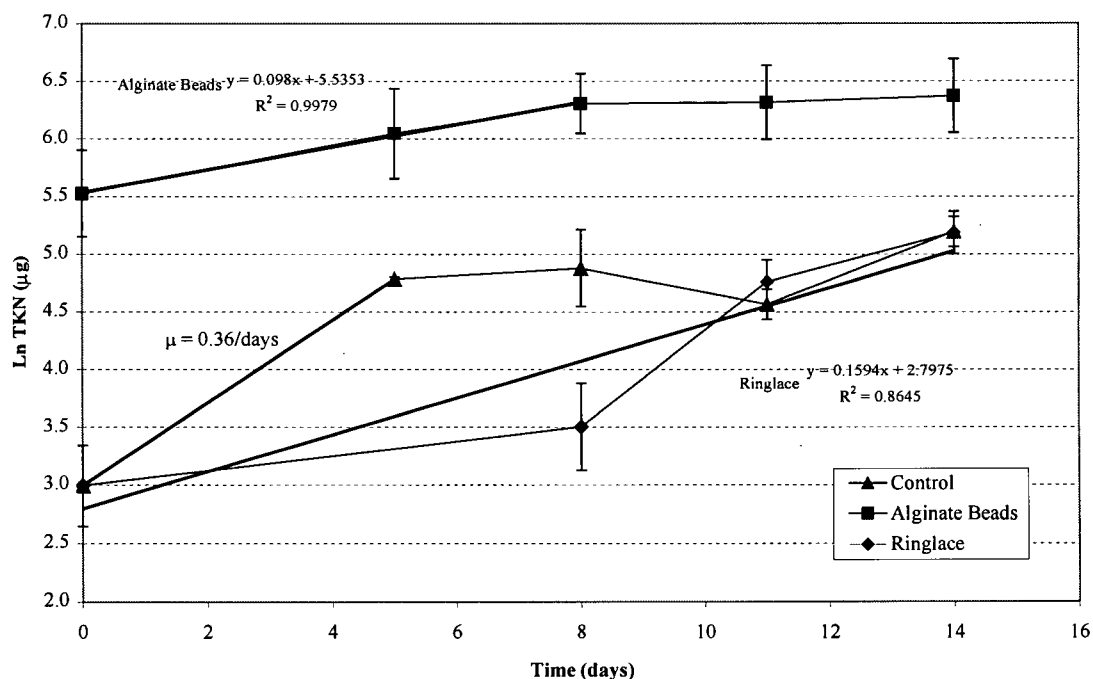
Figure 4.12: Ringlace, and Alginate Bead Support TKN Growth Curves.
Note: T = 31 °C, grown in defined MVH2 nutrient solution, μ = 0.0041, 0.015, 0.0064 h^{-1} for the alginate beads, control and Ringlace, respectively, error bars are based on standard deviations.
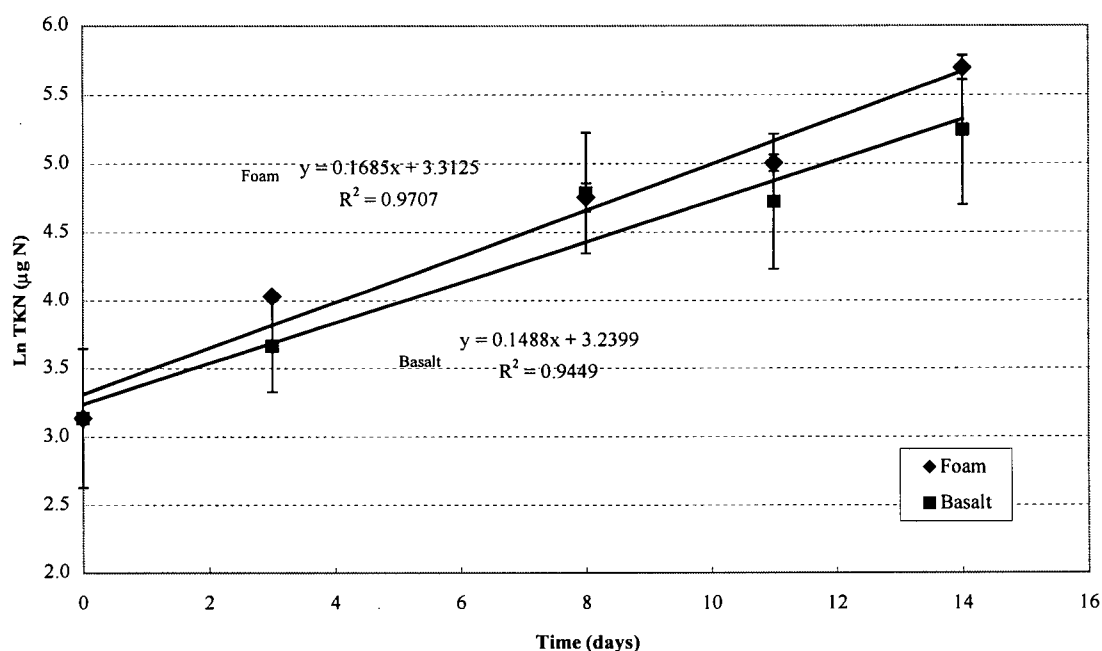
Figure 4.13: Foam and Basalt Support TKN Growth Curves.

Note: T = 31 °C, grown in defined MVH2 nutrient solution, $\mu = 0.007$ and 0.006 h^{-1} for the foam and basalt, respectively, error bars are based standard deviations.

Table 4.12: TKN based Specific Growth Rates and Total Biomass Growth in Set 2 Experiments

Support	TKN μ (hr^{-1})	td (hr)	$T_T = T_F - T_I$ (μg N)	Biomass, X_T (mg)
Control	0.015	46	161	1.41
Foam	0.0070	99	275	2.42
Ringlace	0.0066	104	159	1.40
Basalt	0.0062	112	166	1.46
Alginate Beads	0.0041	170	334	2.93

The covariance value for the first order trend line fitted to growth phase portion of the alginate bead and Ringlace systems is 0.99 and 0.86. The foam and basalt support systems show a linear increase over the length of the experiment. First order trend lines fitted to the data have covariance values of 0.97 for the foam, and 0.94 for the basalt. While a covariance value of 1 represents a perfect linear fit, the covariance values calculated seem to reasonably support the assumption of a first order trend, with the possible exception of the Ringlace support system.

The specific growth rates for the control is based on the differences between only the two data points on days 1 and 5 for the control, since the control system exhibited a large increase in TKN between these points followed by a levelling out, thus it was not possible to fit a first order trend line to this data.

Previous studies, under autotrophic conditions, with various SRB have been performed to establish the specific growth coefficient and yield data with respect to sulphate reduction. This data is summarised in Table 4.13. The specific growth for the control was 0.015/h, which fits within the data reported in the literature.

Table 4.13: Comparison of Specific Growth Rates and Yield Coefficients

Species	Specific growth, μ (h^{-1})	Batch vs. Continuous	pH	Notes	Author
Desulfovibrio vulgaris	0.15	Batch	6.5-7.2	H_2/CO_2, and acetate	Badziong and Thauer, 1978
Desulfovibrio sp. G11	0.05	Batch	6.7	H_2/CO_2 with minerals and vitamins added	Robinson and Tiedge, 1984
Desulfotomaculumn orientis	0.077	Batch	6.9-7.0	H_2/CO_2, basal mineral medium	Klemps, Cypionka, et al 1985
Desulfotomaculumn orientis	0.013-0.044	Continuous	7	H_2/CO_2, basal mineral medium, Sulphate limited	Cypionka and Pfennig, 1986
Desulfotomaculumn orientis	0.09	Continuous	7	H_2/CO_2, basal mineral medium, non-limited	Cypionka and Pfennig, 1986

The specific growth for the control was 0.015/h, which fits within the data reported in the literature, refer to Table 4.15, albeit on low side. The specific growth for the foam, Ringlace, and basalt systems, 0.0070/h, 0.0066/h and 0.0062/h, respectively, were considerably lower than the reported values. The alginate system had the lowest specific growth at 0.004/h. This is not surprising since the nutrients needed to diffuse through two layers, the liquid media and the solid beads before reaching the SRB, as well the electron donor and carbon need to diffuse through the gas, liquid and solid phases. The media used in the literature included trace vitamins, while the defined nutrient media used in this experiment did not, this

difference may have contributed to the specific growth of the SRB reported in the literature generally being higher than the values calculated in this study.

Total Protein

The BioRad DC protein assay was used as an additional indirect method to monitor the increase in biomass over time during the course of the experiment. One of the objectives in using the protein assay was to confirm the trends obtained from the TKN assay. The protein data does tend to follow the same general trend lines as the TKN data with increasing protein concentrations over time, however the error (based on 95%CI) associated with the results is relatively large decreasing confidence in them. The protein data for the alginate beads is not included, as the alginate beads did not digest during the digestion step used in preparing the samples for analysis.

Table 4.14: Total Protein Assay Results for Control, Foam, Basalt and Ringlace

Time	Control		Foam		Basalt		Ringlace	
(days)	mg/mL	SD	mg/mL	SD	mg/mL	SD	mg/mL	SD
0	0.135	0.013	0.154	0.039	0.154	0.039	0.135	0.013
5	0.372	0.014	0.329	0.143	0.295	0.096	---	---
8	0.341	0.013	0.409	0.157	0.320	0.163	0.437	0.087
11	0.419	0.044	0.127	0.046	0.404	0.464	0.478	0.077
14	0.339	0.165	0.240	0.201	0.334	0.486	0.638	0.099

Shown in Figure 4.14 and Figure 4.15 is a comparison between the determined biomass values based on both the TKN and protein analyses. The biomass concentration is calculated by assuming that 55% of the total biomass is protein and is calculated as:

Equation 4.7

$$\text{mg } Biomass = protein\,(\text{mg/ml}) \times Vs \times \left(\frac{1\,\text{mg } Biomass}{0.55\,\text{mg } protein} \right)$$

Where Vs = the digestion volume (10 mL). Both the protein and TKN converted values show a general increasing trend, however the protein based biomass values are much higher than the biomass values that were calculated from the TKN data.

	0	3	8	11	14
■ Foam-tkn	0.20	0.50	1.02	1.31	2.62
□ Basalt-tkn	0.20	0.35	1.05	0.99	1.66
■ Foam-protein	2.81	7.29	7.43	2.31	4.36
□ Basalt-protein	2.81	18.65	5.82	7.35	6.06

Time (days)
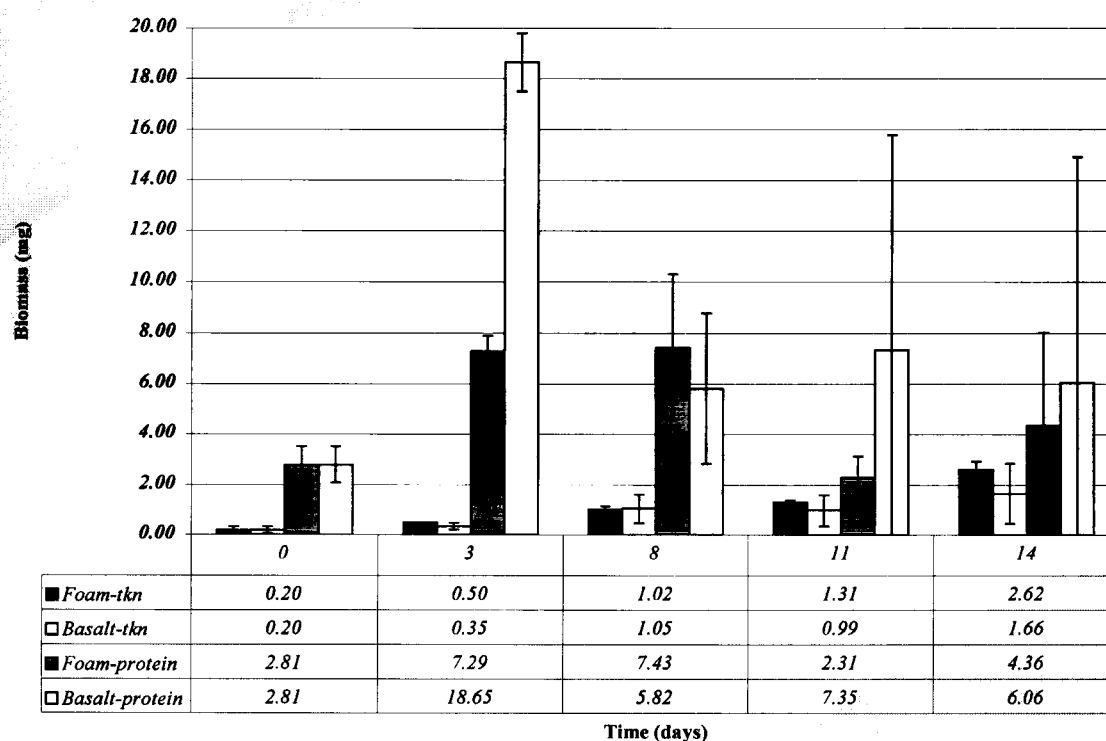
Figure 4.14: Growth Results for Foam and Basalt based on TKN and Protein Measurements.
Note: the values in the table are expressed in mg Biomass and the error bars shown are based on standard deviations.

	0	5	8	11	14
■ *Control-tkn*	0.18	1.05	1.16	0.84	1.59
□ *Ringlace-tkn*	0.18		0.20	1.03	1.57
□ *Control-protein*	2.43	6.77	6.21	7.62	6.16
□ *Ringlace-protein*	2.43		7.95	8.69	11.60

Time (days)
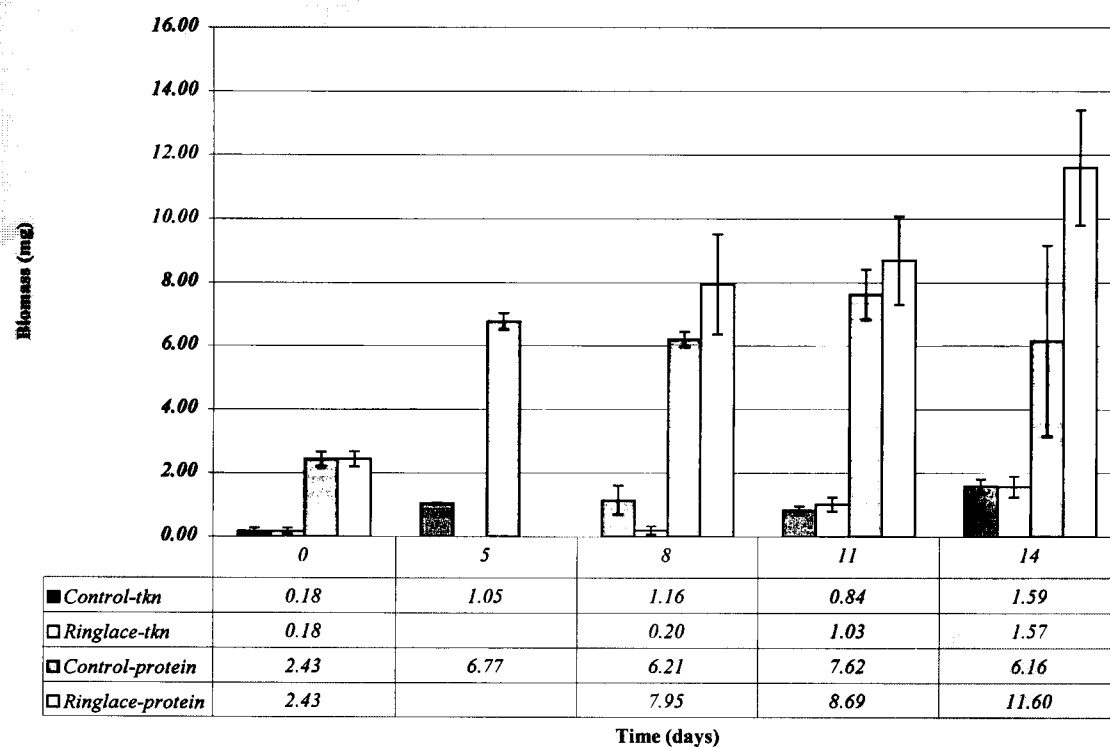
Figure 4.15: Growth Results for Control and Ringlace based on TKN and Protein Measurements.

Note: the values in the table are expressed in mg Biomass and the error bars shown are based on standard deviations.

Finally, the biomass produced per mole of sulphate reduced can be calculated from both the TKN and protein data. This data is summarised in Table 4.15 and Table 4.16. In the case of the protein-based values, the observed yields are high, ranging from 13.22-63.96 g biomass/ mol SO_4, except for the foam, which has a yield of 4.80 g biomass/mol SO_4. It would appear that, in general, the protein assay overpredicted the biomass concentration. The biomass was determined by comparing the measured protein values to a Bovine gamma globulin standard. It is possible that the ratio of proteins in the standard is lower than that present in the SRB, which would account for the higher than expected results. The TKN based values on the other hand range from 5.07 - 9.77 g/mol. As mentioned earlier, the literature values for the yield coefficient have been quoted between 4-12.2 g/mol under similar growth condition (refer to Table 4.5), based on this it is likely the TKN values are a better representation than the protein values for determining the biomass.

Table 4.15: Summary of Biomass Growth based on the Protein Assay

Support	$P_T=P_F-P_I$ mg/ml	Biomass, X_T mg	$(dSO_4/dt)/X_T$ mg/(L.h)/mg	Yield, Y g X_T/mol SO_4 reduced
	Protein			
MVH2	0.204	3.71	0.923	14.65
Basalt	0.180	3.27	0.484	13.22
Foam	0.086	1.56	2.209	4.80
Ringlace	0.503	9.15	0.130	63.96
Alginate Beads	----	----	----	----

Table 4.16: Summary of Biomass Growth based on the TKN Assay

Support	$T_T=T_F-T_I$ ug N	Biomass, X_T mg	$(dSO_4/dt)/X_T$ mg/(L.h)/mg	Yield, Y_{SO_4} g X_T/mol SO_4 reduced
	TKN			
Control	161	1.41	2.42	5.59
Ringlace	159	1.40	0.85	9.77
Basalt	166	1.46	1.09	5.89
Foam	275	2.42	1.46	7.28
Alginate Beads	334	2.93	1.56	5.07

4.3.2 SRB Growth on Support Materials

Since the growth yield values, Y_{SO_4}, calculated using the protein values did not match well with the literature values, the determination of the SRB growth on the support materials was based on the TKN data collected.

The main objective of monitoring the growth on the support materials in the second set of experiments was to show the differences between the amount of immobilized biomass compared to that in free suspension. This data is summarised in Table 4.17, the % of SRB on the support materials in decreasing order is alginate beads>foam>Ringlace>basalt. Figure 4.16 shows the increase of bacteria adhering to the alginate beads, foam, basalt, and Ringlace support materials, as expected the alginate beads values significantly higher than the others since the alginate beads were encapsulated with SRB from the start of the experiment.
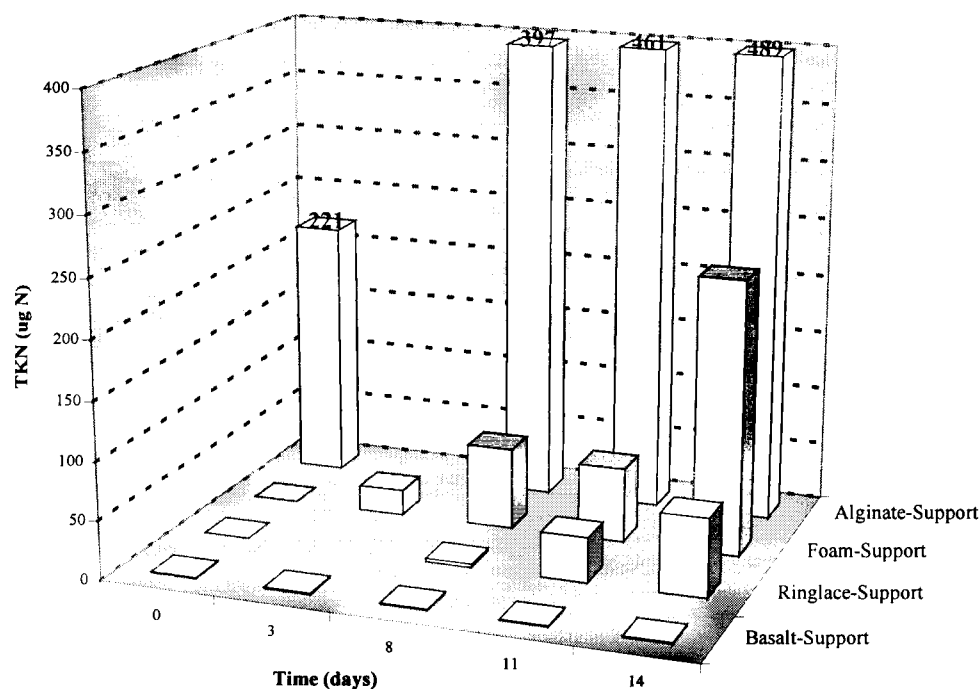
Figure 4.16: Comparison of SRB immobilised on support (TKN)

The foam has a highly porous structure, which may encourage the colonisation of SRB within the pore spaces, accounting for the high percentage (79%) of SRB on the foam support (Huysman et. al., 1983). The Ringlace had 37% adhesion and the results for the basalt were below the method detection limit of the TKN analyser. The Ringlace is a series of thread like material strung together all of which have a smooth surface, the lack of surface roughness and open pore spore spaces for the SRB to colonise may account for reason it has a lower surface adhesion % compared to the foam. The basalt had a rough surface with small crevices, which the SRB could colonise, and was expected to yield good results. However, the lack of large deep pores may have impeded the bacterial colonisation (Van Houten et. al., 1994). Shown in Figure 4.17 is the comparison of the amount of biomass in support versus solution for the foam, basalt, Ringlace, and alginate beads.

101

Table 4.17: SRB Growth in Solution vs. on Support for Set 2 Experiments

Support	Total		% in Solution	% on Support
	µg N	SD		
MVH2	181	25	100	0
Basalt	189	137	100	MDL*
Ringlace	179	25	63	37
Foam	298	35	21	79
Alginate-Beads	586	221	16	84

* the basalt TKN values for the support were below the method detection limit
of the Lachat Autoanalyzer

(a)

(b)

(c)

(d)
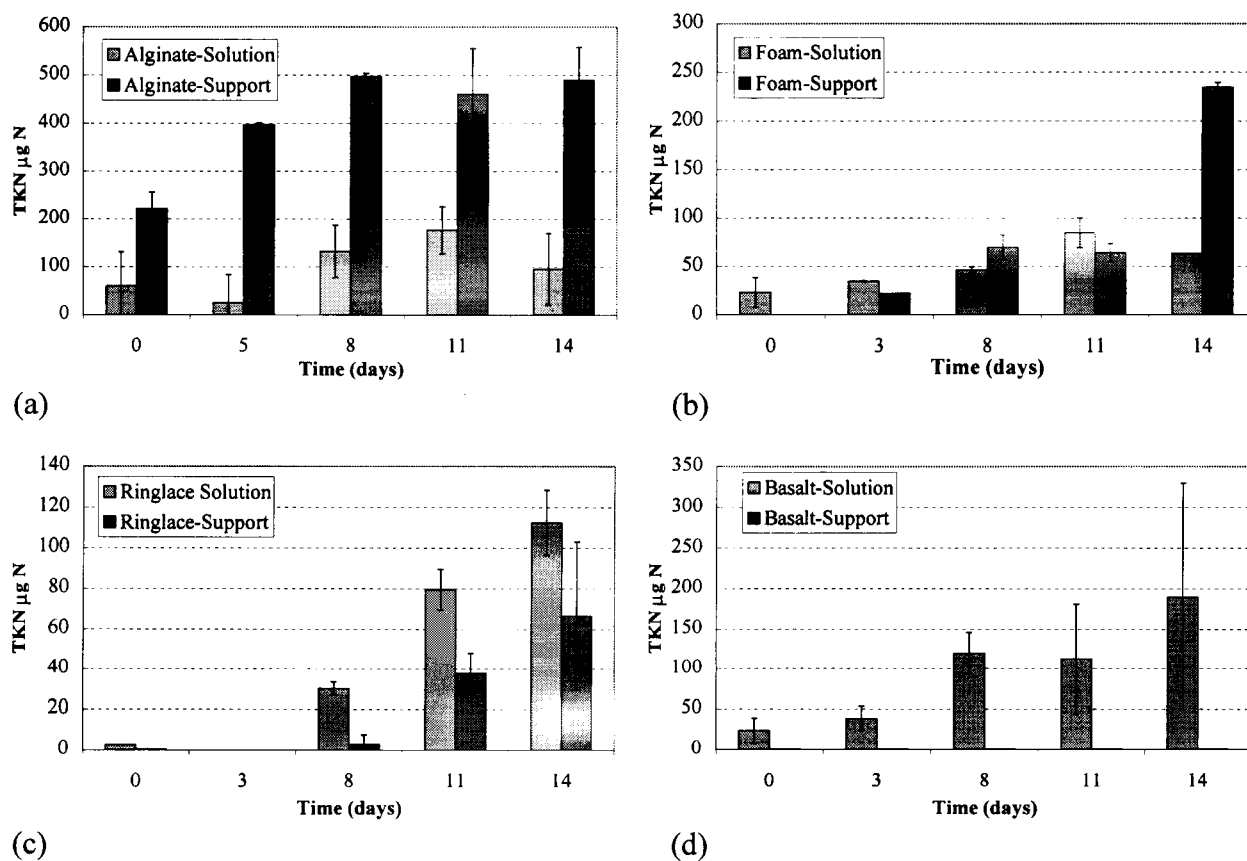
Figure 4.17: Comparison of SRB biomass in solution and immobilised on support.

Note: The above figure shows that the SRB encapsulated within the alginate beads had the highest immobilisation, followed by the foam, and Ringlace, while biomass was not measured on the basalt support. The error bars are based on standard deviations.

4.3.3 Scanning Electron Microscope Images

The purpose of taking the SEM images was to (1) attempt to verify the biomass results in terms of which surfaces had the highest calculated % of bacterial adhesion and (2) to comment on the how the SRB appeared to be adhering or colonising the various surfaces. SEM images were taken for the foam, basalt, Ringlace, and alginate bead supports. The SEM images support the TKN data with more colonies of bacteria observed adhered to the surfaces as follows: foam > Ringlace ≥ basalt. The SRB were encapsulated within the alginate beads and alginate beads which had been cut in half also showed colonies of bacteria, SEM images were also taken of the surface of alginate beads and these showed SRB adhering to outer surface.

The foam has some of the most interesting images (refer to Figure 4.18, Figure 4.19, Figure 4.20). Bacteria were observed attached to the surface of the foam, as well as in flocs inside the pore spaces. These later structures appeared to be attached to the foam via strands of what are assumed to be extracellular polymeric structures (EPS). It was also interesting to note that more SRB colonies and EPS formation was observed between the foam matrix than actually adhered to the surface. These observations are in agreement with a similar study using foam as a support for methanogens (Bolte et. al., 1986).

The alginate beads were observed to have limited growth on the surface of the beads (refer to Figure 4.21) and large colonies of SRB within the beads (refer to Figure 4.22). This was expected since the SRB inoculum was encapsulated within the bead, the SRB observed on the surface of the bead are attributed to a bacterial colony expansion forcing single cells to the bead surface (Wijffels, 1994). The Ringlace SEM images (refer to Figure 4.23) show that small colonies of SRB adhering to the surface but no large groups were found, possibly due to a lack of niches the SRB could colonise. The basalt support had a rough surface with small pores or surface pockets, individual SRB were observed adhered to the surface with the occasional colony found within small surface pockets. The SEM images confirms that SRB were adhering to the basalt but at overall concentrations too small to be enumerated using the TKN assay (refer to Figure 4.24).

(a) (b)
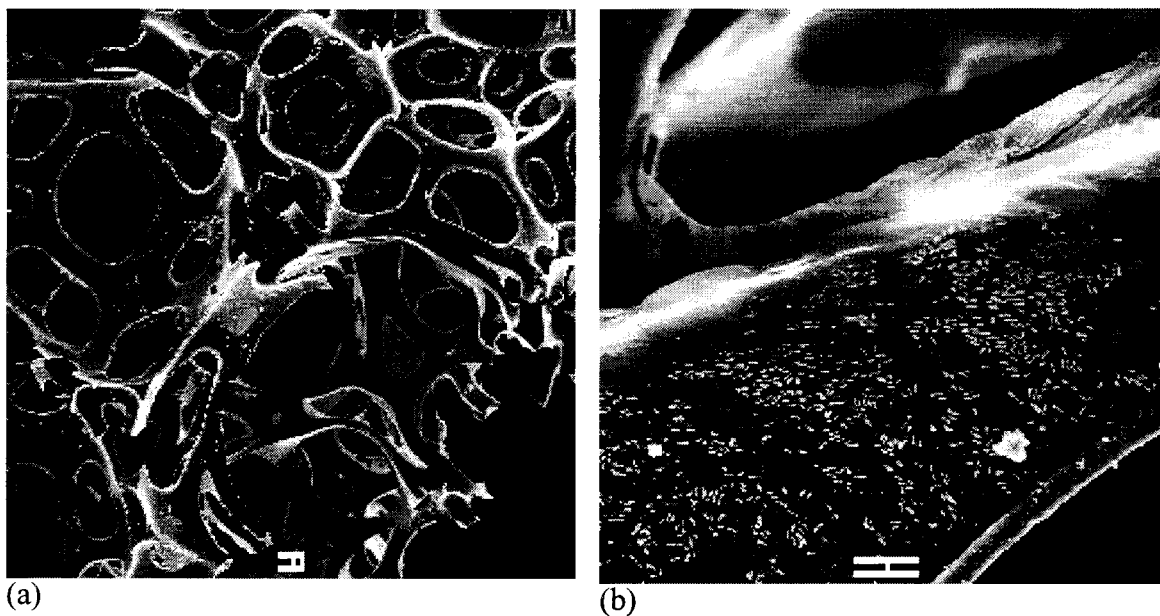
Figure 4.18: SEM Foam 1.

Note: (a) Foam Support, bar 100 μm, (b) SRB on section of foam, taken from inside cross-section, bar 10 μm.

(a) (b)
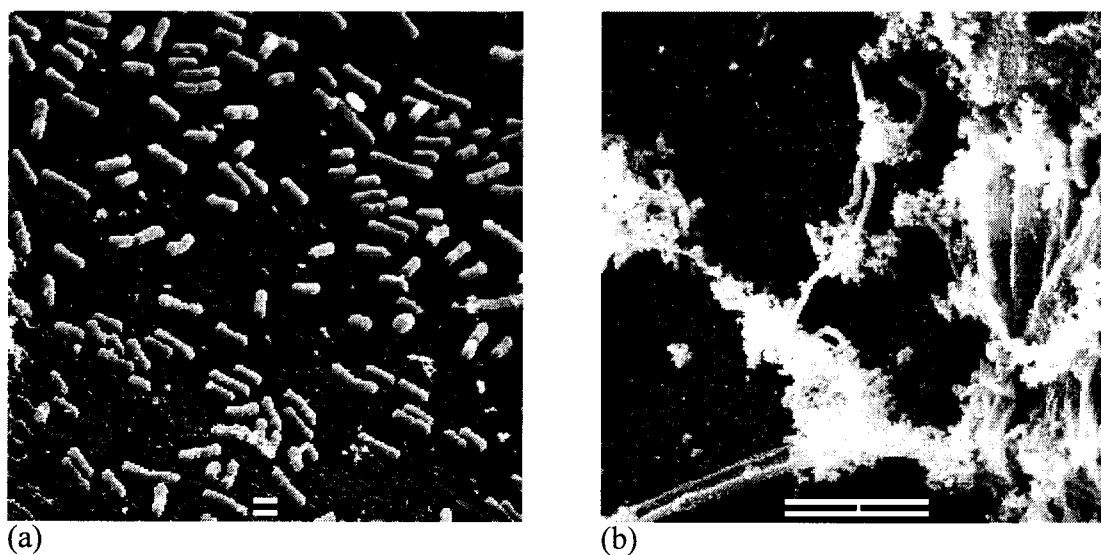
Figure 4.19: SEM Foam 2.

Note: (a) Magnified section of Figure 4.18 (b) above, bar 1 μm, (b) bacterial growth found on outside edge piece of foam, bar 10 μm.

(a)   (b)
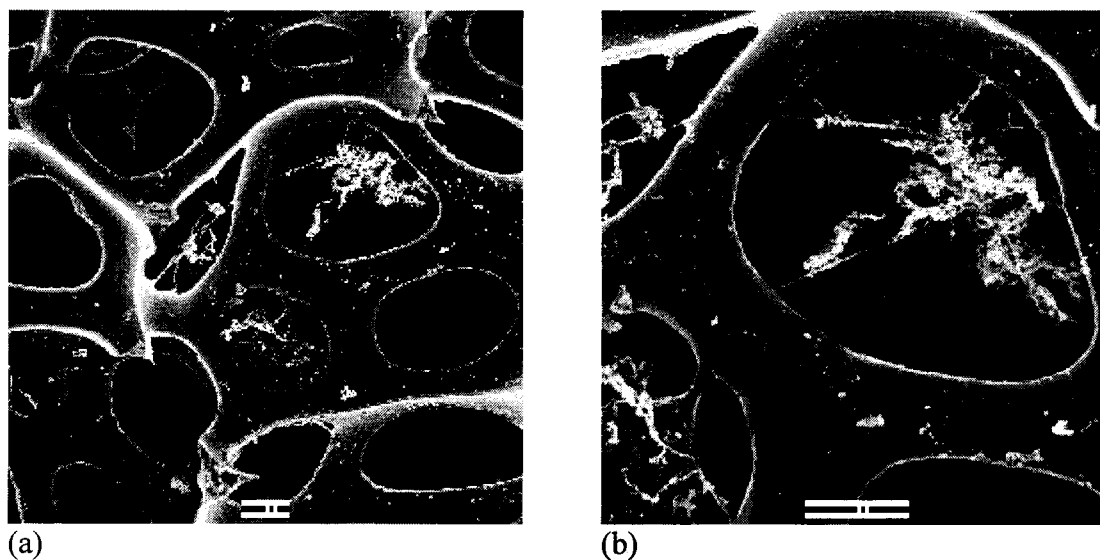
Figure 4.20: SEM Foam 3.

Note: (a) Outside edge of foam with apparent web-like bacterial growth, bar 100 μm, (b) magnified view of upper right hand web structure, bar 100 μm.

(a)   (b)
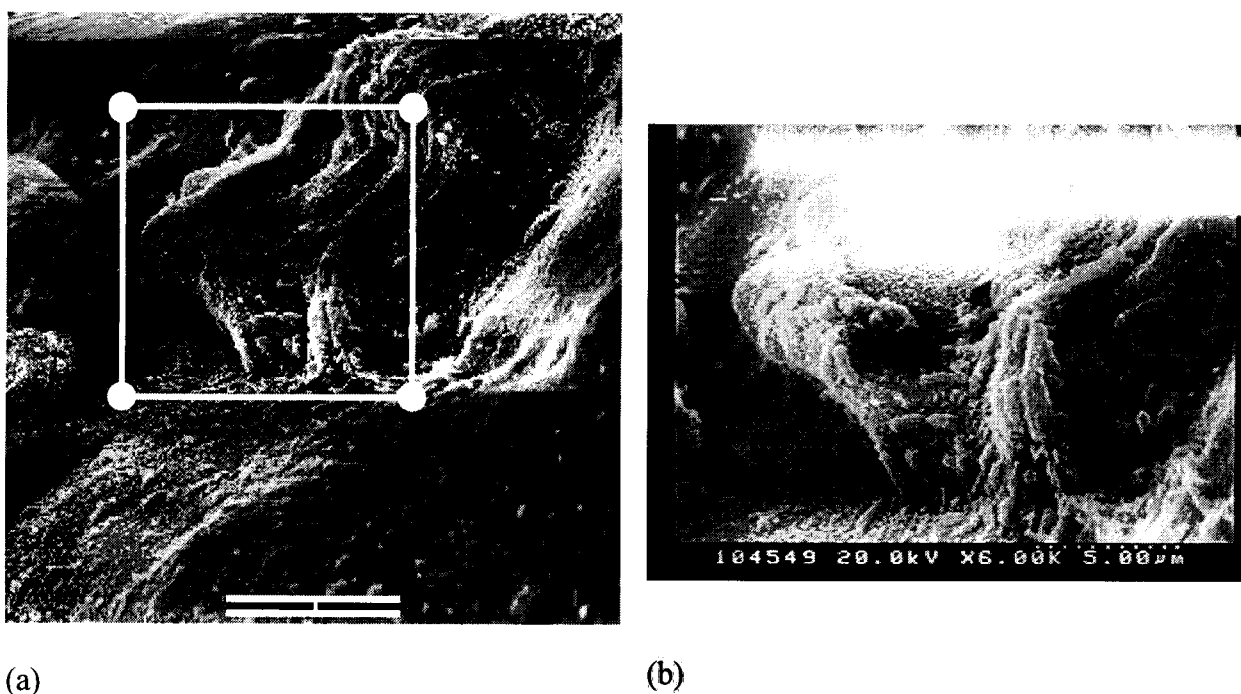
Figure 4.21: SEM Alginate Bead 1.

Note: (a) 2500X Magnification of Alginate Bead Surface, bar 10 μm The area highlighted by the box is shown magnified in (b) 8000X Magnification of surface. Some SRB have been forced to the bead surface.

105
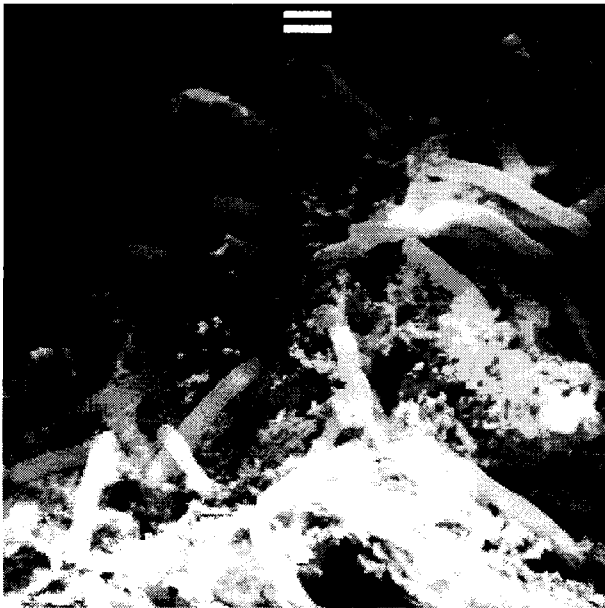
Figure 4.22: SEM Alginate Bead 2.

Note: 7000X Magnification of Inside of Bead, with a large colony of SRB, bar 1μm.
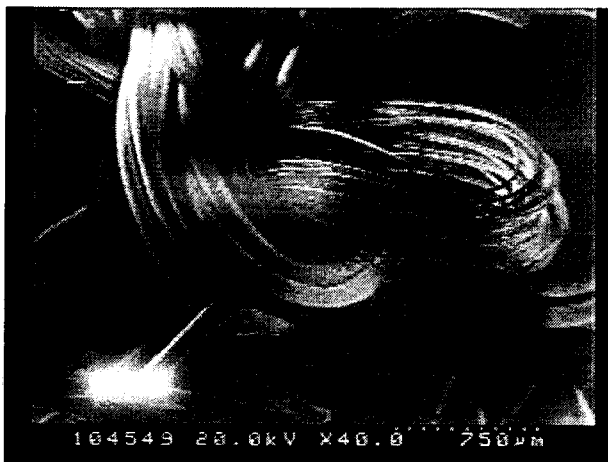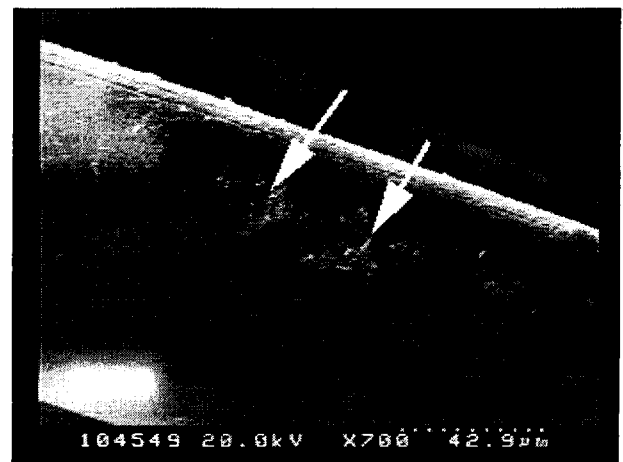
(a)   (b)

Figure 4.23: SEM Ringlace 1.

Note: (a) 40X Magnification of Ringlace, bar 750 μm, (b) 700X Magnification of Ringlace, the lighter areas, indicated by the arrows, denote areas with SRB, bar 42.9 μm.

(a)   (b)
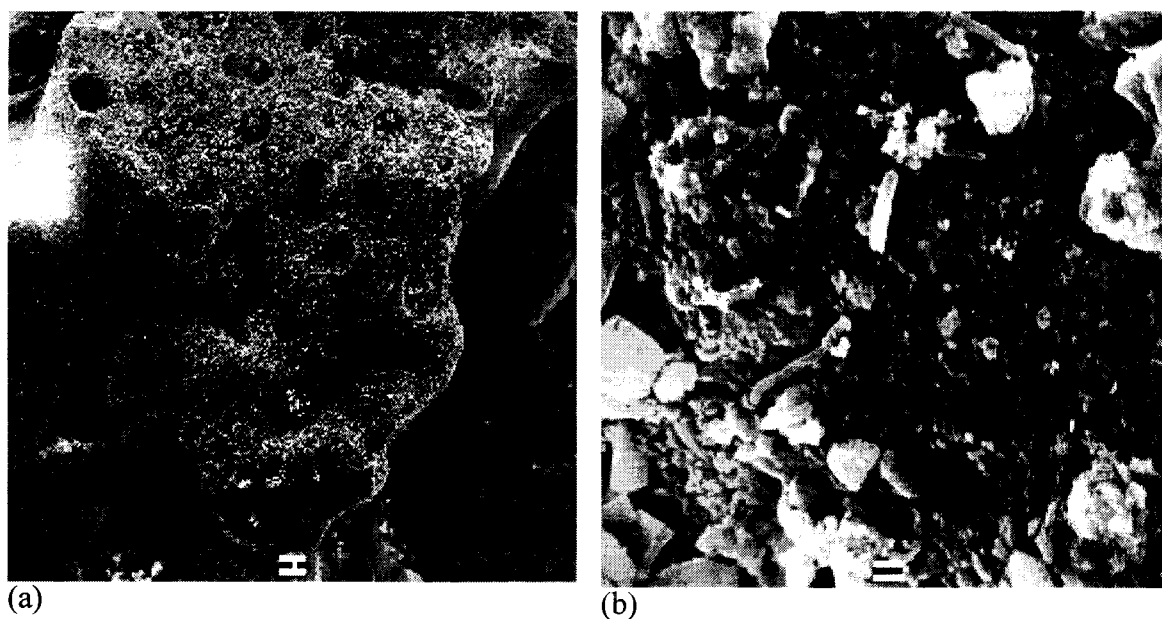
Figure 4.24: SEM Basalt 1.

Note: (a) 400X Magnification of Basalt, bar 10 μm (b): 4500X Magnification of Basalt, notice the sulphate reducing bacteria, bar 1 μm.

(a)   (b)
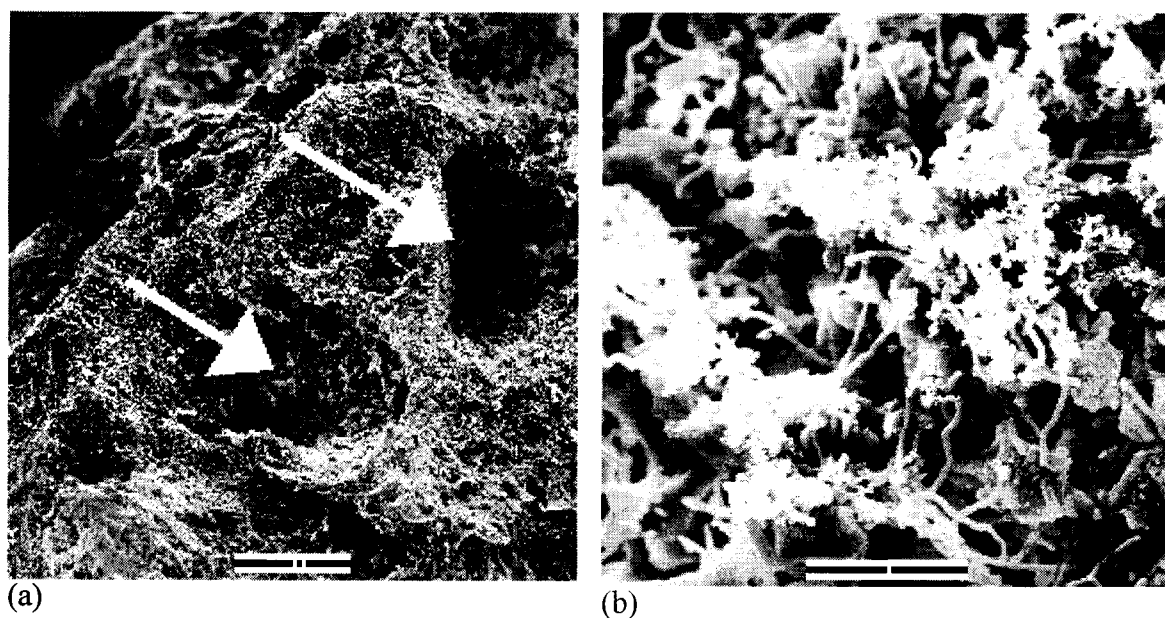
Figure 4.25: SEM Basalt 2.

Note: (a) Surface pockets found on Basalt Support were occasionally found to have colonies of bacteria, bar 100 μm. (b) Left Hand Side Depression from 'a' Note the bacterial colony and the larger elongated and short rods of SRB, bar 10 μm.

Although the exact types of SRB present in the inoculum was not known at the start of the study it appears as though it may be a mixed population of *Desulfotomaculumn* species, which range in size from 2-6 μm. The SEM images show that mainly short vibrio type SRB (1-2 μm in length) were observed on the support but occasionally longer rods (up to 6 μm in length) were also observed. Further, only a few SRB species are capable of mesophilic, autotrophic growth on strictly CO_2/H_2, of which *Desulfotomaculumn* is one of these species and it is the only group, which also falls within the size range observed.

4.3.4 Sulphate Reduction

The sulphate concentration was monitored over two weeks with basalt, foam, Ringlace and alginate beads acting as support surfaces. Figure 4.26 and Figure 4.27 shows plots of the sulphate concentration over time, and the error bars are based on standard deviations. These experiments were carried out in the MVH2 nutrient media. The sulphate reductions all appear to follow zero order kinetics although the rates vary from 1.27-4.58 mg/(L.h), as shown in Table 4.18.

The calcium alginate beads system appears to have the most rapid sulphate removal. Since this system has the highest bacterial concentration (due to the method of inoculation, as discussed earlier) these results were expected. The control also has a higher rate of sulphate reduction compared to the Ringlace although the former has lag phase before the reduction begins. The foam also has an apparently high sulphate reduction while little activity is noted in the basalt system. Zero order trend lines were fitted to the data, the Ringlace covariance value is 0.78, while the covariance values for the alginate beads and control were 0.92 and 0.91, respectively. The covariance values for the zero order trend lines for the basalt and foam support reduction data were 0.86, and 0.90. These values would appear to support the justification for fitting a linear trend line to this data, with the possible exception of the Ringlace support system.
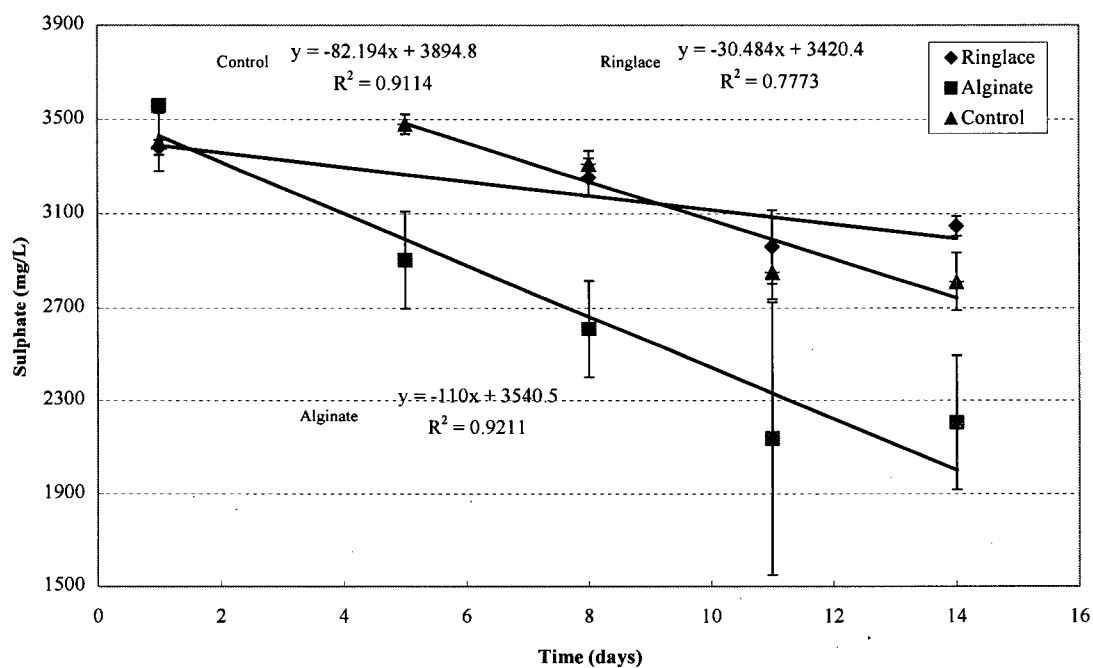
Figure 4.26: Sulphate Reduction with Alginate Beads and Ringlace Supports.

Note: T = 31 °C, the error bars are based on standard deviations and the experiment was conducted with the defined MVH2 nutrient solution.
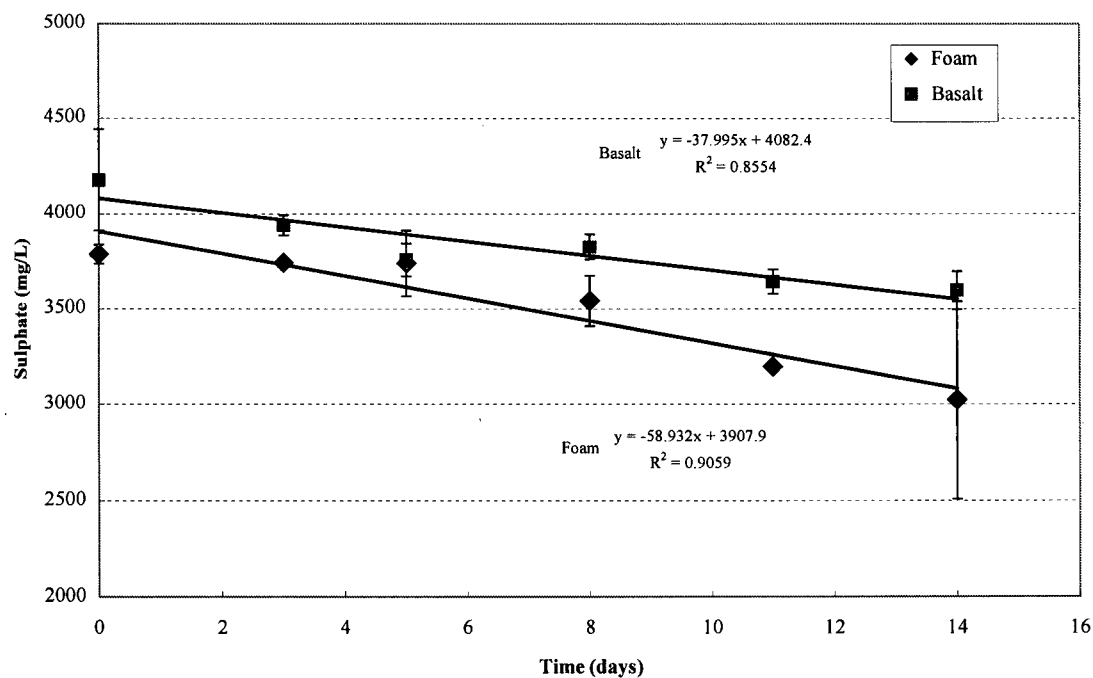
Figure 4.27: Sulphate Reduction with Foam and Pumice Supports.

Note: T = 31 °C, the error bars are based standard deviations and the experiment was conducted with the defined MVH2 nutrient solution.

109

Table 4.18: Sulphate Reduction Data for Set 2 Experiments

Support	TKN			Sulphate			
	$T_T=T_F-T_I$ ug N	Biomass, X_T mg	Yield, Y_{SO_4} g X_T/mol SO_4 reduced	dSO_4/dt mg/(L.h)	Initial mg/L	Final mg/L	Reduced mols x10^{-4}
Control	161	1.41	5.59	3.42 ± 0.75	3405	2812	2.53
Basalt	166	1.46	5.89	1.58 ± 0.33	4176	3596	2.48
Foam	275	2.42	7.42	2.46 ± 0.32	3787	3024	3.26
Ringlace	159	1.40	9.77	1.27 ± 0.48	3383	3048	1.43
Alginate Beads	334	2.93	5.07	4.58 ± 0.78	3560	2205	5.78

As shown in Table 4.18, the sulphate reduction rate in decreasing order was alginate beads>control> foam>basalt> Ringlace. As mentioned earlier, the alginate support system had a larger concentration of SRB than the others, thus it was expected to have the highest sulphate reduction rate. The control exhibited a greater sulphate reduction rate compared to foam despite a higher biomass concentration in the foam system, while the basalt and Ringlace, which had comparable biomass concentrations to the control, also exhibited lower sulphate reduction rates.

Sulphate Kinetics

In a closed, batch system, when the reaction rate is independent of the reaction concentration, the reaction obeys zero order kinetics and the rate will be constant at all times during the reaction. This is expressed as:

Equation 4.8

$$r = \frac{-dS}{dt} = k_o$$

where r = the volumetric rate of reaction ($kg/m^3/s$),

dS/dt = represents the change in concentration over time,

and k_o is the zero order rate constant ($kg/m^3/s$).

By integrating the equation 4,7, we can see that a plot of S versus time will give a straight line with a slope -k_o:

Equation 4.9

$$\int_{So}^{S} -dS = ko \int_{t=o}^{t} dt$$

$$S = So - kot$$

A previous study found that at sulphate concentrations > 30 mg/L at T = 25-31 °C, the growth of acetate utilising SRB was independent of the Sulphate concentrations, with a reduction rate of 12 mg/(L.h) sulphate in a batch system (Middleton and Lawrence, 1977). While another study also found that sulphate reduction followed zero order kinetics (Maree and Strydom, 1987). Based on this, the sulphate reduction data collected in this experiment was plotted as sulphate concentration versus time and fitted to linear trend lines. Both the complex media and defined media controls appeared to agree with the zero order assumption. In general, most of the support systems from the second set of experiments also appear to follow zero order kinetics, with the possible exception of the Ringlace. However, it is difficult to tell if the sulphate reduction data from the first set of experiments also follows zero order kinetics.

4.4 Summary

Two types of experiments were conducted during this project (1) a comparison of SRB growth under autotrophic growth in a complex and defined media, and (2) the immobilisation of SRB on different support materials.

The complex nutrient media solution contained both yeast extract and bactopeptone, which have been shown to facilitate faster growth with SRB (Widdel and Bak, 1992). However, the yeast extract may interfere with the protein analysis and TKN analysis that were conducted in these experiments. As such, it was desirable to see if growth could also be accomplished in a defined media without yeast extract or bactopeptone. A study of SRB growth in the complex

111

and defined media showed that while the SRB did grow in the defined media, although the specific growth of the SRB was much higher in the complex media than the defined media, 0.097 and 0.015/h, respectively. This translates to a doubling time of 7 hours compared to 46 hours. In conjugation with monitoring the increase in biomass over time, the CO_2 uptake rate of the SRB was also monitored. Interestingly, the CO_2 uptake rate was first initiated in the defined media solution before the complex media solution. It is possible that the SRB in the complex nutrient media first utilised any organic carbon available from the addition of the yeast extract and bactopeptone. As well the complex media solution has a higher final biomass value compared to the defined media solution, 6.50 and 1.41 mg biomass, respectively. This also supports the idea that carbon available from the yeast extract and bactopeptone was being utilised by the SRB.

The study of the immobilisation of SRB to different support surfaces was conducted in two parts. In the first study, glass beads, ceramic beads, molecular sieve, Teflon/plastic pieces, and zeolite supports were used. None of these materials proved to be suitable surfaces for SRB attachment, except possibly the Teflon. In the second study, foam, basalt, Ringlace and alginate beads were used as immobilisation surfaces. Teflon could have been included in these studies, except there was a lack of bottle available and it was decided that the other materials had priority. In the first study the following parameters were monitored: total solids, total TKN, CO_2 uptake and sulphate reduction; whereas in the second study: the TKN, and protein both in solution as well as on the supports, and sulphate reduction were measured.

The CO_2 uptake studies during the support experiments were considered invalid as an inconsistent amount of nitrogen (as an inert gas) was initially added to the flasks, which was supposed to be used as a comparison to the change in CO_2 levels. Both TKN and total solids were monitored in the first study, however the total solids did not increase consistently over the time of the experiment and the VSS level was too small to be measured. The TKN values on the other hand did show an increasing level over the time of the experiment. Plots of the TKN versus time appeared to generally follow first order kinetics, with the specific growth values calculated for the control, glass beads, Teflon and zeolite generally falling within the

values reported in literature, $\mu = 0.012 - 0.096$/h compared to values of $\mu = 0.013-0.15$/h reported (Robinson and Tiedge, 1984, Klemps et al., 1985, Badziong and Thauer, 1978). The specific growth values calculated for the molecular sieve and ceramic bead systems however, where an order of magnitude lower than that reported in literature.

The specific growth values calculated for the second set of experiments, which were conducted in the defined media, were generally lower than that determined in the first set of experiments with the complex media. Ranging from $\mu = 0.004$/h for the alginate beads to 0.015/h for the control. The lower specific growth values were expected, based on the results obtained during the nutrient solution experiments.

Since the first set of experiments only monitored the total increase in biomass it was not possible to quantify which support was a better immobilisation surface for growth. However, based on final TKN numbers (as an indirect measurement of biomass) and visual observations, the Teflon support may be a good support surface for SRB. The final biomass in the Teflon system was similar to that in the control, 7.20 and 6.50 mg, respectively. As well biofilm was noticed to be adhering to the Teflon, and it was not easily removed by simply shaking the flask. It has been postulated that hydrophobic surfaces, may encourage bacterial adhesion (Bolte et al., 1986, Huysman et al., 1983). Neither the glass beads nor the zeolite were observed to have good biofilm development on their surfaces and while biofilms were noticed to be adhering to the ceramic beads and molecular sieve, both of these materials were observed to be fracturing. As such, they would probably disintegrate, or crumble, rapidly in a reactor system.

In the second set of experiments with support, the amount of biomass on the surfaces was also quantified. In order of decreasing biomass attached to the surface compared to free suspended biomass was alginate beads (84%)>foam (79%)>Ringlace(37%), while the biomass on the basalt was below the detection limit of the TKN analysis. The results for the foam and alginate beads were as expected. The SRB were encapsulated within the alginate beads and thus SRB were immediately adhered to this immobilisation surface. As such, any biomass in solution was due to either rupturing of the bead walls due to colony expansion or

single cell release to the surface of the beads (Wijffels, 1994). Porous media have been found to be better colonised than nonporous media (Huysman et. al., 1983, Allaoui and Forster, 1994, Van Houten et. al., 1994,). As such the foam was expected to have better results than either the Ringlace or basalt. It has also been noted that microbial colonisation on surfaces tends to increase with increasing surface roughness (Geesey and Costerton, 1979, Baker, 1984, Characklis, 1984). Thus, it was expected that the basalt would perform better than the Ringlace. However the opposite was observed, with approximately, 37% of the biomass adhered to the support in the Ringlace system, while no measurable biomass was found on the basalt system. It has been postulated that the basalt surface lacked sufficiently deep pores, and crevices, for good bacterial colonisation (Van Houten, 1996). While the hydrophobic properties of the Ringlace support are not known, it is possible that this was a contributing reason for the observed bacterial adhesion.

If these experiments were to be repeated, it would be recommended that all bottles be prepared in triplicate for each day of sampling. During this experiment, samples were generally prepared in duplicate, however in some cases there was a large discrepancy between the data obtained during the same day. For instance, in the basalt support system, on day 14 two samples were collected for the TKN measurements, one value was 672 μg N while the other was 448 μg N. A third sample would have weighted the average to the more appropriate TKN value. The results from the total solids and the protein analysis did not agree well with the results of the TKN analysis, although the protein results did show a general increasing biomass trend, which supports the TKN results. A Bovine gamma globulin (BGG) standard was used in the protein assay to determine the biomass content of the SRB, a more appropriate standard would be a purified protein sample of SRB, however this was not available. It is possible that the BGG standard contains a different ratio of proteins than the SRB, which could account for the results being higher than expected. Both the turbidimetric and methylthymol blue sulphate analysis methods appeared to yield good results. The turbidimetric samples were analysed manually while the methythymol blue samples were analysed automatically using flow injection analysis. From a time perspective, the methythymol blue method is significantly faster, as approximately 60 samples/hour could be processed whereas approximately 10 samples/hour were processed using the manual method.

CHAPTER 5: CONCLUSIONS AND RECOMMENDATIONS

5.1 Conclusions

The primary objective of this thesis was to compare the immobilization of SRB to different types of support surfaces, while a secondary objective was monitor the growth of SRB in a complex and defined nutrient media under autotrophic conditions. The objectives were accomplished by monitoring the biomass growth and sulfate reduction in the different support systems, monitoring CO_2 uptake, and with the use of SEM images. The conclusions can be listed as follows:

- The immobilization of SRB was greatest in the alginate beads followed by the foam support, and Ringlace. No significant quantities of biomass were measured on the basalt surfaces. The percentage of immobilized biomass compared to that in free suspension after 14 days of study was 84% for the alginate beads, 79% for the foam, and 37% for the Ringlace.

- The alginate beads had the highest level of immobilized cells as expected, since the SRB were growing within the individual beads. The SRB found in solution was attributed to single cell release and colony eruption of bacteria due to growth at the bead surface.

- The immobilization of the SRB on the foam was also high and is attributed to a bacterial preference for colonizing porous structures, and adhering to hydrophobic materials.

- No quantifiable levels of biomass were measured on the basalt support, despite its rough surface, while a small percentage of biomass was quantified on the Ringlace, it is unclear what properties of the Ringlace, encouraged the bacterial adhesion.

- Porosity and hydrophobicity were found to encourage bacterial adhesion more than surface roughness.

- The complex media control was found to have the largest overall specific growth rate, $\mu = 0.096/h$, when compared to the specific growth rates determined for both the defined and complex nutrient support systems. The specific growth rate for the defined media control, $\mu = 0.015/h$ was less than that calculated for the Ringlace support system, $\mu = 0.023/h$, but greater than the μ values calculated for alginate beads, foam and basalt supports, which were also grown in a defined media.

- The sulfate reduction was found to follow zero order kinetics for the defined and complex nutrient media controls, as well as the support systems with Ringlace, foam, alginate beads, and the basalt. However, the sulfate reduction data for the glass beads, Teflon, and zeolite support systems did not follow the expected trend.

- The molar growth yield, Y_{SO_4} values for the complex and defined nutrient media were 8.47 and 5.59 g biomass/mol SO_4 reduced, respectively. The Y_{SO_4} values for the SRB bacteria cultivated in the complex media support systems varied from 4.88–16.24 g/mol, while the Y_{SO_4} values for the defined media support systems were 5.07, 5.89, 7.28, and 9.77 g/mol for the alginate beads, basalt, foam, and Ringlace, respectively. These values compare well data published in literature, which range from 4-13.5 g/mol (see Table 4.5).

- The nutrient solution studies confirmed that SRB can grow under autotrophic conditions in a defined media, however the complex media was found to have a faster rate of CO_2 uptake compared to the defined media, 1.81×10^{-05} and 0.38×10^{-05} mol $CO_2/(L.h)$, respectively. As well, the CO_2 uptake rate for the intermediate nutrient solution, which had no bactopeptone but did contain yeast extract, was $1.12-0.75 \times 10^{-05}$ mol $CO_2/(L.h)$.

- Monitoring TKN was found to be a valid tool for indirectly estimating the SRB biomass. As well, the complex media did not interfere with the TKN analysis when using the designed experimental protocols.

116

- Although the protein measurements followed the same general increasing biomass trends as the TKN measurements, the calculated growth yields using the protein values were higher than expected. The Bovine gamma globulin protein standard is not appropriate for monitoring SRB biomass.

5.2 Recommendations

The main objective of this project was to determine a suitable immobilization surface for bacterial colonization. This support surface could be used in future reactor studies to compare the ability of the SRB to treat high sulfate, high metal containing effluent at different flow rates. Based on the data gathered from this project, either a hydrophobic, porous structured support (such as foam), or a cell entrapment type immobilization surface would be suitable for future reactor studies. Thus, further work should concentrate on studying the immobilization of SRB under continuous reactor conditions.

The nutrient solution studies confirmed that SRB can grow under autotrophic conditions in a defined media, however, the addition of yeast extract and bactopeptone can increase the rate of CO_2 uptake and has a higher specific growth rate compared to the defined media solution. For the purposes of bench scale research, it is recommended that a complex nutrient media be used in future studies in order to obtain results in a shorter time period.

In this project, three different methods of enumerating bacterial mass were investigated, total solids, TKN, and protein measurements. Of these three methods, TKN appeared the most reliable for estimating the bacterial mass, as such, it is recommended that TKN be used to measure SRB biomass in future studies.

REFERENCES

1. Absolom, D. R., F. V. Lamberti, et al. (1983). "Title Surface thermodynamics of bacterial adhesion." Applied and Environmental Microbiology **46**(1): 90-97.

2. Allaoui, K. and C. F. Forster (1994). "An Examination of Different Support Media in Relation to the Start-up of Anaerobic Expanded Bed Reactors." Environmental Technology **15**: 887-894.

3. Badziong, W. and R. K. Thauer (1978). "Growth Yields and Growth Rates of Desulfovibrio vulgaris (Marburg) Growing on Hydrogen plus Sulfate and Hydrogen plus Thiosulfate as the Sole Energy Sources." Archives of Microbiology **117**: 209-214.

4. Baker, J. H. (1984). Canadian Journal of Microbiology **30**: 511-515.

5. Baldwin, Susan A. (1998) Personnel Communication: Nutrient Solutions.

6. Barnes, L. J., F. J. Jansen, et al. (1991). "Simultaneous Microbial Removal of Sulphate and Heavy Metals from Waste Water." Trans. Instn Min. Metal: C183-C189.

7. Bass, C., J. S. Webb, et al. (1996). "Influences of Surfaces on Sulphidogenic Bacteria." Biofouling **10**(1-3): 95-109.

8. Beeftink, H. H. and P. Staugaard (1986). Applied Environmental Microbiology **52**: 1139-1146.

9. Berube, Pierre (1998) Personnel Communication: Total Solids.

10. Bio-Rad Laboratories (1999) DC Protein Assay Instruction Manual.

11. Bolte, J.P., D.T. Hill, S.A. Cobb. (1986) "Characteristics of Biomass Support Particles for Suspended Particle-Attached Growth Fermentors". Presented at the 1986 Summer Meeting of the American Society of Agricultural Engineers. San Luis Obispo, California June 29-July 2.

12. CIELAP (Canadian Institute for Environmental Law and Policy) (1996) Environmental Law Organizations Call for Strengthening and Moderinzation of Federal Mining Regulations., Press Release: April 16.

13. Chang, J. S., J. C. Huang, et al. (1998). Removal and recovery of lead by fixed-bed biosorption with immobilized bacterial biomass. IAWQ Annual Conference, Vancouver, B.C.

14. Characklis, W. G. (1984). Biofilm Development: A process analysis. <u>Microbial Adhesion and Aggregation</u>. K. C. Marshall. Berlin, Springer-Verlag: 137-157.

15. Characklis, W. G. and K. Marshall, Eds. (1991). Chapter 10: Physiological Ecology in Biofilm Systems. <u>Biofilms</u>, John Wiley & Sons, Inc.

16. Cypionka, H. and N. Pfennig (1986). "Growth yields of *Desulfotomaculum orientis* with hydrogen in chemostat culture." <u>Archives of Microbiology</u> **143**: 396-399.

17. De Vegt, A. L. and C. J. N. Buisman (1995). "Sulfur compounds and Heavy Metal Removal using Bioprocess Technology." <u>The Minerals, Metals and Materials Society</u>: 995-1004.

18. Diels, L., S. V. Roy, et al. (1991). Immobilization of Bacteria in composite membranes and development of tubular membrane reactors for heavy metal recuperation. 3rd International Conference on Effective Biological Processes, BHR Group.

19. Du Preez, L. A., J. P. Odendaal, et al. (1992). "Biological Removal of Sulphate from Industrial Effluents using Producer Gas as Energy Source." <u>Environmental Technology</u> **13**: 875-882.

20. Dudney, A. W. L., A. Narayanan, et al. (1995). Treatment of iron oxalate leachate in anaerobic sludge blanket systems. Editors: C.A. Jerez, T. Vargas, H.Toledo and J.V. Wierz. Biohydrometalurgical Processing.

21. Eccles, H. (1995) Removal of Heavy Metals from Effluent Streams -Why Select a Biological Process?. <u>International Biodeterioration and Biodegradation.</u> pp5-16.

22. Elliott, P., S. Ragusa, et al. (1998). "Growth of Sulfate-Reducing Bacteria Under Acidic Conditions in an Upflow Anaerobic Bioreactor as a Treatment System for Acid Mine Drainage." <u>Water Research</u> **32**(12): 3724-3730.

23. Fisher-Hamilton. (1970). Instruction Manual: Fisher-Hamilton Gas Partitioner. United States, Pittsburgh

24. Fujie, K., T. Tsuchida, et al. (1994). "Development of a Bioreactor System for the Treatment of Chromate Wastewater using *Enterobacter Cloacae* HO1." <u>Water, Science and Technology</u> **30**(3): 235-243.

25. Geesey, G.G. and J.W. Costerton. (1979) Canadian Journal of Microbiology, **25**, 1058-1062.

26. Grappelli, A., L. Campanella, et al. (1992). "Metals Removal and Recovery by *Arthrobacter Sp.* biomass." <u>Water, Science, and Technology</u> **26**(9-11): 2149-2152.

27. Groudeva, V. I. and S. N. Groudev (1994). "A combined chemico-biological treatment of waste waters from coal depyritization with production of elemental sulphur." Fuel Processing Technology **40**: 115-121.

28. Hackl, Ralph P. (1997) Biological Sulfate Reduction for the Treatment of Acid Mine Drainage. Report Presented to: Inco Ltd., J Roy Gordon Research Laboratory, Mississauga, Ontario: 1-40.

29. Humphreys, E. (1999). Personal Communication: Fixation of Bacteria for SEM.

30. Hungate, R. E. (1969) A Methods of Microbiology Roll Tube Method for Cultivation of Strict Anaerobes. Academic Press J.R. Norris and D.W. Ribbons Eds. Volume 3b:118-132.

31. Hunter, P. (1998). The Ugly Canadian, The National Online, July 8, 1998.Heather Abbott.

32. Huysman, P., P. V. Meenen, et al. (1983). "Factors affecting the colonization of non porous and porous packing materials in model upflow methane reactors." Biotechnology Letters **5**(9): 643-648.

33. Ingvosen, Kjeld, and Bo. B. Jorgensen (1984). "Kinetics of sulfate uptake by freshwater and marine species of Desulfovibrio". Archives of Microbiology **139**: 61-66

34. Kim, S. and D. K. Cha (1997). Reduction of Acid Mine Drainage with Sulfate Reducing Bacteria. Hazardous and Industrial Wastes: Proceedings of the Twenty-Ninth Mid-Atlantic Industrial and Hazardous Waste Conference, Technomic Publishing Company.

35. Klemps, R., H. Cypionka, et al. (1985). "Growth with hydrogen, and further physiological characteristics of *Desulfotomaculum* species." Archives of Microbiology **143**: 203-208.

36. Kolmert, A., T. Henrysson, R. Hallberg, and B. Mattiasson.(1997) "Optimization ofsulphide production in anaerobic continuous biofilm process with sulphate reducing bacteria". Biotechnology Letters. **19** No 10 pp 971-975

37. Kuek, C. and T. M. Armitage (1985). "Scanning electron microscopic examination of calcium alginate beads immobilizing growing mycelia of *Aspergillus phoenicus*." Enzyme Microbial Technology **7** March: 121-125.

38. Lachat. (1994) QuikChem Method 10-116-10-2-A. "Sulfate (Methylthymol Blue) in Waters."

39. Lachat. (1976) QuikChem Method 10-107-06-2-E. "Analysis of TKN and ortho-Phosphate in Wastewaters."

40. Ledin, M. and K. Pederson (1996). "The environmental impact of mine wastes - Roles of microorganisms and their significance in treatment of mine wastes." Earth Science Reviews **41**: 67-108.

41. Lefebvre, Jerome and Jean-Claude Vincent. (1997) "Control of the biomass heterogeneity in immobilized cell systems." Enzyme and Microbial Technology **20**:536-543

42. Lens, P. N. L., A. Visser, et al., (1998). "Biotechnological Treatment of Sulfate Rich Wastewaters." Critical Reviews in Environmental Science and Technology: **28**(1): 41-88.

43. Lowry, O. H., N. J. Rosebrough, et al., (1951). "Protein Measurement with the Folin Phenol Reagent." The Journal of Biological Chemistry **193**: 265-275.

44. Madigan, M. T., J. M. Martinko, et al., Eds. (1996). Brock: Biology of Microorganisms.

45. Maree, J. F. and W.F. Strydom (1987). "Biological Sulphate Removal from Industrial Effluent in an Upflow Packed Bed Reactor." Water Resources **21**(2): 141-146.

46. Maree, J. P. and W. F. Strydom (1985). "Biological Sulphate Removal in an Unflow Packed Bed Reactor." Water Resources **19**(9): 1101-1106.

47. Mattuschka, B. and Straube, G. (1993). Biosorption of Metals by a Waste Biomass. Journal of Chemical Technology and Biotechnology. **58**: 57-63.

48. Metcalf and Eddy (1991)."Wastewater Engineering: Treatment, Disposal and Reuse" Third Edition. Publishers McGraw HIll. Revised by: George Tchobanoglous and Franklin L Burton.

49. Monhemius, A.J. (1977) Precipitation diagrams for metal hydroxides, sulphides, arsenates and phosphates. Transactions of the Institute of Mining and Metallurgy C202-C206.

50. Murdock, D.J., Fox, J.R.W. and Benslely, J.G.(1994) Treatment of acid mine drainage by the high density sludge process. International Land Reclamation Conference and Mine Drainage Conference. Proceeding Volume 1, USBM Special Publication SP 06A-94, 241-249.

51. Odom, J.M.Rivers Singleton, Jr. (1993) Sulfate Reducing Bacteria: Contemporary Perspectives. Springer Verlag. Berlin.

52. Perry, K. A. (1995). "Sulfate-Reducing Bacteria and Immobilization of Metals." Marine Geosources and Geotechnology **13**: 33-39.

53. Peters, R.W. and Ku, Y. (1985) Batch precipitation studies for heavy metal removal by sulfide precipitation. American Institute of Chemical Engineers Symposium Series. **81**: 9-27.

54. Philip, L., L. Iyengar, et al. (1996). "Immobilized Microbial Reactor for Heavy Metal Pollution Control." International Journal on the Environment and Pollution **6**(2/3): 277-284.

55. Postek, Michael, Karen S. Howard, Arthur H. Johnson and Kathlyn L. McMichael. (1980). Scanning Electron Microscopy: a student's handbook. Ladd Research Industries, Inc.

56. Postgate, J.R. (1984). The sulphate-reducing bacteria, 2nd edition, Cambridge University Press, Cambridge, England.

57. Revis, N. W., J. Elmore, et al. (1989). Immobilization of Mercury and other Heavy Metals in Soil, Sediment, Sludge, and Water by Sulfate-Reducing Bacteria. Innovative Hazardous Waste Treatment Technology Series. H. Freeman: 97-105.

58. Robinson, J. and J. Tiedje (1984). "Competition between sulfate-reducing and methanogenic bacteria for H2 under resting and growing conditions." Archives of Microbiology **137**: 26-32.

59. Roels, J.A. (1983). Energetics and kinetics in biotechnology. Elsevier Biomedical Press. Amsterdam.

60. Rowley, Michael V (1998) Personal Communication, Biomet Mining Corporation.

61. Rowley, M.V., D.D. Warkentin, V.S. Sicotte (1997). Treatment of Acidic Drainage From the Britannia Mine with the Biosulphide Process - Results of a 10m3 On-Site Pilot Project. 13th Annual BIOMINET Meeting, January 13, 1997, Ottawa, Ontario, Canada.

62. Rowley, M. V., D. D. Warkentin, et al. (1994). The Biosulphide Process: Integrated Biological/Chemical Acid Mine Drainage Treatment - Results of Laboratory Piloting. Proceedings of the International Land Reclamation and Mining Drainage Conference and the Third International Conference on the Abatement of Acid Mine Drainage, April 24 - 29, Pittsburgh, Pennsylvania, USA.

63. Santoyo, A. B., J. B. Rodriguea, et al. (1996). "Immobilization of Pseudomonas sp BA2 by entrapment in calcium alginate and its application for the production of L-alanine." Enzyme and Microbial Technology **19**: 176-180.

64. Schink, B. (1988). Chapter 14: Principles and Limits of Anaerobic Degradation. Biology of Anaerobic Microorganisms. A, Zehnder, John Wiley and Sons.

65. Scott, J. A., A. M. Karanjkar, et al. (1995). "Biofilm Covered Granular Activated Carbon for Decontamination of Streams containing Heavy Metals- and Organic Chemicals." Minerals Engineering **8**(1/2): 221-230.

66. Sengupta, M. (1993). <u>Environmental Impacts of Mining</u>, Lewis Publishers.

67. Shimadzu Corporation. Instruction Manual: Total Organic Carbon Analyzer Model 500. Tokyo, Japan.

68. Smidsrod, O, and Skjak-Braek, G. (1990) Alginate as an Immobilization Matrix for Cells. TIBTECH: 71-78

69. Song, Y. C, Piak, B. C. Shin, H. S .La, S. J. (1998) Influence of electron donor and toxic materials on the activity of sulfate reducing bacteria for the treatment of electroplating wastewater. <u>Water Science and Technology</u> **4** No 5: 187-194.

70. Stams, A.J.M., Grolle, K.C.E., Frijters, et al., (1992) Enrichment of thermophilic propionate-oxidizing bacteria in syntrophy with *Methanobacterium thermoautotrophicum* or *Methanobacterium thermoformicium*. <u>Applied Environmental Microbiology</u>. 58:346-352.

71. Standard Methods. APHA (1995). Greenberg, A., L. Clesceri, et al., Eds.

72. Technicon Industrial Systems (1975). "Digestion and Sample Preparation for the Analysis of TKN." Industrial Method#376-75w.

73. Thauer, R. K., K. Jungermann, et al. (1977). "Energy Conservation in Chemotrophic Anaerobic Bacteria." <u>Bacteriology Reviews</u> **41**: 100-180.

74. Tuttle, J.H., Dugan, P.R., and C.I. Randles (1969). Microbial sulphate reduction and its potential utility as an acid mine water pollution abatement procedure. <u>Applied Microbiology</u>. 17:297-302.

75. Uhrie, J. L., J. I. Drever, et al. (1996). "In situ immobilization of heavy metals associated with uranium leach mines by bacterial sulfate reduction." <u>Hydrometalluryg</u> **43**: 231-239.

76. Vancouver Sun, June 13, 1996, Potent Bacteria Utilized to Harvest Metal While Cleaning Water from Britannia Mine. Page A1

77. Van Houten, R. (1996). Biological sulphate reduction with synthesis gas. Wageningen, The Netherlands, Wageningen Agriculture University: 123.

78. Van Houten, R.T., Van der Spoel, H., Van Aelst, A. et. al. (1996). Biological Sulfate Reduction Using Synthesis Gas as Energy and Carbon Source. <u>Biotechnology and Bioengineering</u> **50**: 136-144.

79. Van Houten, R. T., L. W. H. Pol, et al. (1994). "Biological Sulphate Reduction Using Gas-Lift Reactor fed with Hydrogen and Carbon Dioxide as Energy and Carbon Source." <u>Biotechnology and Bioengineering</u> **44**: 586-594.

80. Visser, A., P. A. Alphenaar, et al. (1993). "Granulation and immobilisation of methanogenic and sulfate-reducing bacteria in high-rate anaerobic reactors." Applied Microbiol Biotechnology **40**: 575-581.

81. Vroblesky, D. A., P. M. Bradley, et al. (1996). "Influence of Electron Donor on the Minimum Sulfate Concentration Required for Sulfate Reduction in a Petroleum Hydrocarbon-Contaminated Aquifer." Environmental Science and Technology **30**(4): 1377-1381.

82. Webb, J., S. McGinness, et al. (1998). "Metal Removal by Sulphate-Reducing Bacteria from Natural and Constructed Wetlands." Journal of Applied Microbiology **84**: 240-248.

83. Widdel, F. and F. Bak (1992). Chapter 183: Gram-Negative Mesophilic Sulfate-Reducing Bacteria. The Prokaryotes: A Handbook on the Biology of Bacteria. A. Balows, Springer-Verlag.

84. Widdel, F. and T. Hansen (1992). Chapter 24: The Dissimilatory Sulfate-and Sulfur-Reducing Bacteri. The Prokaryotes: A Handbook on the Biology of Bacteria. A. Balows, Springer-Verlag.

85. Widdel, F. (1988) Chapter 10: Microbiology and Ecology of Sulfate and Sulfur Reducing Bacteria: Biology of Anaerobic Microoganism. A. Zehnder, John Wiley and Sons.

86. Wijffels, Rene (1994) Nitrification by Immobilized Cells. Ph.D Thesis. Wageningen University.

87. Zobell, C. E. (1943). Journal of Bacteriology **46**: 39-56.

APPENDIX A: RAW AND CALCULATED DATA

Sulphate Raw Data: Control and Glass Beads

Turbimetric Method (Manual)

Description	Day	Sample#1 % Transmittance	Sample#2	Sample#1 Sulphate (mg/L)	Sample#2	Sample#1 Sulphate (mg/L)	Sample#2
(1 mL in 200 mL)				(numbers diluted by 2		(dilution corrected)	
Control	3	83.8	83.8	15.37	15.37	3073	3073
Control	4	78.0	78.0	20.58	20.58	4117	4117
Control	6	79.6	80.4	19.14	18.42	3829	3685
Control	7	81.6	82.8	17.35	16.27	3469	3253
Control	9	87.8	88.2	11.77	11.41	2354	2282
(1 mL in 200 mL)							
Glass Beads	3	85.0		14.29		2858	
Glass Beads	4	80.8	80.4	18.06	18.42	3613	3685
Glass Beads	6	80.2	81.4	18.60	17.53	3721	3505
Glass Beads	7	86.0	86.6	13.39	12.85	2678	2570
Glass Beads	8	85.4	85.4	13.93	13.93	2786	2786

Sulphate Measurements and Standard Deviations

(days)	Control	Glass Beads		Control SD	Glass SD
	Sulphate (mg/L)				
3	3073	2858		0	---
4	4117	3649		0	50.9
6	3757	3613		101.7	152.6
7	3361	2624		152.6	76.3
9	2318	2786		50.9	0

	1	2		Error Analysis of Control	
				1	2
1	m	b			
2	sem	seb	1	-361.063	5735.096
3	r2	sey	2	67.19033	453.2236
4	F	df	3	0.935227	242.2582
5	ssreg	ssresid	4	28.87707	2
			5	1694767	117378.1

where: m = slope
b= y-intercept
sem = error in the slope
seb = error in the y-intercept
r2=variance
sey = error in the y value
F= F statistic, or the F-observed value
df = degrees of freedom
ssreg= regression sum of squares
ssresid = ressidual sum of squares

Sulphate Raw Data: Control and Glass Beads

Sulphate Standard Curve (Manual Method)

Sulphate (mg/L	Percentage Transmittance
0	100
4	96
8	93.4
20	79
40	56

Sulfate Concentratin vs. % Transmittance

$y = -1.1121x + 100.89$

$R^2 = 0.9975$

% Transmittance

Sulfate Concentration (ppm)
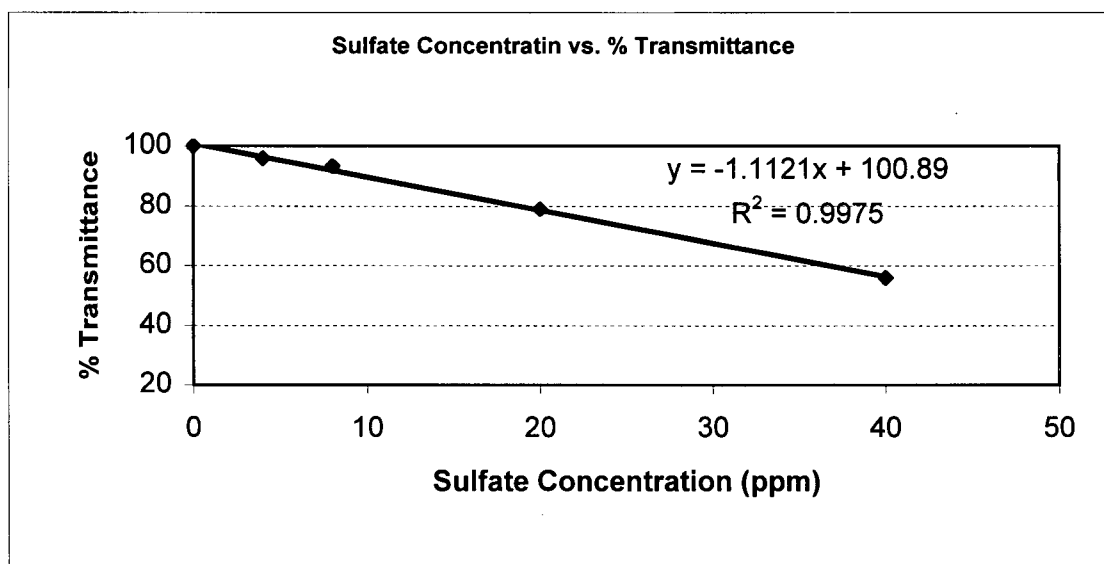
Sulphate Raw and Calculated Data: Teflon and Zeolite

| | | | | | (numbers diluted by 35) | |
| Data | | | Sample#1 | Sample#2 | Sample#1 | Sample#2 |
Bottle#		Date/98	Peak Area		Sulphate (ppm)	
T#0	day 0	27-Nov	11528960		101.49	
Z#0	day 0	27-Nov	11112039		97.54	
T#1	day 1	28-Nov	12205466		107.91	
Z#1	day 1	28-Nov	11248103	11574247	98.83	101.92
Z#3	day 2	29-Nov	11527168	11560755	101.48	101.79
Z#2	day 2	29-Nov	11172941	10933043	98.12	95.84
T#2	day 2	29-Nov	12394138	12407962	109.70	109.83
T#3	day 2	29-Nov	12286208	13257088	108.68	
T#4	day 3	30-Nov	13265626		117.97	
T#5	day 3	30-Nov	10496320		91.70	
Z#4	day 3	30-Nov	11692134		103.04	
Z#5	day 4	1-Dec	10551412		92.22	
T#7	day 4	1-Dec	11002349		96.50	
T#6	day 4	1-Dec	12289044		108.70	
Z#7	day 5	2-Dec	7898445		67.05	
T#8	day 5	2-Dec	8836038		75.95	
T#9	day 5	2-Dec	7864115		66.73	

Sulphate Measurements and Standard Deviations (corrected for dilution)

| | Teflon | Zeolite | | Teflon | Zeolite |
Time	Sulphate (ppm)			S.D.	S.D.
0	3552	3414			
1	3777	3513			77
2	3829	3476		22	100
3	3669	3606		281	
4	3591	3228		302	
5	2497	2347		228	

Sulphate Raw and Calculated Data: Teflon and Zeolite

Sulphate Standard Curve   (Methylthymol Blue Method)

Sulphate (ppm)	Peak Area
77	9084135
55	5881908
40	5176756
24	3900570
16	3284531
0	0

Sulfate Calibration Curve

$y = 105417x + 829920$

$R^2 = 0.9524$

Peak Area

SO42- Standard (ppm)
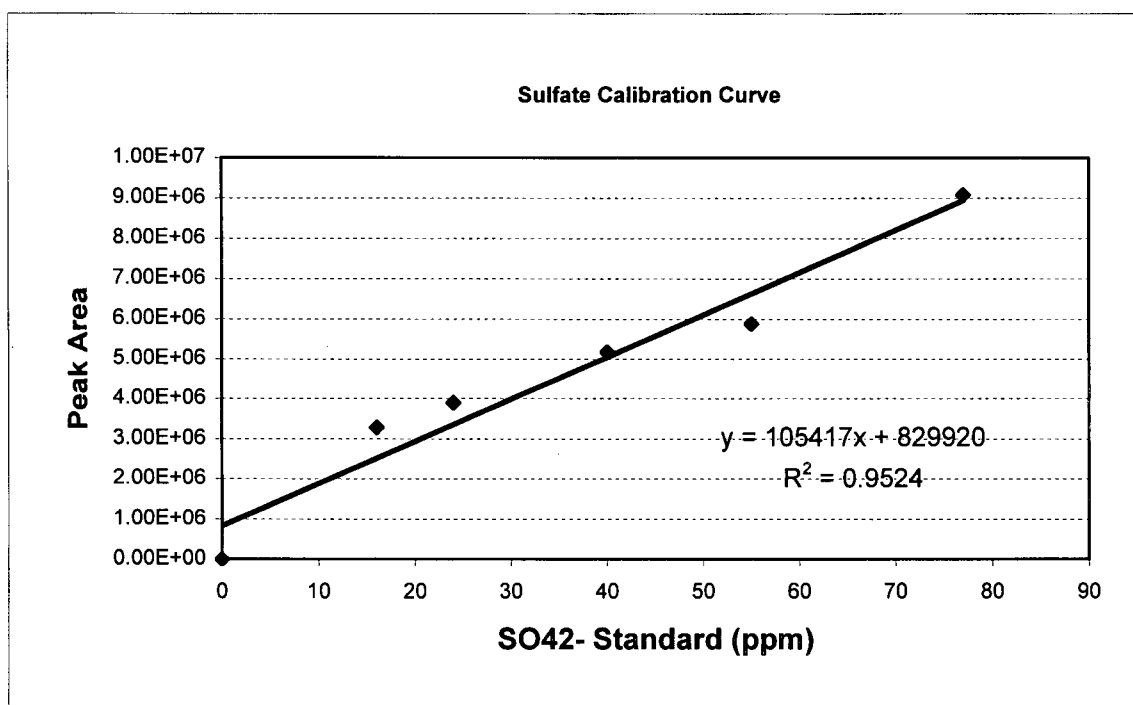
Sulphate Raw Data: Basalt and Foam

April 19- May 2/99 Experiment

Bottle#	Desc	Sampling Day	Sample#1 Sulphate	Sample#2 Concentration (ppm)	
3	Basalt	5	38.63	37.89	numbers diluted by 100
5	Basalt	8	37.50		
6	Basalt	14	37.07	36.54	
7	Basalt	3	39.67	40.01	
8	Basalt	11	35.96	36.87	
10	Basalt	3	39.05	38.88	
11	Basalt	14	35.02	35.21	
12	Basalt	5	36.70	37.05	
13	Basalt	8	38.73	38.54	
14	Basalt	11	dropped		
21	Basalt	blank	43.93	43.67	
31	foam	14	24.80	24.61	
33	foam	11	32.00	31.95	
34	foam	3	37.24	37.58	
35	foam	8	34.76	33.86	
36	foam	11	dropped		
39	foam	8	36.37	36.65	
42	foam	5	37.33	39.85	
43	foam	14	34.44	34.91	
44	foam nsrb	blank	38.19	37.88	
45	foam nsrb	blank	37.16		
46	foam	5	36.41	35.96	
47	foam	14	32.48		
70	control	blank	37.57	37.37	
71	control	blank	37.52	36.53	
72	Basalt	blank	38.28	41.18	
73	foam	blank	38.26		

Sulphate Measurments (corrected for dilution)

Day	Foam (Sulphate ppm)	Basalt (Sulphate ppm)		Foam S.D	C.I=0.95%	Basalt S.D.	.I. =0.95%
0	3787	4177		50	49	263	195
3	3741	3940		24	---	53	52
5	3739	3757		174	170	86	85
8	3541	3825		133	130	66	75
11	3198	3641		3	---	64	---
14	3025	3596		514	451	100	139

Sulphate Raw Data: Basalt and Foam

	Error Analysis - Foam			Error Analysis - Basalt	
	1	2		1	2
1	-58.9	4163		-38.0	4082
2	7.56	76.2		7.81	65.0
3	0.984	50.7		0.855	90.7
4	120	2		23.7	4
5	309174	5147		194644	32915

	1	2
1	m	b
2	sem	seb
3	r2	sey
4	F	df
5	ssreg	ssresid

where: m = slope
b= y-intercept
sem = error in the slope
seb = error in the y-intercept
r2=variance
sey = error in the y value
F= F statistic, or the F-observed value
df = degrees of freedom
ssreg= regression sum of squares
ssresid = ressidual sum of squares

Sulphate Raw Data: MVH3, MVH2, Alginate, Ringlace

Batch Subset 1:June/July/99 Experiments

Bottle #	Desc	Sampling Day	Sample#1	Sample#2	
			Sulfate Concentration (ppm)		
10	MVH3	5	35.4	34	numbers diluted by 100
12	MVH3	5	35.5	35.3	
13	MVH3	8	31.8	31.6	
14	MVH3	14	29.6	29.7	
15	MVH3	11	28.7	30.6	
16	MVH3	8	32.6	32.7	
17	MVH3	11	30	30.5	
18	MVH3	5	32.4	33.2	
19	MVH3	1	33.4	33.8	
21	MVH3	14	27.8	28	
23	MVH3	11	30	30.5	
30	Alginate	14	25	24	
31	Alginate	11	26.5	27.2	
32	Alginate	5	30.9	31.7	
33	Alginate	8	27.9	27.8	
36	Alginate	5	26.7	26.8	
37	Alginate	11	13.6	14.6	
40	Alginate	5	28.9	29.2	
41	Alginate	8	24.8	23.8	
42	Alginate	14	19.4	19.8	
44	Alginate	0	35.5	35.7	
45	Alginate	11	23.1	23.2	
47	Alginate	0			
50	MVHII	0	32.8	33.2	
51	MVHII	0	35	35.2	
52	MVHII	5	34.5	35.1	
53	MVHII	14	29.7	29.6	
56	MVHII	8	33	33.4	
57	MVHII	8	32.4	33.7	
60	MVHII	14	26.9	27.4	
61	MVHII	11	29.5	29.2	
62	MVHII	11	28.9	29.3	
63	MVHII	blank	31	30.4	
64	MVHII	blank	31.1	30.7	
65	MVHII	11	27.5	26.7	
67	MVHII	14	27.2	27.9	
71	Ringlace	8	33.3	31.4	
72	Ringlace	11	28	28.7	
73	Ringlace	14	30	30.6	
74	Ringlace	8	32.9	32.6	
75	Ringlace	14	31	30.3	
78	Ringlace	11	30.2	31.5	

Sulphate Raw Data: MVH3, MVH2, Alginate, Ringlace

Sulphate Measurements (ppm) (corrected for dilution)

(days)	1	5	8	11	14
Ringlace	3383		3255	2960	3048
Ca-Beads	3560	2903	2608	2137	2205
MVH2	3405	3480	3313	2852	2812
MVH3	3360	3430	3218	3005	2878

Sulphate Standard Deviations and Confidence Limits

	0		5		8	
	S.D	C.I=0.95%	S.D	C.I=0.95%	S.D	C.I=0.95%
Ringlace	32	---	---	---	82	80
Ca-Beads	14	---	205	164	209	205
MVH2	123	120	42	---	56	55
MVH3	28	---	131	105	56	54

	11		14	
	S.D	C.I=0.95%	S.D	C.I=0.95%
Ringlace	156	153	43	42
Ca-Beads	588	470	286	281
MVH2	114	91	123	99
MVH3	71	57	101	99

133

Sulphate Raw Data: MVH3, MVH2, Alginate, Ringlace

Excel Linear Error Analysis
Error Analysis - MVH2 sulfate reduction

	1	2			1	2
1	-82.2	3895		1	m	b
2	18.1	182.6		2	sem	seb
3	0.9	121.6		3	r2	sey
4	20.6	2.0		4	F	df
5	304017	29566		5	ssreg	ssresid

Error Analysis - Ringlace

	1	2
1	-28.5	3397
2	11.6	113.8
3	0.7	112.3
4	6.0	2.0
5	75368	25219

where: m = slope
b= y-intercept
sem = error in the slope
seb = error in the y-intercept
r2=variance
sey = error in the y value
F= F statistic, or the F-observed value
df = degrees of freedom
ssreg= regression sum of squares
ssresid = ressidual sum of squares

Error Analysis - Alginate

	1	2
1	-109.995	3540
2	18.6	167.7
3	0.9	188.5
4	35.0	3.0
5	1243770	106569

Errot Analysis - MVH3

	1	2
1	-42.3346	3508.21012
2	10.52715	94.9780363
3	0.843524	106.735169
4	16.17222	3
5	184240.3	34177.1887

Total Solids and TKN Values for MVH Control, Ceramic Beads, Molecular Sieve, and Glass Beads

Day 0=Oct 28/98 **Batch V** Sample ID	KN (ug N)		Crucible (before) (g)	Crucible (after) (g)	Filter (g) (g)	Crucible w Filter+Solids (g)	otal Solids#1 (g)	Total Solids#2 (g)
C#1	470	day 1	26.8951	26.8949	0.1084	27.0423	0.0388	0.0390
M#1	382	day 1	28.1811	28.1807	0.1096	28.31	0.0193	0.0197
G#1	383	day 1	25.1775	26.1771	0.1086	26.3019	1.0158	0.0162
V#1	456	day 1	28.4446	28.4443	0.1086	28.5688	0.0156	0.0159
C#2	765	day 3	19.8794	19.8799	0.1043	20.0208	0.0371	0.0366
C#3	766	day 3	18.9048	18.9043	0.105	19.0474	0.0376	0.0381
M#2	690	day 3	28.7936	28.7936	0.105	28.941	0.0424	0.0424
M#3	dropped	day 3	26.2075		0.1039			
G#2	732	day 3		27.6373	0.1031	27.7617		0.0213
V#2	771	day 3	18.8199	18.8198	0.1048	18.9397	0.015	0.0151
C#4	739	day 4	18.5684	18.5687	0.1084	18.6992	0.0224	0.0221
C#5	717	day 4	18.9525	18.953	0.1067	19.0747	0.0155	0.015
M#4	588	day 4	17.9152	17.9162	0.1043	18.0511	0.0316	0.0306
M#5	629	day 4	19.6196	19.6199	0.1043	19.7524	0.0285	0.0282
G#3	664	day 4	18.8339	18.8343	0.1039	18.9577	0.0199	0.0195
V#3		day 4	18.6791	18.679	0.107	18.7922	0.0061	0.0062
C#6	638	day 5	18.3688	18.3689	0.1078	18.49	0.0134	0.0133
M#6	672	day 5	19.0019	19.002	0.107	19.301	0.1921	0.192
G#6	601	day 5	17.8225	17.8228	0.1087	17.9552	0.024	0.0237
V#4	848	day 5	18.9989	18.9993	0.108	19.1172	0.0103	0.0099
C#8	710	day 6	18.5305	18.513	0.1086	18.6636	0.0245	0.042
MS	748	day 6	18.9526	18.9537	0.1086	19.0872	0.026	0.0249
V#5	785	day 6	18.2195	18.2203	0.1082	18.3377	0.01	0.0092
Glass	722	day 6	18.8625	18.8631	0.1085	18.9863	0.0153	0.0147
C#7	798	day 7	18.8488	18.8497	0.1094	18.9909	0.0327	0.0318
C#9	685	day 7	18.7466	18.7505	0.109	18.8731	0.0175	0.0136
V#6	839	day 7	19.0823	19.0833	0.1086	19.1993	0.0084	0.0074

Glass	42	day 0
No Support	45	day 0

Note: Total Solids#1 = (Crucible with Filter +Solids)-(Filter+Crucible wt before firing)
Note: Total Solids#2 = (Crucible with Filter +Solids)-(Filter+Crucible wt after firing)

C=Ceramic Beads
M=Molecular Sieve
G=Glass Beads
V=Control

**Total Solids and TKN Values for MVH Control, Ceramic Beads,
Molecular Sieve, and Glass Beads**

Total Solids

Day	Ceramic Beads		Molecular Sieve		Glass Beads		Control	
1	0.039	0.039	0.019	0.020		0.016	0.016	0.016
3	0.037	0.037	0.042	0.042		0.021	0.015	0.015
4	0.019	0.019	0.030	0.029	0.020	0.020	0.006	0.006
5	0.013	0.013	0.192	0.192	0.024	0.024	0.010	0.010
6	0.024	0.042	0.026	0.025	0.015	0.015	0.010	0.009
7	0.017	0.014					0.008	0.007

Summary of TKN Results

Day	Ceramic	Mol Sieve	Glass	Control
0			42	45
1	470	382	383	456
3	765	690	732	771
4	728	608	663	
5	638	671	600	847
6	710	748	723	785

Standard Deviations

Day	Ceramic SD	Mol Sieve SD
1		
3	0.69	
4	16.14	
5	16.14	28.50
6		
7	79.99	

TKN Values for Teflon and Zeolite

TKN (ug N)

Batch VI	Day	Run 1	Run 2	
V#1	0	44	45	V= Control (No Support)
T#0	0	52		T= Teflon
Z#0	0	78		Z = Zeolite
Z#1	1	103		
T#1	1	263		
T#2	2	348	354	
T#3	2	408		
Z#2	2	140		
Z#3	2	130		
T#4	3	475		
T#5	3	738	754	
Z#4	3	196		
V#2	4	513		
T#6	4	791		
T#7	4	603		
Z#7	5	331		
T#8	5	832		
T#9	5	890	894	

Total TKN Measurements

Day	Teflon	Zeolite	Control
0	52	78	45
1	263	103	
2	370	135	
3	656	196	
4	697		513
5	872	331	

	Standard Deviation	
Day	Teflon	Zeolite
0		
1		
2	33	7
3	156	
4	132	
5	35	

TKN Values for MVH, Basalt, and Foam

TKN (ug N) April/99 Experiments   TKN Results

Vial No	Desc	Sampling Day	Run 1 Solution	Run2 Solution	Run 1 Support	Run 2 Support	Filter
3	basalt	5	389.55		327.93		whatman
5	basalt	8	485		368		whatman
6	basalt	14	671.8		408.98		whatman
7	basalt	3	20.43		1.9		millipore
8	basalt	11	543.9		415.41		whatman
10	basalt	3	45.72	48.38	1.7		millipore
11	basalt	14	473		359		whatman
12	basalt	5	446.74		371.1		whatman
13	basalt	8	521.74		446		whatman
14	basalt	11	447		377		whatman
31	foam	14	503	465	658		whatman
33	foam	11	533		501		whatman
34	foam	3	34.31	35.13	21.69		millipore
35	foam	8	496.77		527.3		whatman
36	foam	11			514		whatman
39	foam	8	491.79		509.3	502.74	whatman
42	foam	5	435.13		422.55		whatman
43	foam	14	88	93	241	248	millipore
46	foam	5	424	410.83	456		whatman
60	srb	April 19 (Day 0)	33.87				millipore
62	srb	April 19 (Day 0)	12.22				millipore
65	pumice	blank	383		409		whatman
70	foam	blank	448		443		whatman
71	whatman	blank	386				whatman
72	millipore	blank	0				millipore

TKN Values for MVH, Basalt, and Foam

Total TKN Measurements (ug N)

Day	Foam	Basalt
0	23.0	23.0
3	56.4	40.0
5	-28.4	-24.3
8	116.4	120.4
11	149.5	112.5
14	297.9	189.4

Note: TKN Values based on TKN less value of filter blanks for Whatman or Millipore

Total TKN Standard Deviations and Confidence Intervals

Day	Foam SD	Foam CI=95%	Basalt SD	Basalt CI=95%
0	15.3	21.2	15.3	21.2
3	0.6	0.8	15.4	17.5
5	---	---	---	---
8	12.7	14.4	65.8	64.5
11	9.2	12.7	71.4	69.9
14	35.4	28.3	137.2	134.5

TKN Measurements (Solution vs Support) (ug N)

Day	Foam Solution	Foam Support	Basalt Solution	Basalt Support
0	23.0	0.0	23.0	0.0
3	34.7	21.7	38.2	0.0
8	46.3	70.1	120.4	0.0
11	85.0	64.5	112.5	0.0
14	63.3	234.7	189.4	0.0

TKN Measurements (Solution vs Support) Standard Deviations and Confidence Limits

	0 SD	0 CI=95%	3 SD	3 CI=95%	8 SD	8 CI=95%
Foam-Solution	15.3	21.2	0.6	0.8	3.5	4.9
Foam-Support	---	---	---	---	12.7	14.4
Basalt-Solution	15.3	21.2	15.4	17.5	26.0	29.4
Basalt-Support	---	---	0.1	0.2	55.2	62.4

	11 SD	11 CI=95%	14 SD	14 CI=95%
Foam-Solution	---	---	15.2	14.9
Foam-Support	9.2	12.7	4.9	6.9
Basalt-Solution	68.5	95.0	140.6	194.8
Basalt-Support	27.2	37.6	---	---

TKN Values for MVH3, MVH2, Calcium Alginate, Ringlace

TKN (ug N) June 14-July 3/99 Experiments

Batch Subset 1 Label #	Desc	Sampling Day	Run 1 Solution	Run 2 Solution	Run 1 Support	Run 2 Support
10	MVH3	5	82	82		
12	MVH3	5	100	103		
13	MVH3	8	148	151		
14	MVH3	14	261	268		
15	MVH3	11	156	160		
16	MVH3	8	95	96		
17	MVH3	11	114	117		
18	MVH3	5	96	98		
21	MVH3	14	242	251		
23	MVH3	11	145	151		
30	Alginate Beads	14	37	37	418	433
31	Alginate Beads	11	8	9	512	494
33	Alginate Beads	8	121	119	393	409
36	Alginate Beads	5	29	29	341	352
40	Alginate Beads	5	21	23	443	452
41	Alginate Beads	8	130	135	382	502
42	Alginate Beads	14	152	157	545	563
44	Alginate Beads	0	0	0	275	289
45	Alginate Beads	11	176	178	414	424
47	Alginate Beads	0	59	62	157	164
50	MVHII	0	2.0	3.9		
51	MVHII	0	1.6	2.2		
52	MVHII	5	118	121		
53	MVHII	14	180	184		
56	MVHII	8	87	89		
57	MVHII	8	159	192		
60	MVHII	14	151	153		
61	MVHII	11	80	79		
62	MVHII	11	102	110		
63	MVHII	blank	0.0	0.0		
64	MVHII	blank	19	20		
65	MVHII	11	100	107		
67	MVHII	14	206	210		

TKN Values for MVH3, MVH2, Calcium Alginate, Ringlace

TKN (ug N)

Batch Subset 1 Label #	Desc	Sampling Day	Run 1 Solution	Run 2 Solution	Run 1 Support	Run 2 Support
71	Ringlace	8	34	35	5	6
72	Ringlace	11	70	71	28	30
73	Ringlace	14	80	81	51	54
74	Ringlace	8	26	27	0	0
75	Ringlace	14	151	138	79	82
78	Ringlace	11	86	91	45	48
90	Foam	14	88	93	241	248
	Millipore	blank	0	0		
	Millipore	blank	0	0		

TKN Values for MVH3, MVH2, Calcium Alginate, Ringlace

Total TKN Measurements (ug N)

(days)	0	5	8	11	14
Ringlace	20.0	---	33.3	117.3	179.0
Ca-Beads	251.5	422.5	547.8	553.8	585.5
MVH2	20.0	120.0	131.8	96.3	180.7
MVH3	20.0	94.0	122.5	140.5	255.5

note: TKN = 20 was used as day 0 values based on blanks run from MVH2 solutions

Total TKN Standard Deviations and Confidence Limits

(days)	0		5		8	
	SD	CI=95%	SD	CI=95%	SD	CI=95%
Ringlace	---	---	---	---	15.3	10.6
Ca-Beads	114.3	79.2	202.3	140.2	161.9	112.2
MVH2	11.3	7.8	2.1	2.9	52.3	51.2
MVH3	11.3	5.8	9.2	7.4	31.2	30.6

	11		14	
	SD	CI=95%	SD	CI=95%
Ringlace	24.3	16.8	36.3	25.1
Ca-Beads	209.4	145.1	220.7	153.0
MVH2	13.5	10.8	25.1	20.1
MVH3	20.0	16.0	11.4	11.2

TKN Measurements (Solution vs Support) (ug N)

	0	5	8	11	14
Ringlace - solution	---	---	30.5	79.5	112.5
Ringlace - support	---	---	2.8	37.8	66.5
Ca-Beads - solution	30.25	25.5	126.3	92.8	95.8
Ca-Beads - support	221.25	397	421.5	461.0	489.8

TKN Measurements (Solution vs Support) Standard Deviation and Confidence Limits

	0		5		8	
	SD	CI=95%	SD	CI=95%	SD	CI=95%
Ringlace -support	---	---	---	---	4.7	4.6
Ringlace - solution	---	---	---	---	3.2	3.1
Alginate - support	35.0	34.3	4.1	4.0	7.5	7.4
Alginate - solution	70.4	69.0	58.6	57.4	54.8	53.7

	11		14	
	SD	CI=95%	SD	CI=95%
Ringlace -support	10.6	10.4	37.3	36.6
Ringlace - solution	10.2	10.0	16.3	15.9
Alginate - support	93.9	92.0	67.9	66.5
Alginate - solution	49.2	48.2	74.8	73.3

Protein Raw Data: Basalt, and Foam

April Experment

Protein OD reading 750 nm modified Lowry Assay

Vial #	Desc	Sampling	Standard		Protein Absorbance Values			Biomass (mg/ml)		
Solution		day								
3	Basalt	5	whatman	1	0.502	0.504	0.506	0.831	0.844	0.858
5	Basalt	8	whatman	1	0.512	0.514	0.502	0.899	0.913	0.831
6	Basalt	14	whatman	1	0.496	0.504	0.506	0.790	0.844	0.858
7	Basalt	3	millipore	2	0.4	0.402	0.4	0.164	0.175	0.164
8	Basalt	11	whatman	1	0.496	0.498	0.5	0.790	0.803	0.817
10	Basalt	3	millipore	2	0.41	0.406	0.406	0.222	0.198	0.198
11	Basalt	14	whatman	1	0.538	0.536	0.536	1.077	1.064	1.064
12	Basalt	5	whatman	1	0.492	0.492	0.498	0.762	0.762	0.803
13	Basalt	8	whatman	1	0.494	0.492	0.492	0.776	0.762	0.762
14	Basalt	11	whatman	1	0.486	0.482	0.484	0.721	0.694	0.707
15	Basalt	8	whatman	1	0.526	0.532	0.52	0.995	1.036	0.954
20	Basalt	11	whatman	1	0.526	0.528	0.526	0.995	1.009	0.995
Support										
3	Basalt	5	whatman	1	0.526	0.522	0.526	0.995	0.968	0.995
5	Basalt	8	whatman	1	0.488	0.48	0.48	0.735	0.680	0.680
6	Basalt	14	whatman	1	0.418	0.416	0.418	0.255	0.241	0.255
7	Basalt	3	millipore	2	0.518	0.504	0.504	0.849	0.767	0.767
8	Basalt	11	whatman	1	0.4	0.396	0.396	0.132	0.104	0.104
10	Basalt	3	millipore	2	0.524	0.528	0.52	0.883	0.907	0.860
11	Basalt	14	whatman	1	0.498	0.5	0.498	0.803	0.817	0.803
12	Basalt	5	whatman	1	0.504	0.5	0.502	0.844	0.817	0.831
13	Basalt	8	whatman	1	0.524	0.52	0.516	0.981	0.954	0.927
14	Basalt	11	whatman	1	0.516	0.516	0.516	0.927	0.927	0.927
15	Basalt	8	whatman	1	0.516	0.516	0.52	0.927	0.927	0.954
20	Basalt	11	whatman	1						

Protein Raw Data: Basalt, and Foam

	Desc	Sampling	Standard		Protein OD reading 750 nm modified Lowry Assay					
					Protein Absorbance Values			Biomass (mg/ml)		
	Solution									
31	foam	14	whatman	1	0.494	0.496	0.488	0.776	0.790	0.735
33	foam	11	whatman	1						
34	foam	3	millipore	2	0.412	0.404	0.404	0.233	0.187	0.187
35	foam	8	whatman	2	0.502	0.516	0.51	0.756	0.837	0.802
36	foam	11	whatman	2						
39	foam	8	whatman	1	0.534	0.53	0.532	1.050	1.023	1.036
42	foam	5	whatman	1	0.51	0.516	0.512	0.886	0.927	0.899
43	foam	14	millipore	1						
44	foam	14	whatman	1	0.504	0.502	0.496	0.844	0.831	0.790
45	foam	14	whatman	1	0.48	0.48	0.482	0.680	0.680	0.694
46	foam	5	whatman	2	0.482	0.486	0.484	0.640	0.663	0.651
	Support									
31	foam	14	whatman	1	0.528	0.53	0.518	1.009	1.023	0.940
33	foam	11	whatman	1	0.5	0.496	0.496	0.817	0.790	0.790
34	foam	3	millipore	2	0.41	0.404	0.404	0.222	0.187	0.187
35	foam	8	whatman	1	0.5	0.506	0.504	0.817	0.858	0.844
36	foam	11	whatman	2	0.524	0.522	0.524	0.883	0.872	0.883
39	foam	8	whatman	1	0.524	0.526	0.526	0.981	0.995	0.995
42	foam	5	whatman	1	0.5	0.502	0.5	0.817	0.831	0.817
43	foam	14	millipore	1						
44	foam	14	whatman	1	0.464	0.462	0.46	0.570	0.557	0.543
45	foam	14	whatman	1	0.502	0.5	0.5	0.831	0.817	0.817
46	foam	5	whatman	1	0.508	0.51	0.508	0.872	0.886	0.872
60	srb	0	0.34	1	0.404	0.408	0.412	0.159	0.186	0.214
62	srb	0	0.34	1	0.398	0.398	0.4	0.118	0.118	0.132
71	filter	blank	whatman	1	0.496	0.478	0.48	0.712		
72	filter	blank	millipore	2	0.372	0.376	0.374	0.001		

Protein Raw Data: Basalt, and Foam

Total Protein Measurements (mg/ml)

(day)	0	3	5	8	11	14
Basalt	0.154	1.026	0.295	0.320	0.404	0.334
Foam	0.154	0.401	0.329	0.409	0.127	0.240

note: if values is less than blank taken as zero

Total Biomass Standard Deviations and Confindence Limits

	0		3		5		8	
	SD	CI=95%	SD	CI=95%	SD	CI=95%	SD	CI=95%
Basalt	0.039	0.032	0.063	0.036	0.096	0.054	0.163	0.092
Foam	0.039	0.032	0.034	0.027	0.143	0.081	0.157	0.073

	11		14	
	SD	CI=95%	SD	CI=95%
Basalt	0.464	0.235	0.486	0.275
Foam	0.046	0.036	0.201	0.093

Protein Raw Data: Basalt, and Foam

    Protein Standard Curves

Standard Curve 1				Standard Curve 2			
mg/mL	Protein Absorbance Values			mg/mL	Protein Absorbance Values		
0	0.376	0.376	0.376	0	0.371	0.364	0.3675
0.73	0.498	0.496	0.497	0.73	0.51	0.502	0.506
1.46	0.598	0.58	0.589	1.46	0.62	0.618	0.619

Standard Curve 1

Plot of OD @ 750 nm versus Gamma Gobulin Protein (mg/ml).

$$y = 0.1459x + 0.3808$$
$$R^2 = 0.9939$$

Standard Curve 2

Plot of OD @ 750 nm versus Gamma Gobulin Protein (mg/mL).

$$y = 0.1723x + 0.3718$$
$$R^2 = 0.9966$$

146
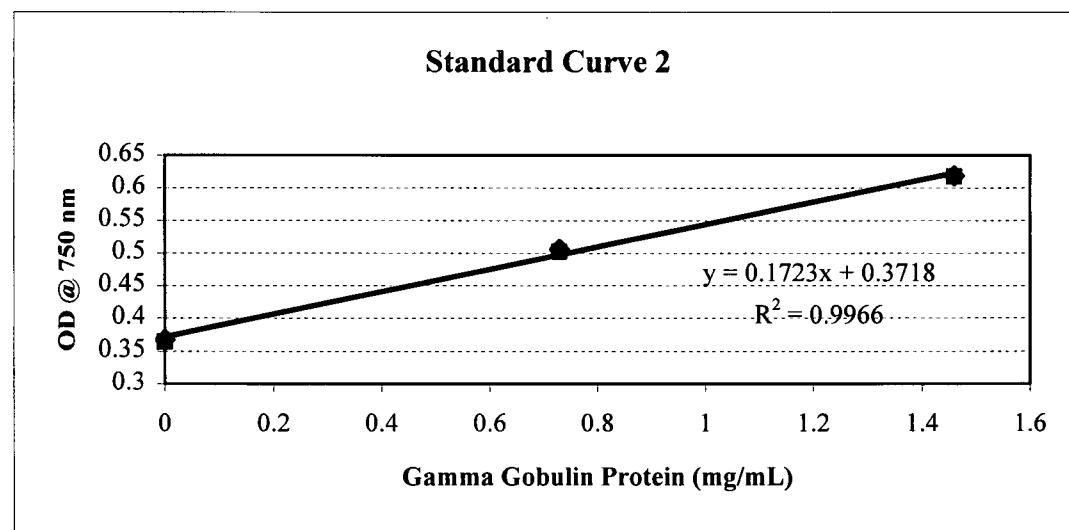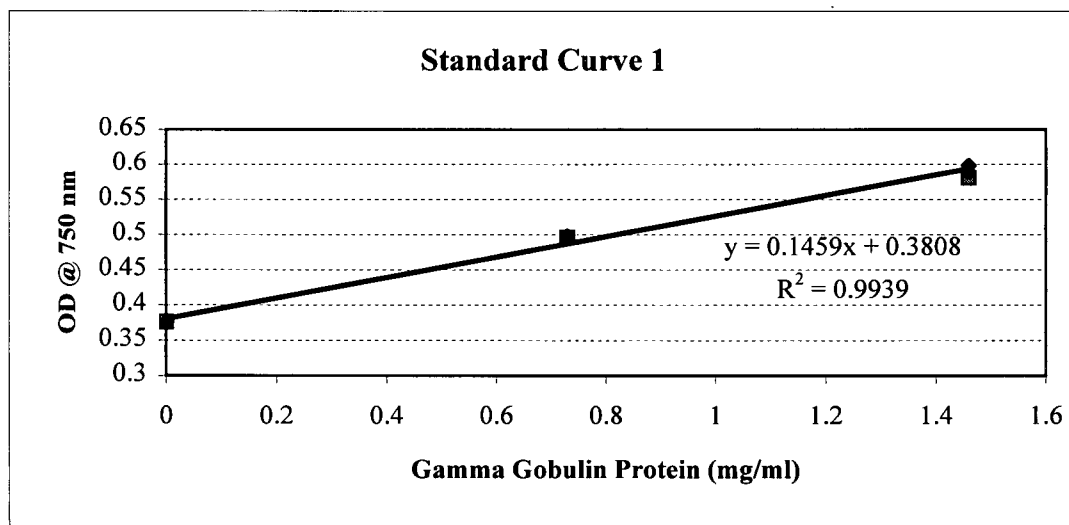
Protein Raw Data: MVH2, MVH3, Ringlace, and Alginate Beads

Batch Subset 1

(Absorbance @ 750 nm)

Bottle#	Desc	Sampling Day	Std Curve	Protein Absorbance Values			Biomass (mg/ml)		
10	MVH3	5	1	0.418	0.418	0.418	0.313	0.313	0.313
12	MVH3	5	2	0.41	0.408	0.408	0.172	0.157	0.157
13	MVH3	8	1	0.44	0.438	0.438	0.470	0.456	0.456
14	MVH3	14	1	0.434	0.434	0.438	0.427	0.427	0.456
15	MVH3	11							
16	MVH3	8	2	0.42	0.418	0.422	0.487	0.458	0.515
17	MVH3	11	1	0.45	0.442	0.442	0.542	0.485	0.485
18	MVH3	5	1	0.416	0.416	0.416	0.298	0.298	0.298
19	MVH3	0	2	0.392	0.394	0.398	0.086	0.115	0.172
21	MVH3	14	1	0.418	0.42	0.422	0.313	0.327	0.341
22	MVH3	0	2	0.376	0.378	0.378	-0.143	-0.115	-0.115
23	MVH3	11	1	0.426	0.428	0.426	0.370	0.384	0.370
Solution									
30	Alginate	14	1	0.424	0.42	0.422	0.356	0.327	0.341
31	Alginate	11					.		
32	Alginate	8	1	0.428	0.424	0.424	0.384	0.356	0.356
33	Alginate	5	1	0.394	0.394	0.392	0.141	0.141	0.127
36	Alginate	5	1	0.442	0.438	0.442	0.485	0.456.	0.485
37	Alginate	11	1	0.498	0.502	0.498	0.885	0.914	0.885
40	Alginate	5	1	0.43	0.426	0.43	0.399	0.370	.0.399
41	Alginate	8	1	0.434	0.432	0.43	0.427	0.413	0.399
42	Alginate	14	1	0.434	0.438	0.436	0.427	0.456	0.442
44	Alginate	0	2	0.402	0.4		0.229	0.200	
45	Alginate	11	1	0.468	0.466	0.464	0.671	0.656	0.642
47	Alginate	0	2	0.424	0.422	0.42	0.544	0.515	0.487

Note: The alginate beads would not digest using the divised protocal
thus no support values were calculated

50	MVHII	0	2	0.406	0.404	0.406	0.143	0.129	0.143
51	MVHII	0	2	0.406	0.402		0.143	0.115	
52	MVHII	5	2	0.44	0.436	0.438	0.387	0.358	0.372
53	MVHII	14	2	0.402	0.404	0.404	0.115	0.129	0.129
56	MVHII	8	1	0.42	0.424	0.42	0.327	0.356	0.327
57	MVHII	8	1	0.422	0.424	0.422	0.341	0.356	0.341
60	MVHII	14	1	0.444	0.44	0.442	0.499	0.470	0.485
61	MVHII	11	1	0.436	0.434	0.436	0.442	0.427	0.442
62	MVHII	11	1	0.43	0.43	0.42	0.399	0.399	0.327
63	MVHII	blank							
64	MVHII	blank							
65	MVHII	11	1	0.418	0.418		0.458	0.458	
67	MVHII	14	1	0.432	0.432	0.43	0.413	0.413	0.399

Protein Raw Data: MVH2, MVH3, Ringlace, and Alginate Beads

Vial No.	Desc	Sampling Day	Std Curve	Protein Absorbance Values			Biomass (mg/ml)		
	Solution								
71	Ringlace	8	1	0.398	0.398	0.398	0.170	0.170	0.170
72	Ringlace	11	1	0.418	0.418	0.416	0.313	0.313	0.298
73	Ringlace	14	1	0.416	0.416	0.416	0.298	0.298	0.298
74	Ringlace	8	1	0.42	0.422	0.426	0.327	0.341	0.370
75	Ringlace	14		dropped					
78	Ringlace	11		lost					
	Support								
72	Ringlace	11	1	0.396	0.4	0.398	0.155	0.184	0.170
73	Ringlace	14	1	0.438	0.438	0.436	0.456	0.456	0.442
74	Ringlace	8	1	0.4	0.4	0.398	0.184	0.184	0.170
75	Ringlace	14	1	0.406	0.406	0.406	0.227	0.227	0.227
78	Ringlace	11		lost					

Total Protein Measurements (mg/ml)

(days)	0	5	8	11	14
Ringlace	0.135		0.437	0.478	0.638
MVH2	0.135	0.372	0.341	0.419	0.339
MVH3	0.124	0.258	0.474	0.439	0.382

Total Protein Standard Deviations and Confidence Limits

(days)	0		5		8	
	SD	CI=95%	SD	CI=95%	SD	CI=95%
Ringlace	0.013				0.087	0.057
MVH2	0.013	0.011	0.014	0.016	0.013	0.010
MVH3	0.044	0.049	0.072	0.047	0.024	0.019

(days)	11		14	
	SD	CI=95%	SD	CI=95%
Ringlace	0.0765	0.0612	0.0993	0.0649
MVH2	0.0438	0.0303	0.1648	0.1142
MVH3	0.0738	0.0590	0.0617	0.0494

Protein Raw Data: MVH2, MVH3, Ringlace, and Alginate Beads

Protein Standard Curves

| Standard Curve 1 | | | | Standard Curve 2 | | | |
mg/L	Protein Absorbance Values			mg/L	Protein Absorbance Values		
0	0.374	0.374	0.373	0	0.38	0.382	0.378
0.71	0.47	0.476	0.476	0.73	0.5	0.496	
1.41	0.572	0.572	0.57	1.46	0.58	0.586	

Standard Curve 1

$y = 0.1397x + 0.3743$

$R^2 = 0.9995$

OD 750 nm vs. Gamma Gobulin Protein mg/mL

Standard Curve 2

$y = 0.1397x + 0.386$

$R^2 = 0.9954$

OD 750 nm vs. Gamma Globulin Protein mg/mL
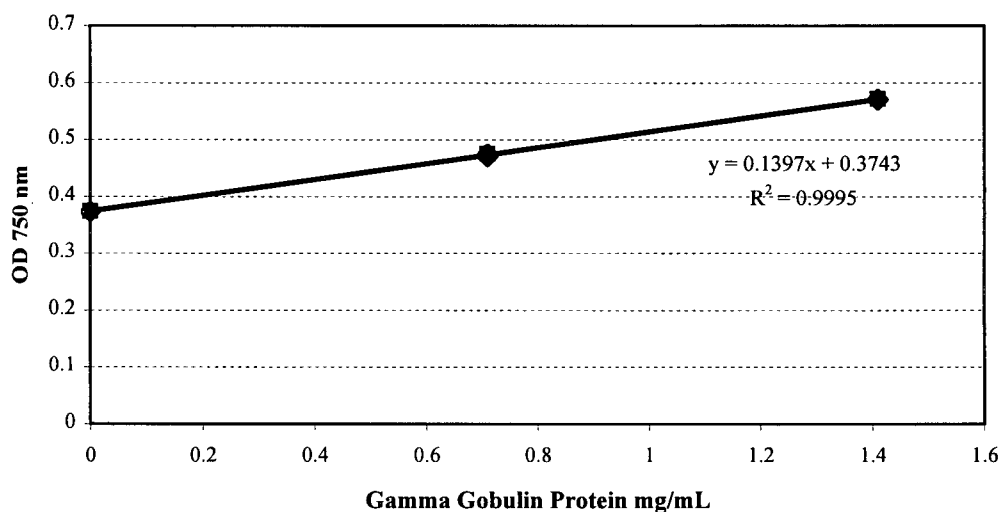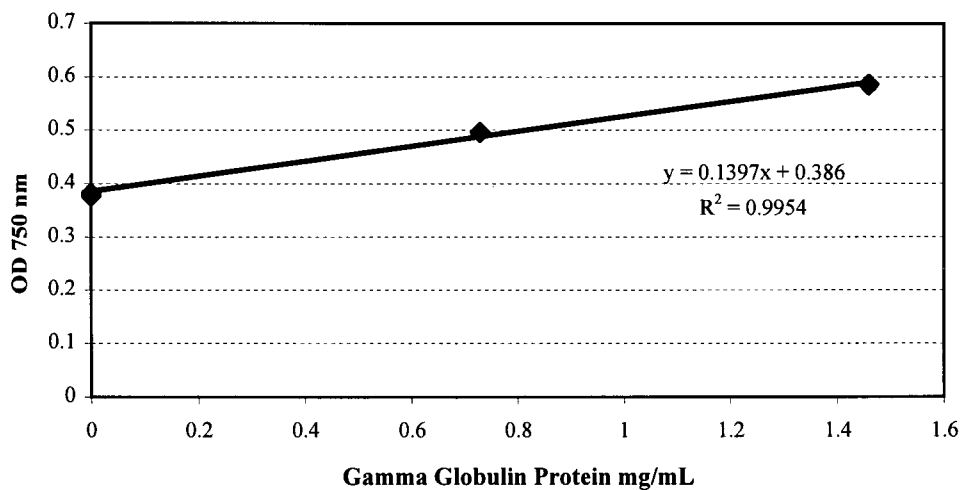
Molecular Sieve, Ceramic Beads, Glass Beads, Control - CO2 Raw Data
Sample Size Injected = 0.5 mL (unless stated otherwise)
Date = Oct 29/98

Sample Data Batch V	Peak Number	Area %	Retention time (min)	Area	BC	Gas
Molecular Sieve	1	43.004	0.17	4487	2	
M#1	2	31.282	0.33	3264	2	composite
Run 1	3	6	0.59	626	3	CO2
Day 1	4	2.616	1.04	273	1	O2
	5	17.098	1.89	1784	1	N2
Total		100		5947		

Sample Data Batch V	Peak Number	Area %	Retention time (min)	Area	BC	Gas
Molecular Sieve	1	31.228	0.12	2126	2	
M#1	2	32.065	0.3	2183	3	composite
Run 2	3	7.902	0.55	538	1	CO2
Day 1	4	3.775	1.01	257	1	O2
	5	25.029	1.82	1704	1	N2
Total		100		4682		

Sample Data Batch V	Peak Number	Area %	Retention time (min)	Area	BC	Gas
Molecular Sieve	1	21.738	0.11	1281	2	
M#1	2	350551	0.28	2095	3	composite
Run 3	3	9.248	0.54	545	1	CO2
Day 1	4	4.31	0.98	254	1	O2
	5	29.153	1.82	1718	1	N2
Total		100		4612		

Sample Data Batch V	Peak Number	Area %	Retention time (min)	Area	BC	Gas
No Support	1	28.059	0.13	1949	2	
V#1	2	30.809	0.3	2140	3	composite
Run 1	3	16.153	0.55	1122	1	CO2
Day 1	4	3.513	1.02	244	1	O2
	5	21.466	1.86	1491	1	N2
Total		100		4997		

Sample Data Batch V	Peak Number	Area %	Retention time (min)	Area	BC	Gas
No Support	1	17.616	0.13	1036	2	
V#1	2	33.022	0.3	1942	3	composite
Run 2	3	19.333	0.55	1137	1	CO2
Day 1	4	3.809	1	224	1	O2
	5	26.22	1.84	1542	1	N2
Total		100		4845		

Molecular Sieve, Ceramic Beads, Glass Beads, Control - CO2 Raw Data

Sample Data Batch V	Peak Number	Area %	Retention time (min)	Area	BC	Gas
No Support	1	13.21	0.13	709	2	junk
V#1	2	33.11	0.3	1777	3	composite
Run 3	3	20.738	0.55	1113	1	CO2
Day 1	4	4.397	1.01	236	1	O2
	5	28.454	1.82	1532	1	N2 a
Total		100		4658		

Sample Data Batch V	Peak Number	Area %	Retention time (min)	Area	BC	Gas
Glass Beads	1	12.664	0.11	762	2	
G#1	2	34.103	0.27	2052	3	composite
Run 1	3	17.65	0.52	1062	1	CO2
Day 1	4	5.684	0.98	342	1	O2
	5	29.899	1.81	1799	1	
Total		100		5255		

Sample Data Batch V	Peak Number	Area %	Retention time (min)	Area	BC	Gas
Glass Beads	1	18.728	0.11	1337	2	
G#1	2	32.736	0.28	2337	3	composite
Run 3	3	15.955	0.53	1139	1	CO2
Day 1	4	5.477	1	391	1	O2
	5	27.105	1.81	1935	1	N2
Total		100		5802		

Sample Data Batch V	Peak Number	Area %	Retention time (min)	Area	BC	Gas
Glass Beads	1	18.9825	0.16	1276	2	
G#1	2	32.282	0.34	2170	3	composite
Run 4	3	16.201	0.58	1089	1	CO2
Day 1	4	5.281	1.04	355	1	O2
	5	27.254	1.85	1832	1	N2
Total		100		5446		

Sample Data Batch V	Peak Number	Area %	Retention time (min)	Area	BC	Gas
Ceramic Bead	1	2.001	0.04	107	2	
C#1	2	39.125	0.14	2092	2	
Run 1	3	29.811	0.32	1594	3	composite
Day 1	4	6.751	0.57	361	1	CO2
	5	2.431	1.05	130	1	O2
	6	19.88	1.85	1063	1	N2
Total		100		3148		

Molecular Sieve, Ceramic Beads, Glass Beads, Control - CO2 Raw Data

Sample Data Batch V	Peak Number	Area %	Retention time (min)	Area	BC	Gas
Ceramic Bead	1	1.628	0.05	73	2	
C#1	2	30.821	0.13	1382	2	
Run 2	3	31.869	0.31	1429	3	composite
Day 1	4	8.095	0.56	363	1	CO2
	5	2.966	1.02	133	1	O2
	6	24.621	1.84	1104	1	N2
Total		100		3029		

Sample Data Batch V	Peak Number	Area %	Retention time (min)	Area	BC	Gas
Ceramic Bead	1	2.876	0.04	131	2	
C#1	2	28.452	0.15	1296	2	
Run 3	3	32.448	0.33	1478	3	composite
Day 1	4	8.342	0.58	380	1	CO2
	5	2.942	1.06	134	1	O2
	6	24.94	1.85	1136	1	N2
Total		100		3128		

October 31/98

Sample Data Batch V	Peak Number	Area %	Retention time (min)	Area	BC	Gas
Ceramic Bead	1	0.908	0.04	76	2	
C#2	2	8.46	0.14	708	2	
Run 1	3	44.151	0.32	3695	3	composite
Day 3	4	1.219	0.61	102	1	CO2
	5	2.294	1.08	192	1	O2
	6	42.968	1.93	3596	1	N2
Total		100		7585		

Sample Data Batch V	Peak Number	Area %	Retention time (min)	Area	BC	Gas
Ceramic Bead	1	0.97	0.07	81	2	
C#2	2	7.996	0.15	668	2	
Run 2	3	43.991	0.33	3675	3	composite
Day 3	4	1.161	0.61	97	1	CO2
	5	2.61	1.09	218	1	O2
	6	43.273	1.93	3615	1	N2
Total		100		7605		

Molecular Sieve, Ceramic Beads, Glass Beads, Control - CO2 Raw Data

Sample Data Batch V	Peak Number	Area %	Retention time (min)	Area	BC	Gas
Ceramic Bead	1	0.415	0.04	30	2	
C#2	2	0.968	0.08	70	2	
Run 3	3	5.63	0.12	407	2	
Day 3	4	44.736	0.31	3234	3	composite
	5	1.162	0.59	84	1	CO2
	6	3.168	1.08	229	1	O2
Total	7	43.92	1.92	3175	1	N2
				6722		

Sample Data Batch V	Peak Number	Area %	Retention time (min)	Area	BC	Gas
Ceramic Bead	1	0.506	0.03	40	2	
C#3	2	11.603	0.12	918	2	
Run 1	3	43.415	0.31	3435	3	composite
Day 3	4	0.784	0.59	62	1	CO2
	5	2.793	1.09	221	1	O2
	6	40.9	1.89	3236	1	N2
Total				6954		

Sample Data Batch V	Peak Number	Area %	Retention time (min)	Area	BC	Gas
Ceramic Bead	1	0.506	0.04	31	2	
C#3	2	1.045	0.08	64	2	
Run 2	3	3.299	0.12	202	3	
Day 3	4	45.566	0.31	2790	1	composite
	5	0.947	0.58	58	1	CO2
	6	2.809	1.08	172	1	O2
Total	7	45.827	1.92	2806	1	N2
				5826		

Sample Data Batch V	Peak Number	Area %	Retention time (min)	Area	BC	Gas
Ceramic Bead	1	1.386	0.07	88	2	
C#3	2	2.741	0.13	174	3	
Run 3	3	45.825	0.33	2909	1	composite
Day 3	4	0.914	0.61	58	1	CO2
	5	2.914	1.09	185	1	O2
	6	46.219	1.92	2934	1	N2
Total				6086		

Molecular Sieve, Ceramic Beads, Glass Beads, Control - CO2 Raw Data

Sample Data Batch V	Peak Number	Area %	Retention time (min)	Area	BC	Gas
Molecular Sieve	1	1.01	0.03	64	2	
M#2	2	8.962	0.08	568	2	
Run 1	3	43.61	0.31	2764	3	composite
Day 3	4	4.071	0.59	258	1	CO2
	5	42.348	1.9	2684	1	N2
				5706		

Sample Data Batch V	Peak Number	Area %	Retention time (min)	Area	BC	Gas
Molecular Sieve	1	0.542	0.04	38	2	
M#2	2	10.923	0.12	766	2	
Run 2	3	43.79	0.31	3071	3	composite
Day 3	4	3.821	0.59	268	1	CO2
	5	40.924	1.92	2870	1	N2
				6209		

Sample Data Batch V	Peak Number	Area %	Retention time (min)	Area	BC	Gas
Molecular Sieve	1	0.318	0.03	19	2	
M#2	2	9.579	0.06	573	2	
Run 3	3	44.266	0.3	2648	3	composite
Day 3	4	3.828	0.58	229	1	CO2
	5	42.009	1.88	2513	1	N2
				5390		

Sample Data Batch V	Peak Number	Area %	Retention time (min)	Area	BC	Gas
Molecular Sieve	1	0.695	0.03	43	2	
M#3	2	11.632	0.07	720	2	
Run 1	3	43.15	0.31	2671	3	composite
Day 3	4	3.99	0.59	247	1	CO2
	5	40.533	1.9	2509	1	N2
				5427		

Sample Data Batch V	Peak Number	Area %	Retention time (min)	Area	BC	Gas
Molecular Sieve	1	1.193	0.03	78	2	
M#3	2	12.439	0.13	813	2	
Run 2	3	42.901	0.32	2804	3	composite
Day 3	4	4.207	0.6	275	1	CO2
	5	39.259	1.92	2566	1	N2
				5645		

Molecular Sieve, Ceramic Beads, Glass Beads, Control - CO2 Raw Data

Sample Data Batch V	Peak Number	Area %	Retention time (min)	Area	BC	Gas
Molecular Sieve	1	0.867	0.03	55	2	
M#3	2	12.541	0.13	796	2	
Run3	3	42.634	0.32	2706	3	composite
Day 3	4	4.222	0.6	268	1	CO2
	5	39.735	1.92	2522	1	N2
				5496		

Sample Data Batch V	Peak Number	Area %	Retention time (min)	Area	BC	Gas
No Support	1	1.096	0.04	66	2	???
V#2	2	14.395	0.14	867	2	???
Run 1	3	32.276	0.34	1944	3	composite
Day 3	4	23.825	0.61	1435	1	CO2
	5	28.408	1.93	1711	1	N2
				5090		

Sample Data Batch V	Peak Number	Area %	Retention time (min)	Area	BC	Gas
No Support	1	1.239	0.04	83	2	
V#2	2	20.287	0.14	1359	2	
Run 2	3	30.408	0.33	2037	3	composite
Day 3	4	21.585	0.6	1446	1	CO2
	5	26.482	1.93	1774	1	N2
				5257		

Sample Data Batch V	Peak Number	Area %	Retention time (min)	Area	BC	Gas
No Support	1	1.277	0.04	78	2	
V#2	2	13.47	0.14	823	2	
Run3	3	33.028	0.33	2018	3	composite
Day 3	4	24.664	0.6	1507	1	CO2
	5	27.5614	1.93	1684	1	N2
				5209		

Date = Nov 1/98 Day 4

Sample Data Batch V	Peak Number	Area %	Retention time (min)	Area	BC	Gas
Molecular Sieve	1	2.413	0.03	142	2	
M#4	2	2.77	0.14	163	2	
Run 1	3	47.171	0.33	2776	3	composite
Day4	4	2.379	1.09	140	1	O2
	5	45.268	1.86	2664	1	N2
Total				5580		

Molecular Sieve, Ceramic Beads, Glass Beads, Control - CO2 Raw Data

Sample Data Batch V	Peak Number	Area %	Retention time (min)	Area	BC	Gas
Molecular Sieve	1	2.291	0.13	131	2	
M#4	2	48.575	0.32	2778	3	composite
Run 2	3	2.868	1.08	164	1	O2
Day4	4	46.267	1.86	2646	1	N2
				5588		
Total						

Sample Data Batch V	Peak Number	Area %	Retention time (min)	Area	BC	Gas
Molecular Sieve	1	1.715	0.02	90	1	
M#4	2	50.2	0.3	2635	1	composite
Run 3	3	48.085	1.84	2524	1	N2
Day4				5159		

Sample Data Batch V	Peak Number	Area %	Retention time (min)	Area	BC	Gas
Molecular Sieve	1	2.539	0.06	150	2	
M#5	2	3.588	0.13	212	2	
Run 1	3	46.378	0.33	2740	3	composite
Day4	4	3.825	0.6	226	1	CO2
	5	2.59	1.08	153	1	O2
	6	41.08	1.86	2427	1	N2
Total				5546		

Sample Data Batch V	Peak Number	Area %	Retention time (min)	Area	BC	Gas
Molecular Sieve	1	4.146	0.16	254	2	
M#5	2	47.968	0.32	2939	3	
Run 2	3	3.787	0.6	232	1	composite
Day4	4	2.579	1.06	158	1	O2
	5	41.521	1.88	2544	1	N2
Total				2934		

Sample Data Batch V	Peak Number	Area %	Retention time (min)	Area	BC	Gas
Molecular Sieve	1	2.102	0.03	132	2	
M#5	2	2.818	0.12	177	2	
Run 3	3	46.768	0.32	2937	3	composite
Day 4	4	3.631	0.6	228	1	CO2
	5	3.041	1.08	191	1	O2
	6	41.64	1.86	2615	1	N2
Total				5971		

Molecular Sieve, Ceramic Beads, Glass Beads, Control - CO2 Raw Data

Sample Data Batch V	Peak Number	Area %	Retention time (min)	Area	BC	Gas
Glass Beads	1	1.485	0.05	76	2	
G#3	2	6.469	0.13	331	2	
Run 1	3	32.265	0.31	1651	3	composite
Day4	4	28.454	0.59	1456	1	CO2
	5	31.327	1.88	1603	1	N2
Total				4710		

Sample Data Batch V	Peak Number	Area %	Retention time (min)	Area	BC	Gas
Glass Beads	1	1.784	0.03	98	2	junk
G#3	2	0.673	0.08	37	2	
Run 2	3	3.786	0.12	208	2	
Day4	4	33.018	0.31	1814	3	composite
	5	28.813	0.59	1583	1	CO2
	6	31.926	1.86	1754	1	N2
Total				5151		

Sample Data Batch V	Peak Number	Area %	Retention time (min)	Area	BC	Gas
Glass Beads	1	1.776	0.03	103	2	
G#3	2	0.535	0.09	31	2	
Run 3	3	4.795	0.13	278	2	
Day4	4	32.58	0.31	1889	3	composite
	5	28.613	0.58	1659	1	CO2
	6	31.701	1.86	1838	1	N2
Total				5386		

Sample Data Batch V	Peak Number	Area %	Retention time (min)	Area	BC	Gas
Ceramic Beads	1	1.581	0.03	136	2	
C#4	2	4.151	0.13	357	2	
Run 1	3	45.983	0.33	3955	3	composite
Day4	4	0.918	0.61	79	1	CO2
	5	2.814	1.07	242	1	O2
	6	44.553	1.88	3832	1	N2
Total				8108		

Sample Data Batch V	Peak Number	Area %	Retention time (min)	Area	BC	Gas
Ceramic Beads	1	1.266	0.03	106	2	
C#4	2	4.406	0.13	369	2	
Run 2	3	47.444	0.32	3973	3	composite
Day4	4	0.908	0.6	76	1	CO2
	5	3.129	1.06	262	1	O2
	6	42.847	1.86	3588	1	N2
Total				7899		

Molecular Sieve, Ceramic Beads, Glass Beads, Control - CO2 Raw Data

Sample Data Batch V	Peak Number	Area %	Retention time (min)	Area	BC	Gas
Ceramic Beads	1	1.237	0.03	119	2	
C#4	2	7.534	0.15	725	2	
Run 3	3	44.882	0.33	4319	3	composite
Day4	4	0.707	0.62	68	1	CO2
	5	3.793	1.09	365	1	O2
	6	41.848	1.89	4027	1	N2
Total				8779		

Sample Data Batch V	Peak Number	Area %	Retention time (min)	Area	BC	Gas
Ceramic Beads	1	2.726	0.07	233	2	
C#5	2	4.704	0.17	402	2	
Run 1	3	45.717	0.36	3907	3	composite
Day4	4	0.62	0.64	53	1	CO2
	5	4.154	1.11	355	1	O2
	6	42.078	1.9	3596	1	N2
Total				7911		

Sample Data Batch V	Peak Number	Area %	Retention time (min)	Area	BC	Gas
Ceramic Beads	1	1.602	0.03	146	2	
C#5	2	10.916	0.15	995	2	
Run 2	3	44.355	0.34	4043	3	composite
Day4	4	0.603	0.62	55	1	CO2
	5	3.928	1.1	358	1	O2
	6	38.596	1.88	3518	1	N2
Total				7974		

Sample Data Batch V	Peak Number	Area %	Retention time (min)	Area	BC	Gas
Ceramic Beads	1	5.925	0.16	490	2	
C#5	2	47.582	0.34	3935	3	composite
Run 3	3	0.762	0.61	63	1	CO2
Day4	4	3.724	1.08	308	1	O2
	5	42.007	1.9	3474	1	N2
				7780		

November 2/98 Day 5

Sample Data Batch V	Peak Number	Area %	Retention time (min)	Area	BC
Ceramic Beads	1	0.695	0.03	76	2	
C#6	2	9.214	0.14	1007	2	
Run 1	3	45.475	0.33	4970	3	composite
Day 5	4	0.393	0.61	43	1	CO2
	5	4.429	1.06	484	1	O2
	6	39.793	1.83	4349	1	N2
				9846		

Molecular Sieve, Ceramic Beads, Glass Beads, Control - CO2 Raw Data

Sample Data Batch V	Peak Number	Area %	Retention time (min)	Area	BC	
Ceramic Beads	1	0.884	0.03	93	2	
C#6	2	5.734	0.09	603	2	
Run 2	3	46.234	0.32	4862	3	composite
Day 5	4	0.418	0.61	44	1	CO2
	5	3.718	1.06	391	1	O2
	6	43.011	1.82	4523	1	N2
				9820		

Sample Data Batch V	Peak Number	Area %	Retention time (min)	Area	BC	
Ceramic Beads	1	1.923	0.07	247	2	
C#6	2	6.33	0.16	813	2	
Run 3	3	45.235	0.35	5810	3	composite
Day 5	4	0.413	0.63	53	1	CO2
	5	4.617	1.08	593	1	O2
	6	41.482	1.86	5328	1	N2
				11784		

Sample Data Batch V	Peak Number	Area %	Retention time (min)	Area	BC	
Molecular Sieve	1	1.237	0.04	115	2	
M#6	2	11.037	0.15	1026	2	
Run 1	3	45.009	0.34	4184	3	composite
Day 5	4	2.291	0.62	213	1	CO2
	5	2.915	1.08	271	1	O2
	6	37.511	1.85	3487	1	N2
				8155		

Sample Data Batch V	Peak Number	Area %	Retention time (min)	Area	BC	
Molecular Sieve	1	1.388	0.08	119	2	
M#6	2	4.655	0.14	399	2	
Run 2	3	46.669	0.33	4000	3	composite
Day 5	4	2.368	0.62	203	1	CO2
	5	3.512	1.08	301	1	O2
	6	41.407	1.82	3549	1	N2
				8053		

Molecular Sieve, Ceramic Beads, Glass Beads, Control - CO2 Raw Data

Sample Data Batch V	Peak Number	Area %	Retention time (min)	Area	BC	
Molecular Sieve	1	1.639	0.02	138	2	
M#6	2	5.298	0.13	446	2	
Run 3	3	46.431	0.32	3909	3	composite
Day 5	4	2.91	0.61	245	1	CO2
	5	2.174	1.05	183	1	O2
	6	41.549	1.81	3498	1	N2
				7835		

Sample Data Batch V	Peak Number	Area %	Retention time (min)	Area	BC	
No Support	1	0.933	0.02	71	2	
V#4	2	5.413	0.13	412	2	
Run 1	3	37.538	0.31	2857	3	composite
Day 5	4	21.101	0.59	1606	1	CO2
	5	35.015	1.81	2665	1	N2
				7128		

Sample Data Batch V	Peak Number	Area %	Retention time (min)	Area	BC	
No Support	1	1.58	0.02	118	2	
V#4	2	5.331	0.13	398	2	
Run 2	3	38.387	0.32	2866	3	composite
Day 5	4	21.23	0.59	1585	1	CO2
	5	33.472	1.84	2499	1	N2
				6950		

Sample Data Batch V	Peak Number	Area %	Retention time (min)	Area	BC	
No Support	1	1.089	0.03	88	2	
V#4	2	9.874	0.13	798	2	
Run 3	3	36.884	0.32	2981	3	composite
Day 5	4	19.203	0.6	1552	1	CO2
	5	32.95	1.81	2663	1	N2
				7196		

Sample Data Batch V	Peak Number	Area %	Retention time (min)	Area	BC	
Glass Beads	1	0.621	0.06	44	2	
G#4	2	9.086	0.13	644	2	
Run 1	3	34.283	0.32	2430	3	composite
Day 5	4	23.49	0.59	1665	1	CO2
	5	32.52	1.81	2305	1	N2
				6400		

Molecular Sieve, Ceramic Beads, Glass Beads, Control - CO2 Raw Data

Sample Data Batch V	Peak Number	Area %	Retention time (min)	Area	BC	
Glass Beads	1	8.521	0.12	665	2	
G#4	2	34.739	0.31	2711	2	composite
Run 2	3	23.552	0.59	1838	3	CO2
Day 5	4	33.188	1.82	2590	1	N2
				7139		

Sample Data Batch V	Peak Number	Area %	Retention time (min)	Area	BC	
Glass Beads	1	11.363	0.13	938	2	
G#4	2	35.239	0.32	2909	2	composite
Run 3	3	21.333	0.59	1761	3	CO2
Day 5	4	32.065	1.84	2647	1	N2
				7317		

November 3/98 Day 6

Sample Data Batch V	Peak Number	Area %	Retention time (min)	Area	BC	
Ceramic Beads	1	1.176	0.06	98	2	???
C#8	2	3.241	0.14	270	2	?
Run 1	3	47.065	0.3	3921	3	composite
Day 6	4	4.513	0.95	376	1	O2
	5	44.004	1.61	3666	1	N2
				7963		

Sample Data Batch V	Peak Number	Area %	Retention time (min)	Area	BC	
Ceramic Beads	1	1.501	0.06	125	2	???
C#8	2	2.785	0.14	232	2	?
Run 2	3	46.987	0.3	3917	3	composite
Day 6	4	5.27	0.95	439	1	O2
	5	43.457	1.62	3620	1	‹ N2
				7976		

Sample Data Batch V	Peak Number	Area %	Retention time (min)	Area	BC	
Ceramic Beads	1	2.347	0.06	210	2	
C#8	2	3.946	0.14	353	2	
Run 3	3	47.15	0.31	4218	3	composite
Day 6	4	4.941	0.95	442	1	O2
	5	41.616	1.6	3723	1	N2
				8383		

Molecular Sieve, Ceramic Beads, Glass Beads, Control - CO2 Raw Data

Sample Data Batch V	Peak Number	Area %	Retention time (min)	Area	BC	
Molecular Sieve	1	1.934	0.13	169	2	
M#7	2	48.724	0.3	4258	2	composite
Run 1	3	1.19	0.55	104	3	CO2
Day 6	4	4.726	0.94	413	1	O2
	5	43.426	1.61	3795	1	N2
				8570		

Sample Data Batch V	Peak Number	Area %	Retention time (min)	Area	BC	
Molecular Sieve	1	5.122	0.14	484	2	
M#7	2	49.751	0.3	4701	2	composite
Run 2	3	0.868	0.56	82	3	CO2
Day 6	4	5.958	0.96	563	1	O2
	5	38.3	1.61	3619	1	N2
				8965		

Sample Data Batch V	Peak Number	Area %	Retention time (min)	Area	BC	
Molecular Sieve	1	1.178	0.05	110	2	
M#7	2	1.873	0.14	175	2	
Run 3	3	46.601	0.3	4353	3	composite
Day 6	4	0.749	0.56	70	1	CO2
	5	6.777	0.95	633	1	O2
		42.822	1.62	4000		N2
				9056		

Sample Data Batch V	Peak Number	Area %	Retention time (min)	Area	BC	
No Support	1	11.587	0.15	939	2	
V#5	2	39.832	0.3	3228	2	composite
Run 1	3	13.388	0.55	1085	3	CO2
Day 6	4	3.43	0.94	278	1	O2
	5	31.762	1.61	2574	1	N2
				7165		

Sample Data Batch V	Peak Number	Area %	Retention time (min)	Area	BC	
No Support	1	1.439	0.04	113	2	
V#5	2	10.445	0.14	820	2	
Run 2	3	39.613	0.31	3110	3	composite
Day 6	4	13.693	0.55	1075	1	CO2
	5	3.312	0.95	260	1	O2
		31.499	1.64	2473		N2
				6918		

Molecular Sieve, Ceramic Beads, Glass Beads, Control - CO2 Raw Data

Sample Data Batch V	Peak Number	Area %	Retention time (min)	Area	BC	
No Support	1	4.826	0.14	349	2	
V#5	2	41.98	0.3	3036	2	composite
Run 3	3	15.169	0.55	1097	3	CO2
Day 6	4	3.498	0.95	253	1	O2
	5	34.527	1.62	2497	1	N2
				6883		

Sample Data Batch V	Peak Number	Area %	Retention time (min)	Area	BC	
Glass Beads	1	6.145	0.15	519	2	???
G#5	2	40.658	0.31	3434	2	composite
Run 1	3	13	0.56	1098	3	CO2
Day 6	4	4.914	0.96	415	1	O2
	5	35.283	1.62	2980	1	N2
				7927		

Sample Data Batch V	Peak Number	Area %	Retention time (min)	Area	BC	
Glass Beads	1	3.02	0.13	247	2	
G#5	2	40.523	0.29	3314	2	composite
Run 2	3	13.928	0.54	1139	3	CO2
Day 6	4	3.962	0.94	324	1	O2
	5	38.567	1.62	3154	1	N2
				7931		

Sample Data Batch V	Peak Number	Area %	Retention time (min)	Area	BC	
Glass Beads	1	5.42	0.11	460	2	
G#5	2	39.767	0.28	3375	2	composite
Run 3	3	11.465	0.53	973	3	CO2
Day 6	4	4.902	0.93	416	1	O2
	5	38.447	1.6	3263	1	N2
				8027		

Teflon and Zeolite CO2 Raw Data

Sample Data Batch VI	Peak Number	Area %	Retention time (min)	Area	BC	
Teflon	1	19.732	0.13	780	2	
T#0	2	33.392	0.31	1320	3	composite
Run 1	3	32.355	0.59	1279	1	CO2
Day 0	4	14.521	1.79	574	1	N2
	5			3173		

Sample Data Batch VI	Peak Number	Area %	Retention time (min)	Area	BC	
Teflon	1	11.345	0.13	398	2	
T#0	2	21.009	0.31	737	2	composite
Run 2	3	14.31	0.32	502	3	composite
Day 0	4	36.887	0.6	1294	1	
	5	16.448	1.79	577	1	
				3110		

Sample Data Batch VI	Peak Number	Area %	Retention time (min)	Area	BC	
Teflon	1	24.009	0.12	1018	2	
T#0	2	32.123	0.31	1362	3	composite
Run 3	3	30.425	0.59	1290	1	
Day 0	4	13.443	1.79	570	1	
	5			3222		

Sample Data Batch VI	Peak Number	Area %	Retention time (min)	Area	BC	
Zeolite	1	28.892	0.16	1119		
Z#0	2	30.648	0.34	1187		composite
Run 1	3	40.46	0.62	1567		
Day 0				2754		

Sample Data Batch VI	Peak Number	Area %	Retention time (min)	Area	BC	
Zeolite	1	17.582	0.14	541		
Z#0	2	30.452	0.32	937		composite
Run 2	3	51.966	0.6	1599		
Day 0				2536		

Sample Data Batch VI	Peak Number	Area %	Retention time (min)	Area	BC	
Zeolite	1	15.584	0.15	482	2	
Z#0	2	32.396	0.34	1002	3	composite
Run 3	3	52.021	0.62	1609	1	
Day 0				2611		

Teflon and Zeolite CO2 Raw Data

Sample Data Batch VI	Peak Number	Area %	Retention time (min)	Area	BC	
Zeolite	1	34.988	0.13	1776	2	
Z#1	2	30.871	0.33	1567	3	composite
Run 1	3	34.141	0.63	1733	1	
Day 1				3300		

Sample Data Batch VI	Peak Number	Area %	Retention time (min)	Area	BC	
Zeolite	1	0.669	0.02	24	2	
Z#1	2	0.752	0.05	27	22	
Run 2	3	19.304	0.13	693	3	
Day 1		33.398	0.33	1199	1	composite
		45.877	0.63	1647		
				2846		

Sample Data Batch VI	Peak Number	Area %	Retention time (min)	Area	BC	
Zeolite	1	16.941	0.11	524	2	
Z#1	2	34.465	0.32	1066	3	
Run 3	3	48.594	0.61	1503	1	composite
Day 1				2569		

Sample Data Batch VI	Peak Number	Area %	Retention time (min)	Area	BC	
Teflon	1	38.4	0.15	1145	2	
T#1	2	21.472	0.34	808	3	composite
Run 1	3	40.128	0.64	1510	1	
Day 1				2318		

Sample Data Batch VI	Peak Number	Area %	Retention time (min)	Area	BC	
Teflon	1	27.145	0.13	794	2	
T#1	2	23.045	0.33	674	3	composite
Run 2	3	49.812	0.63	1457	1	
Day 1				2131		

Sample Data Batch VI	Peak Number	Area %	Retention time (min)	Area	BC	
Teflon	1	35.648	0.14	1350	2	
T#1	2	22.815	0.34	864	3	composite
Run 3	3	41.537	0.64	1573	1	
Day 1				2437		

Teflon and Zeolite CO2 Raw Data

Sample Data Batch VI	Peak Number	Area %	Retention time (min)	Area	BC
Teflon	1	28.131	0.11	1195	2
T#2	2	24.411	0.31	1037	3
Run 1	3	33.781	0.6	1435	1
Day 2		13.677	1.68	581	1
				3053	

Sample Data Batch VI	Peak Number	Area %	Retention time (min)	Area	BC
Teflon	1	24.609	0.13	1022	2
T#2	2	25.692	0.33	1067	3
Run 2	3	34.674	0.61	1440	1
Day 2		15.025	1.68	624	1
				3131	

Sample Data Batch VI	Peak Number	Area %	Retention time (min)	Area	BC
Teflon	1	26.696	0.12	1106	2
T#2	2	23.727	0.31	983	3
Run 3	3	35.071	0.6	1453	1
Day 2		14.506	1.66	601	1
				3037	

Sample Data Batch VI	Peak Number	Area %	Retention time (min)	Area	BC
Zeolite	1	19.28	0.11	970	2
Z#2	2	31.962	0.31	1608	3
Run 3	3	34.824	0.6	1752	1
Day 2		13.934	1.66	701	1
				4061	

Sample Data Batch VI	Peak Number	Area %	Retention time (min)	Area	BC
Zeolite	1	23.403	0.11	1099	2
Z#2	2	29.77	0.31	1398	3
Run 4	3	33.22	0.59	1560	1
Day 2		13.607	1.68	639	1
				3597	

Teflon and Zeolite CO2 Raw Data

Sample Data Batch VI	Peak Number	Area %	Retention time (min)	Area	BC
Zeolite	1	0.671	0.03	36	2
Z#3	2	29.601	0.12	1589	2
Run 1	3	27.385	0.32	1470	3
Day 2		30.756	0.61	1651	1
		11.587	1.71	622	1
				3743	

Sample Data Batch VI	Peak Number	Area %	Retention time (min)	Area	BC
Zeolite	1	0.525	0.03	30	2
Z#3	2	0.56	0.05	32	2
Run 2	3	32.354	0.14	1850	2
Day 2		27.632	0.35	1580	3
		28.227	0.63	1614	1
		10.703	1.71	612	1
				3806	

Sample Data Batch VI	Peak Number	Area %	Retention time (min)	Area	BC
Zeolite	1	0.497	0.03	26	2
Z#3	2	0.612	0.06	32	2
Run 3	3	26.864	0.13	1405	2
Day 2		28.585	0.34	1495	3
		31.778	0.62	1662	1
		11.663	1.68	610	1
				3767	

Sample Data Batch VI	Peak Number	Area %	Retention time (min)	Area	BC
Teflon	1	20.395	0.12	1220	2
T#4	2	32.029	0.31	1916	3
Run 1	3	25.493	0.6	1525	1
Day 3		22.083	1.68	1321	1
				4762	

Sample Data Batch VI	Peak Number	Area %	Retention time (min)	Area	BC
Teflon	1	26.759	0.15	1848	2
T#4	2	31.161	0.33	2152	3
Run 2	3	22.256	0.62	1537	1
Day 3		19.823	1.71	1369	1
				5058	

Teflon and Zeolite CO2 Raw Data

Sample Data Batch VI	Peak Number	Area %	Retention time (min)	Area	BC
Teflon	1	10.071	0.12	525	2
T#4	2	35.603	0.31	1856	3
Run 3	3	28.045	0.6	1462	1
Day 3		26.28	1.68	1370	1
				4688	

Sample Data Batch VI	Peak Number	Area %	Retention time (min)	Area	BC
Teflon	1	13.62	0.12	1204	2
T#5	2	42.215	0.31	3997	3
Run 1	3	9.072	0.6	802	1
Day 3		5.656	1.09	500	2.
		26.437	1.7	2337	3
				7636	

Sample Data Batch VI	Peak Number	Area %	Retention time (min)	Area	BC
Teflon	1	5.996	0.12	461	2
T#5	2	47.679	0.31	3666	3
Run 2	3	11.016	0.6	847	1
Day 3		6.334	1.09	487	2
		28.976	1.69	2228	3
				7228	

Sample Data Batch VI	Peak Number	Area %	Retention time (min)	Area	BC
Teflon	1	8.349	0.11	696	2
T#5	2	46.905	0.31	3910	3
Run 3	3	9.465	0.6	789	1
Day 3		6.322	1.13	527	2
		28.959	1.69	2414	3
				7640	

Sample Data Batch VI	Peak Number	Area %	Retention time (min)	Area	BC
Zeolite	1	18.133	0.12	606	2
Z#4	2	31.658	0.31	1058	3
Run1	3	50.209	0.6	1678	1
Day 3				2736	

Sample Data Batch VI	Peak Number	Area %	Retention time (min)	Area	BC
Zeolite	1	43.738	0.16	2609	2
Z#4	2	28.533	0.34	1702	3
Run 2	3	27.728	0.62	1654	1
Day 3				3356	

Teflon and Zeolite CO2 Raw Data

Sample Data Batch VI	Peak Number	Area %	Retention time (min)	Area	BC
Zeolite	1	20.472	0.11	712	2
Z#4	2	30.88	0.3	1074	3
Run 3	3	48.649	0.59	1692	1
Day 3				2766	

Sample Data Batch VI	Peak Number	Area %	Retention Time (min)	Area	BC
Teflon		4.802	0.11	603	2
T#6		49.243	0.31	6183	3
Run 2		3.592	0.6	451	1
Day 4		8.386	1.1	1053	2
		33.976	1.66	4266	3
				11953	

Sample Data Batch VI	Peak Number	Area %	Retention Time (min)	Area	BC
Teflon		12.075	0.11	1414	2
T#6		55.884	0.31	6544	3
Run 3		3.365	0.61	394	1
Day 4		28.676	1.66	3358	1
				10296	

Sample Data Batch VI	Peak Number	Area %	Retention Time (min)	Area	BC
Teflon		10.103	0.1	758	2
T#7		44.942	0.31	3372	3
Run1		12.662	0.6	950	1
Day 4		4.092	1.09	307	2
		28.202	1.68	2116	3
				6745	

Teflon and Zeolite CO2 Raw Data

Sample Data Batch VI	Peak Number	Area %	Retention Time (min)	Area	BC
Teflon		11.353	0.12	859	2
T#7		44.343	0.31	3355	3
Run 2		12.741	0.6	964	1
Day 4		3.873	1.12	293	2
		27.69	1.68	2095	3
				6707	

Sample Data Batch VI	Peak Number	Area %	Retention Time (min)	Area	BC
Teflon		10.371	0.09	889	2
T#7		7.07	0.19	606	2
Run 3		40.877	0.3	3504	3
Day 4		0.467	0.48	40	1
		9.449	0.59	810	1
		4.281	1.08	367	2
		27.485	1.66	2356	3
				7077	

Sample Data Batch VI	Peak Number	Area %	Retention Time (min)	Area	BC
Zeolite		0.93	0.03	40	2
Z#7		30.792	0.14	1325	2
Run 1		23.658	0.35	1018	3
Day 5		44.62	0.65	1920	1
				2938	

Sample Data Batch VI	Peak Number	Area %	Retention Time (min)	Area	BC
Zeolite		1.086	0.03	43	2
Z#7		23.662	0.14	937	2
Run 2		24.672	0.34	977	3
Day 5		50.581	0.65	2003	1
				2980	

Sample Data Batch VI	Peak Number	Area %	Retention Time (min)	Area	BC
Zeolite		1.36	0.02	54	2
Z#7		27.884	0.13	1107	2
Run 3		23.476	0.34	932	3
Day 5		47.28	0.65	1877	1
				2809	

Teflon and Zeolite CO2 Raw Data

Sample Data Batch VI	Peak Number	Area %	Retention Time (min)	Area	BC
Teflon		0.498	0.03	80	2
T#8		5.509	0.15	885	2
Run 1		43.552	0.35	6997	3
Day 5		3.753	0.66	603	1
		6.305	1.24	1013	2
		40.383	1.84	6488	3
				15101	

Sample Data Batch VI	Peak Number	Area %	Retention Time (min)	Area	BC
Teflon	.	0.449	0.03	63	2
T#8		6.212	0.13	872	2
Run 2		48.351	0.34	6787	3
Day 5		4.937	0.65	693	1
		7.345	1.22	1031	2
		32.706	1.79	4591	3
				13102	

Sample Data Batch VI	Peak Number	Area %	Retention Time (min)	Area	BC
Teflon		0.573	0.02	87	2
T#8		10.572	0.15	1605	2
Run 3		47.48	0.36	7208	3
Day 5		3.979	0.67	604	1
		7.061	1.21	1072	2
		30.334	1.83	4605	3
				13489	

Sample Data Batch VI	Peak Number	Area %	Retention Time (min)	Area	BC
Teflon		0.265	0.02	42	2
T#9		5.208	0.13	824	2
Run 1		44.135	0.33	6983	3
Day 5		3.356	0.64	531	1
		6.99	1.21	1106	2
		40.046	1.8	6336	3
				14956	

Sample Data Batch VI	Peak Number	Area %	Retention Time (min)	Area	BC
Teflon		0.4	0.03	58	2
T#9		7.487	0.14	1085	2
Run 2		48.737	0.34	7063	3
Day 5		3.533	0.65	512	1
		8.018	1.2	1162	2
		31.824	1.82	4612	3
				13349	

171

Teflon and Zeolite CO2 Raw Data

Sample Data Batch VI	Peak Number	Area %	Retention Time (min)	Area	BC
Teflon		4.57	0.12	719	2
T#9		45.068	0.33	7091	3
Run 3		2.638	0.63	415	1
Day 5		6.985	1.2	1099	2
		40.74	1.8	6410	3
				15015	

Carbon Dioxide Analysis: No Support, Glass Gas Partitioner

R=Aco2/(Aco2+composite)

Day	No Support			Glass Beads		
1	0.344	0.369	0.385	0.341	0.328	0.334
3	0.425	0.415	0.428			
4				0.469	0.466	0.468
5	0.360	0.356	0.356	0.407	0.404	0.377
6	0.252	0.257	0.265	0.242	0.256	0.224

Day	No Support		Glass Beads	
	Average	SD	Average	SD
1	0.366	0.021	0.334	0.007
3	0.422	0.006		
4			0.467	0.001
5	0.358	0.002	0.396	0.016
6	0.258	0.007	0.241	0.016

Carbon Dioxide Analysis: Teflon and Zeolite Gas Partitioner

R=Aco2/(Aco2+composite)

Day	Teflon			Zeolite		
0	0.492	0.486	0.486	0.569	0.631	0.616
1	0.651	0.684	0.645	0.525	0.579	0.585
2	0.470	0.460	0.478		0.521	0.527
2				0.529	0.505	0.526
3	0.443	0.417	0.441	0.613	0.493	0.612
3	0.167	0.188	0.168			
4		0.068	0.057			
4	0.220	0.223	0.188			
5	0.079	0.093	0.077	0.654	0.672	0.668

Day	Teflon		Zeolite	
	Avg	SD	Avg	SD
0	0.4883	0.0033	0.6053	0.0322
1	0.6602	0.0206	0.5630	0.0329
2	0.4695	0.0093	0.5219	0.0097
3	0.3039	0.1425	0.5726	0.0691
4	0.2344	0.0823		
5	0.0831	0.0083	0.6646	0.0098

Carbon Dioxide Analysis: Ceramic Beads, Molecular Sieve
Gas Partitioner

R=Aco2/(Aco2+composite)

Day	Ceramic Beads			Molecular Sieve		
1	0.185	0.203	0.205	0.161	0.198	0.206
3	0.027	0.026	0.025	0.085	0.080	0.080
3	0.018	0.020	0.020	0.085	0.089	0.090
4	0.020	0.019	0.016	0.000	0.000	0.000
4	0.013	0.013	0.016	0.076	0.072	0.000
5	0.009	0.009	0.009	0.048	0.048	0.059
6	0.000	0.000	0.000	0.024	0.017	0.016

Day	Ceramic Beads		Molecular Sieve	
	Average	SD	Average	SD
1	0.1972	0.0109	0.1884	0.0242
3	0.0226	0.0038	0.0849	0.0044
4	0.0161	0.0026	0.0224	0.0383
5	0.0089	0.0003	0.0519	0.0061
6	0.0000	0.0000	0.0189	0.0043

Sample of Gas Partitioner Data

Note: this particular sample has no CO2 present. The combined peak
is present at 0.29 minutes. The peak at 0.12 minutes is from a flux
in the air pressure in the column as the sample is injected.

```
CHANNEL A        INJECT  10/05/98 01:43:01

      .129
       1.03  ◄──────  O2 Peak
      1.92  ◄──────  N2 Peak


                        10/05/98 01:43:01      CH= "A"  PS= 1.

FILE  1.      METHOD  0.      RUN   5    INDEX   5

PEAK#    AREA%        RT       AREA BC

   1      3.445      0.12      200 02
   2     49.078      0.29     2849 03
   3      7.924      1.03      460 01
   4     39.552      1.92     2296 01

TOTAL   100.                 5805
```
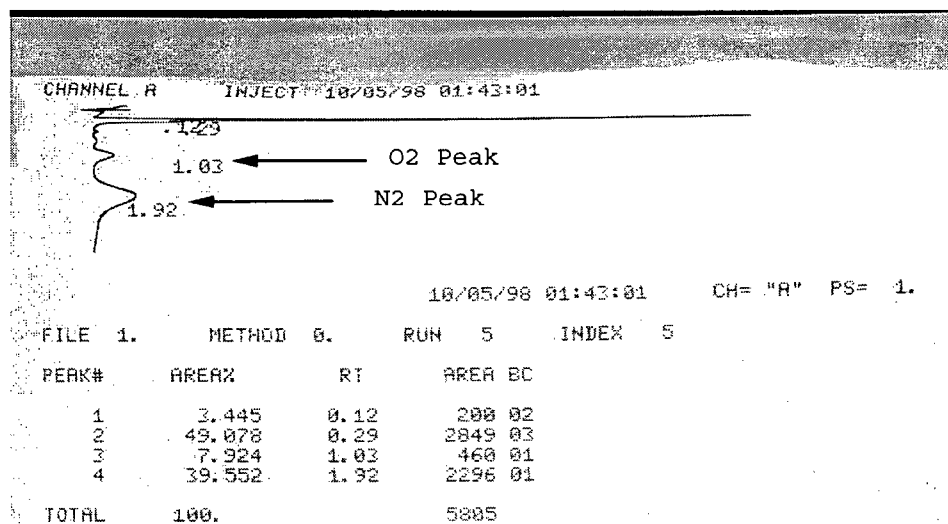
Nutrient Solution: CO2 Uptake Experiments Raw Data

		Peak Area Data						
		noon 24-May	noon 25-May	noon 26-May	midnight 26-May	8:00 AM 27-May	4:00 PM 27-May	midnight 27-May
Solution	Sample							
MVH2	1	18660	19266	18780	17410	18732	15559	17716
MVH2	2	17656	18658	18243	16655	18128	15854	17530
MVH2	3	18160	18408	18316	16611	17448	15456	17201
MVH3	4	15393	17524	16913	15286	16607	14262	16100
MVH3	5	15268	16394	17202	16049	16679	15008	16634
MVH3	6	15748	17185	16792	15484	16348	14565	15927

Standards (CO2)

Injected vol (uL)	Conc. mol*10-07							
15	6.24	47846	45922	46966	43259	43413	38949	43676
15	6.24	48181	45985	46327	42706	44587	38990	44041
10	4.16	33142	30918	31219	27966	30134	25622	27229
10	4.16	33142	29767	31219	27973	30451	26452	28725
5	2.08	15870	15274	14909	13715	15353	12811	14393
5	2.08	15866	15191	15136	14401	15031	13226	14719
0	0.00	0	0	0	0	0	0	0

Linear Fit Data to CO2 Standards

Where:

y=mx+b

y=CO2 concentration

x=peak area

m=slope

b=intercept

	m=slope	b=intercept
May 24 noon	7749	90
May 25 noon	7361	-98
May 26 noon	7529	-305
May 26 midnight	6888	-271
May 27 8am	7038	471
May 27 4pm	6245	26
May 27 midnight	6988	-233

Nutrient Solution: CO2 Uptake Experiments Raw Data

		Peak Area Data							
		8:00 AM 28-May	4:00 PM 28-May	Midnight 28-May	8:00 AM 29-May	4:00 PM 29-May	Midnight 29-May	8:00 AM 30-May	4:00 PM 30-May
Solution	Sample								
MVH2	1	17342	18861	15396	16087	18375	20569	16011	19732
MVH2	2	17026	18556	15075	15336	17777	20046	15584	19066
MVH2	3	16813	17280	15153	16338	17647	19961	14936	19632
MVH3	4	14872	16753	13598	12730	14388	15405	11844	13858
MVH3	5	15973	17367	15498	15246	17137	19526.5	15329	18831
MVH3	6	15347	15876	14777	14592	16185	17389	13438	16707

Standards (CO2)

Injected vol (uL)	Conc. mol*10-07								
15	6.24	42326	45415	40592	39876	45579	51607	39969	51136
15	6.24	42513	45723	40221	40330	45980	51227	38848	50597
10	4.16	27877	30723	26849	27392	30531	33692	26312	33270
10	4.16	28402	30513	27132	27353	30778	34335	26312	33227
5	2.08	14146	15767	13214	13202	15254	16799	14023	15776
5	2.08	14516	14794	13352	13660	15237	16584	13550	16799
0	0.00	0	0	0	0	0	0	0	0

Linear Fit Data to CO2 Standards
Where:
y=mx+b
y=CO2 concentration
x=peak area
m=slope
b=intercept

	m=slope	b=intercept
May 28 8am	6775	96
May 28 4pm	7303	93
May 28 midnight	6495	-106
May 29 8am	6444	137
May 29 4pm	7343	12
May 29 Midnight	8271	-316
May 30 8am	6257	406
May 30 4pm	8189	-513

Nutrient Solution: CO2 Uptake Experiments Raw Data

					Peak Area Data				
Solution	Sample	Midnight 30-May	8:00 AM 31-May	4:00 PM 31-May	Midnight 31-May	8am 1-Jun	4:00 PM 1-Jun	8am 2-Jun	4:00 PM 2-Jun
MVH2	1	18810	15924	18043	17470	15243	---	16160	15391
MVH2	2	18800	15398	18870	17399	16118	---	16480	15115
MVH2	3	18602	15021	17857	16945	15071	---	15914	14477
MVH3	4	13743	10525	12919	12477	10489	10987	10973	10352
MVH3	5	18808	15020	18322	17524	15894	15995	16882	15532
MVH3	6	16235	13142	15095	14603	12836	13177	12977	12132

Standards (CO2)

Injected vol (uL)	Conc. mol*10-07								
15	6.24	50616	38078	47107	46563	41122	42419	44509	40776
15	6.24	49657	38953	47767	47221	40696	41083	44529	40860
10	4.16	32804	25513	31657	31799	28305	28260	30935	26661
10	4.16	32726	25513	31657	31111	27477	28260	30277	27137
5	2.08	16077	13190	16453	15028	13696	14000	14611	13580
5	2.08	16093	12865	16255	15658	13668	13451	14691	13950
0	0.00	0	0	0	0	0	0	0	0

Linear Fit Data to CO2 Standards
Where:
y=mx+b
y=CO2 concentration
x=peak area
m=slope
b=intercept

	m=slope	b=intercept
May 30 Midnight	8068	-487
May 31 8am	6257	-517
May 31 4pm	7725	-477
May 31 Midnight	7549	-147
June 1 8am	6575	123
June 1 4pm	6542	1044
June 1 Midnight	-	-
June 2 8am	7186	26
June 2 4pm	6515	50

Nutrient Solution: CO2 Uptake Experiments Raw Data

		Peak Area Data						
		4:00 PM 3-Jun	4:00 PM 4-Jun	Midnight 4-Jun	4:00 PM 5-Jun	4:00 PM 8-Jun	4:00 PM 9-Jun	4:00 PM 10-Jun
Solution	Sample							
MVH2	1	15007	17752	14671	20569	16058	15107	15348
MVH2	2	15189	17420	14741	19257	15418	14946	15073
MVH2	3	15107	16982	14508	19690	15006	14341	14290
MVH3	4	9600	11251	9188	12895	9285	8149	8244
MVH3	5	15138	17904	14773	19990	15371	14528	14943
MVH3	6	11935	13043	10933	15061	9895	9069	9469

Standards (CO2)

Injected vol (uL)	Conc. mol*10-07							
15	6.24	41002	50069	40607	56233	46215	43129	45532
15	6.24	41420	49999	39583	56798	46879	43259	44954
10	4.16	27711	32781	27040	38906	31417	29241	30590
10	4.16	27678	33431	26511	38612	31806	28637	29919
5	2.08	13964	16192	14060	19032	15606	14572	15702
5	2.08	14039	15350	13746	19829	15293	14598	14810
0	0.00	0	0	0	0	0	0	0

Linear Fit Data to CO2 Standards
Where:
$y=mx+b$
$y=CO2$ concentration
$x=$peak area
$m=$slope
$b=$intercept

	m=slope	b=intercept
June 3 4pm	6588	197
June 4 4pm	8093	-597
June 4 midnight	6377	338
June 5 4pm	9042	531
June 8 4pm	7487	49
June 9 4pm	6910	137
June 10 4pm	7238	122

Nutrient Solution: CO2 Uptake Experiments Raw Data

		Peak Area Data					
		4:00 PM 11-Jun	9:00 PM 14-Jun	4:00 PM 16-Jun	4:00 PM 18-Jun	10:00 AM 19-Jun	10:00 AM 20-Jun
Solution	Sample						
MVH2	1	13058	13951	12788	8801	13649	13790
MVH2	2	13842	14441	13139	8884	14816	13701
MVH2	3	12987	10690	12588	12091	14456	12965
MVH3	4	7923	4847	6758	6657	7499	27839
MVH3	5	13429	12635	11183	10719	11439	38520
MVH3	6	8489	7279	3408	5614	7213	21845

Standards (CO2)

Injected vol (uL)	Conc. mol*10-07						
15	6.24	42670	41145	40909	45056	42497	41353
15	6.24	42115	41159	40919	43504	43392	41176
10	4.16	28250	28061	27258	28095	28841	28116
10	4.16		28575	26486	27453	29119	28496
5	2.08	14360	13876	13987	14178	14181	14280
5	2.08	14321	14628	13702	13951	14291	14224
0	0.00	0	0	0	0	0	0

Linear Fit Data to CO2 Standards		m=slope	b=intercept
Where:	June 11 4pm	6847	-233
y=mx+b	June 14 9pm	6578	465
y=CO2 concentration	16-Jun-99	6523	65
x=peak area	June 18 4pm	7096	-697
m=slope	June 19 10am	6902	5
b=intercept	June 20 10am	6596	428

Nutrient Solution: CO2 Uptake Experiments Raw Data

Peak Area Data

Solution	Sample	10:00 AM 21-Jun	10:00 AM 22-Jun	10:00 AM 23-Jun	5:00 PM 25-Jun	Midnight 25-Jun	5:00 PM 26-Jul
MVH2	1	12730	13173	13779	13201	---	27104
MVH2	2	13738	13880	14493	14360	---	28949
MVH2	3	13122	13883	14156	13311	---	27305
vol (uL)		25	25	25	25	---	50
MVH3	4	29568	29889	29848	30621	---	15153
MVH3	5	41127	37645	38680	37162	---	18281
MVH3	6	22819	23638	23945	27761	---	13795
vol (uL)		25	25	25	100		50
MVH	7				14414	14592	14727
MVH	8				14375	14824	15056
vol (uL)					25	25	25

Standards (CO2)

Injected vol (uL)	Conc. mol*10-07						
15	6.24	43099	42972	43703	43287	45515	45515
15	6.24	43033	44144	43562	43613	45324	45300
10	4.16	29401	28839	29600	29104	30299	29988
10	4.16	29275	29719	29340	28687	29558	29244
5	2.08	14393	14796	14744	14698	14212	15068
5	2.08	14015	14376	14344	14700	14181	15068
0	0.00	0	0	0	0	0	0

Linear Fit Data to CO2 Standards		m=slope	b=intercept
Where:	June 21 10am	6939	3
y=mx+b	June 22 10am	6983	78
y=CO2 concentration	June 23 10am	7007	59
x=peak area	June 25 5pm	6941	122
m=slope	June 25 Midnight	7353	-635
b=intercept	June 26 5pm	7259	-143

180

Nutrient Solution: CO2 Uptake Experiments Raw Data

		Peak Area Data							
		Midnight 26-Jun	9:00 AM 27-Jun	Midnight 27-Jun	10:00 AM 28-Jun	4:00 PM 28-Jun	Midnight 28-Jun	9:00 AM 29-Jun	Midnight 29-Jun
Solution	Sample								
MVH2	1	---	---	27179	---	---	---	---	---
MVH2	2	---	---	28391	---	---	---	---	---
MVH2	3	---	---	26669	---	---	---	---	---
		---	---	50	---	---	---	---	---
MVH3	4	---	---	---	13943	---	---	---	---
MVH3	5	---	---	---	18296	---	---	---	---
MVH3	6	---	---	---	12550	---	---	---	---
					50				
MVH	7	14858	14943	15040	14357	14451	13858	14098	14339
MVH	8	15376	14777	15427	14803	14602	14388	14434	14769
		25	25	25	25	25	25	25	25

Standards (CO2)

Injected vol (uL)	Conc. mol*10-07								
15	6.24	44550	45184	46364	42853	43886	43037	44058	41574
15	6.24	44550	45717	46279	43123	43467	42874	42607	42556
10	4.16	30175	29728	30184	28667	28872	28554	28530	27767
10	4.16	30175	30015	30376	28202	28783	28554	28777	27937
5	2.08	15109	15216	15111	14202	14278	14230	13976	14322
5	2.08	15109	15216	15111	14220	14278	14230	13976	14722
0	0.00	0	0	0	0	0	0	0	0

Linear Fit Data to CO2 Standards		m=slope	b=intercept
Where:	June 26 Midnight	7133	232
y=mx+b	June 27 9am	7262	-25
y=CO2 concentration	June 27 Midnight	7432	-295
x=peak area	June 28 10am	6892	-107
m=slope	June 28 4pm	7015	-217
b=intercept	June 28 Midnight	6889	-67
	June 29 9am	6979	-324
	June 29 Midnight	6688	278

181

Nutrient Solution: CO2 Uptake Experiments Raw Data

		Peak Area Data							
		9:00 AM	Midnight	10:00 AM	Midnight	9:00 AM	Midnight	Noon	Midnight
Solution	Sample	30-Jun	30-Jun	1-Jul	1-Jul	2-Jul	4-Jul	5-Jul	5-Jul
MVH	7	14383	14799	15144	14555	14312	18290	12292	13856
MVH	8	14658	15015	15422	14990	14550	17910	12809	13119
vol (uL)		25	25	25	25	25	25	25	25

Standards (CO2)									
Injected vol (uL)	Conc. mol*10-07								
15	6.24	41165	42812	42904	42124	41680	49665	39985	41965
15	6.24	41444	42438	43709	42013	41008	50157	39634	41328
10	4.16	27594	28767	28880	28823	27066	32742	26475	27530
10	4.16	27052	28126	29668	28724	27133	32974	26576	27602
5	2.08	14043	14329	14663	14725	14522	17227	13440	14139
5	2.08	13792	14506	14543	14770	14114	17459	13753	13855
0	0.00	0	0	0	0	0	0	0	0

Linear Fit Data to CO2 Standards

Where:			m=slope	b=intercept
		June 30 9am	6598	59
y=mx+b		June 30 Midnight	6813	133
y=CO2 concentration		July 1 10am	6940	165
x=peak area		July 1 Midnight	6702	558
m=slope		July 2 9am	6559	259
b=intercept		July 4 Midnight	7918	370
		July 5 Noon	6349	199
		July 5 Midnight	6656	40

		Peak Area Data				
		Noon	Midnight	Noon	Noon	Noon
Solution	Sample	6-Jul	6-Jul	8-Jul	9-Jul	10-Jul
MVH	7	14040	10864	9296	7663	9696
MVH	8	14589	12283	10220	7889	9422
vol (uL)		25	25	25	25	25

Standards (CO2)						
Injected vol (uL)	Conc. mol*10-07					
15	6.24	43926	45479	39574	34701	43972
15	6.24	43819	45343	39531	34652	45612
10	4.16	29138	30039	26880	22827	30682
10	4.16	29361	30163	26907	23617	31284
5	2.08	14632	14704	13475	11898	15279
5	2.08	14423	14731	13025	12287	15567
0	0.00	0	0	0	0	0

Linear Fit Data to CO2 Standards

Where:			m=slope	b=intercept
		July 6 Noon	7040	-59
y=mx+b		July 6 Midnight	7310	-285
y=CO2 concentration		July 8 Noon	6352	121
x=peak area		July 9 Noon	5512	344
m=slope		July 10 Noon	7174	476
b=intercept				

Nutrient Solution: CO2 Uptake Experiments Raw Data
CO2 Concentration determined from Peak Area Data

Concentration (mol/L)

Solution	Sample	24-May noon	25-May noon	26-May 10:00AM	26-May Midnight	27-May 8:00 AM	27-May 4:00 PM	27-May Midnight
	(Hours)	0	24	48	60	68	76	84
	1	0.00959	0.01026	0.01014	0.01027	0.01038	0.00995	0.01027
MVH2	2	0.00907	0.00997	0.00985	0.00983	0.01004	0.01014	0.01017
	3	0.00933	0.01001	0.00989	0.00980	0.00965	0.00988	0.00998
	(Hours)	0	24	48	60	68	76	84
	4	0.00790	0.00924	0.00915	0.00903	0.00917	0.00912	0.00935
MVH3	5	0.00783	0.00940	0.00930	0.00948	0.00921	0.00960	0.00966
	6	0.00808	0.00918	0.00908	0.00915	0.00902	0.00931	0.00925

Solution	Sample	28-May 8:00 AM	28-May 4:00 PM	28-May Midnight	29-May 8:00 AM	29-May 4:00 PM	29-May Midnight	30-May 8:00 AM
	(Hours)	92	100	108	116	124	132	140
	1	0.01018	0.01028	0.00955	0.00990	0.01000	0.01010	0.00998
MVH2	2	0.01000	0.01011	0.00935	0.00943	0.00968	0.00985	0.00970
	3	0.00987	0.00941	0.00940	0.01006	0.00961	0.00981	0.00929
	(Hours)	92	100	108	116	124	132	140
	4	0.008723614	0.009125037	0.008440468	0.007816312	0.007831419	0.007602531	0.007312162
MVH3	5	0.009373637	0.00946133	0.009610683	0.009377961	0.009328946	0.009595641	0.009540136
	6	0.009004051	0.008644696	0.009166617	0.008972032	0.008810341	0.008561971	0.008331212

Solution	Sample	30-May 4:00 PM	30-May Midnight	31-May 8:00 AM	31-May 4:00 PM	31-May Midnight	1-Jun 8:00 AM	1-Jun 4:00 PM
	(Hours)	148	156	164	172	180	188	196
	1	0.00989	0.00957	0.01051	0.00959	0.00934	0.00920	---
MVH2	2	0.00956	0.00956	0.01017	0.01002	0.00930	0.00973	---
	3	0.00984	0.00946	0.00993	0.00949	0.00906	0.00909	---
	(Hours)	148	156	164	172	180	188	196
	4	0.00702	0.00705	0.00706	0.00694	0.00669	0.00631	0.00608
MVH3	5	0.00945	0.00957	0.00993	0.00973	0.00936	0.00960	0.00914
	6	0.00841	0.00829	0.00873	0.00806	0.00782	0.00773	0.00742

Nutrient Solution: CO2 Uptake Experiments Raw Data
CO2 Concentration determined from Peak Area Data

		Concentration (mol/L)						
Solution	Sample	1-Jun Midnight	2-Jun 8:00 AM	2-Jun 4 pm	3-Jun 4:00 PM	4-Jun 4:00 PM	4-Jun midnight	5-Jun 4:00 PM
	(Hours)	204	212	220	244	268	276	292
	1		0.00898	0.00942	0.00899	0.00907	0.00899	0.00886
MVH2	2		0.00916	0.00925	0.00910	0.00890	0.00903	0.00828
	3		0.00884	0.00886	0.00905	0.00869	0.00889	0.00848
	(Hours)	204	212	220	244	268	276	292
	4		0.00609	0.00633	0.00571	0.00586	0.00555	0.00547
MVH3	5		0.00938	0.00951	0.00907	0.00914	0.00905	0.00861
	6		0.00721	0.00742	0.00713	0.00674	0.00665	0.00643

Solution	Sample	8-Jun 4:00 PM	9-Jun 4:00 PM	10-Jun 4:00 PM	11-Jun 4:00 PM	14-Jun 9:00 PM	16-Jun 4:00 PM	18-Jun 4:00 PM
	(Hours)	364	388	412	436	513	556	580
	1	0.00855	0.00867	0.00841	0.00776	0.00820	0.00780	0.00535
MVH2	2	0.00821	0.00857	0.00826	0.00822	0.00850	0.00802	0.00540
	3	0.00799	0.00822	0.00783	0.00772	0.00622	0.00768	0.00721
	(Hours)	364	388	412	436	513	556	580
	4	0.00493	0.00464	0.00449	0.00476	0.00266	0.00410	0.00415
MVH3	5	0.00819	0.00833	0.00819	0.00798	0.00740	0.00682	0.00644
	6	0.00526	0.00517	0.00517	0.00510	0.00414	0.00205	0.00356

Solution	Sample	19-Jun 10:00 AM	20-Jun 10:00 AM	21-Jun 10:00 AM	22-Jun 10:00 AM	23-Jun 10:00 AM
	(Hours)	598	622	646	670	694
	1	0.00791	0.00810	0.00734	0.00750	0.00783
MVH2	2	0.00858	0.00805	0.00792	0.00791	0.00824
	3	0.00837	0.00760	0.00756	0.00791	0.00805
	(Hours)	598	622	646	670	694
	4	0.00434	0.00416	0.00426	0.00427	0.00425
MVH3	5	0.00663	0.00577	0.00593	0.00538	0.00551
	6	0.00418	0.00325	0.00329	0.00337	0.00341

Nutrient Solution: CO2 Uptake Experiments Raw Data

CO2 Concentration determined from Peak Area Data

		Concentration (mol/L)						
Solution	Sample	25-Jun 5:00 PM	25-Jun Midnight	26-Jul 5:00 PM	26-Jun Midnight	27-Jun 9:00 AM	27-Jun Midnight	28-Jun 10:00 AM
	(Hours)	749	756	773	780	789	804	814
	1	0.00754	---	0.00751	---	---	0.00739	---
MVH2	2	0.00821	---	0.00802	---	---	0.00772	---
	3	0.00760	---	0.00756	---	---	0.00726	---
	(Hours)	749	756	773	780	789	804	814
	4	0.00439	---	0.00421	---	---	---	0.00408
MVH3	5	0.00534	---	0.00508	---	---	---	0.00534
	6	0.00398	---	0.00384	---	---	---	0.00367
	(Hours)	0	7	24	31	40	55	65
MVH	7	0.00823692	0.00828	0.00819	0.00820	0.00825	0.00825	0.00840
	8	0.00821444	0.00841	0.00838	0.00849	0.00815	0.00846	0.00865

Solution	Sample	28-Jun 4:00 PM	28-Jun Midnight	29-Jun 9:00 AM	29-Jun Midnight	30-Jun 9:00 AM	30-Jun Midnight	1-Jul 10:00 AM
	(Hours)	71	79	88	103	112	127	137
MVH	7	0.00836	0.00809	0.00827	0.00841	0.00868	0.00861	0.00863
	8	0.00845	0.00839	0.00846	0.00867	0.00885	0.00874	0.00879

Solution	Sample	1-Jul Midnight	2-Jul 9:00 AM	4-Jul Midnight	5-Jul Noon	5-Jul Midnight	6-Jul Noon	6-Jul Midnight
	(Hours)	151	160	223	235	247	259	271
MVH	7	0.00835	0.00857	---	0.00762	0.00830	---	0.00610
	8	0.00861	0.00872	---	0.00794	0.00786	---	0.00688

Solution	Sample	8-Jul Noon	9-Jul Noon	10-Jul Noon
	(Hours)	307	331	355
MVH	7	0.00578	0.00531	0.00514
	8	0.00636	0.00548	0.00499

Nutrient Solution: CO2 Uptake Experiments Raw Data
Excel Linear Error Analysis

	1	2
1	m	b
2	sem	seb
3	r2	sey
4	F	df
5	ssreg	ssresid

where: m = slope
b= y-intercept
sem = error in the slope
seb = error in the y-intercept
r2=variance
sey = error in the y value
F= F statistic, or the F-observed value
df = degrees of freedom
ssreg= regression sum of squares
ssresid = ressidual sum of squares

MVH Linear analysis+

	1	2
1	-1.813E-05	0.01166129
2	2.3779E-06	0.00063357
3	0.90639963	0.00046964
4	58.1023074	6
5	1.2815E-05	1.3233E-06

+fitted through averaged
values from Sample 7 and 8

MVH2 Linear analysis*

	1	2
1	-3.847E-06	0.01012257
2	3.1836E-07	0.00012779
3	0.80224951	0.00045692
4	146.04759	36
5	3.0491E-05	7.5159E-06

*fitted through averaged
values from Samples 1, 2, and 3

MVH3 Linear analsysis++

	1	2
1	-1.196E-05	0.00958546
2	4.3123E-07	0.00011881
3	0.97095264	0.00027507
4	768.810338	23
5	5.8171E-05	1.7403E-06

++fitted through averaged
values from Samples 5 and 6

MVH3 Linear analsysis**

	1	2
	-7.453E-06	0.01093825
	3.0839E-07	0.00011696
	0.96529116	0.00024712
	584.033153	21
	3.5666E-05	1.2824E-06

**fitted through values
from Sample 4

Nutrient Solution: CO2 Uptake Experiments -TKN Raw Data

Bottle #	Description	TKN (ug N) Sample #1	Sample #2
1	MVH2	376	388
2	MVH2	371	385
3	MVH2	436	456
4	MVH3	347	357
5	MVH3	411	430
6	MVH3	328	339
7	MVH	568	585
8	MVH	526	552

Descriptive Statistics using Excel 97 Analysis Package

MVH	MVH2	MVH3
568	376	347
526	371	411
585	436	328
552	388	357
	385	430
	456	339

MVH		*MVH2*		*MVH3*	
Mean	558	Mean	402	Mean	369
Standard Erro	13	Standard Error	14	Standard Error	17
Median	560	Median	387	Median	352
SD	25	SD	35.2	SD	41.7
Sample Varia	630	Sample Variance	1238.8	Sample Variance	1738.7
Kurtosis	-0.2	Kurtosis	-1.1	Kurtosis	-1.4
Skewness	-0.5	Skewness	1.0	Skewness	0.8
Range	59	Range	85	Range	102
Minimum	526	Minimum	371	Minimum	328
Maximum	585	Maximum	456	Maximum	430
Count	4	Count	6	Count	6
C.l.= 95.0%	40	C.l.= 95.0%	37	C.l.= 95.0%	44